

Advances in Human Computer Interaction and Artificial Intelligence

Research in Computing Science

Series Editorial Board

Editors-in-Chief:

Grigori Sidorov (Mexico)
Gerhard Ritter (USA)
Jean Serra (France)
Ulises Cortés (Spain)

Associate Editors:

Jesús Angulo (France)
Jihad El-Sana (Israel)
Alexander Gelbukh (Mexico)
Ioannis Kakadiaris (USA)
Petros Maragos (Greece)
Julian Padget (UK)
Mateo Valero (Spain)

Editorial Coordination:

Alejandra Ramos Porras

Research in Computing Science es una publicación trimestral, de circulación internacional, editada por el Centro de Investigación en Computación del IPN, para dar a conocer los avances de investigación científica y desarrollo tecnológico de la comunidad científica internacional. **Volumen 121**, noviembre 2016. Tiraje: 500 ejemplares. *Certificado de Reserva de Derechos al Uso Exclusivo del Título* No. : 04-2005-121611550100-102, expedido por el Instituto Nacional de Derecho de Autor. *Certificado de Licitud de Título* No. 12897, *Certificado de licitud de Contenido* No. 10470, expedidos por la Comisión Calificadora de Publicaciones y Revistas Ilustradas. El contenido de los artículos es responsabilidad exclusiva de sus respectivos autores. Queda prohibida la reproducción total o parcial, por cualquier medio, sin el permiso expreso del editor, excepto para uso personal o de estudio haciendo cita explícita en la primera página de cada documento. Impreso en la Ciudad de México, en los Talleres Gráficos del IPN – Dirección de Publicaciones, Tres Guerras 27, Centro Histórico, México, D.F. Distribuida por el Centro de Investigación en Computación, Av. Juan de Dios Bátiz S/N, Esq. Av. Miguel Othón de Mendizábal, Col. Nueva Industrial Vallejo, C.P. 07738, México, D.F. Tel. 57 29 60 00, ext. 56571.

Editor responsable: *Grigori Sidorov, RFC SIGR651028L69*

Research in Computing Science is published by the Center for Computing Research of IPN. **Volume 121**, November 2016. Printing 500. The authors are responsible for the contents of their articles. All rights reserved. No part of this publication may be reproduced, stored in a retrieval system, or transmitted, in any form or by any means, electronic, mechanical, photocopying, recording or otherwise, without prior permission of Centre for Computing Research. Printed in Mexico City, in the IPN Graphic Workshop – Publication Office.

Advances in Human Computer Interaction and Artificial Intelligence

Obdulia Pichardo Lagunas (ed.)



Instituto Politécnico Nacional
"La Técnica al Servicio de la Patria"



Instituto Politécnico Nacional, Centro de Investigación en Computación
México 2016

ISSN: 1870-4069

Copyright © Instituto Politécnico Nacional 2016

Instituto Politécnico Nacional (IPN)
Centro de Investigación en Computación (CIC)
Av. Juan de Dios Bátiz s/n esq. M. Othón de Mendizábal
Unidad Profesional “Adolfo López Mateos”, Zacatenco
07738, México D.F., México

<http://www.rcs.cic.ipn.mx>

<http://www.ipn.mx>

<http://www.cic.ipn.mx>

The editors and the publisher of this journal have made their best effort in preparing this special issue, but make no warranty of any kind, expressed or implied, with regard to the information contained in this volume.

All rights reserved. No part of this publication may be reproduced, stored on a retrieval system or transmitted, in any form or by any means, including electronic, mechanical, photocopying, recording, or otherwise, without prior permission of the Instituto Politécnico Nacional, except for personal or classroom use provided that copies bear the full citation notice provided on the first page of each paper.

Indexed in LATINDEX, DBLP and Periodica

Printing: 500

Printed in Mexico

Editorial

The present volume of the journal "Research in Computing Science" contains articles from different fields of research such as: bioinspired algorithms, machine learning, and image processing among others. The papers chosen by the editorial board were subjected to rigorous evaluation by specialist in the area (peer review), taking into consideration the originality, scientific contribution to the field and technical quality.

Each of the works addressed in this issue seeks to solve problems in different fields by providing solutions from the computational point of view.

It is important to recognize the importance of the application of scientific development in the treatment of problems of strong social impact. The papers selected for this volume contains different proposals of computational solutions for problems ranging "*Identification of fungi in corn using Artificial Vision techniques*" to "*Oncological Analysis Using Data Mining*".

On the other hand, the creation of new computer models or techniques to improve those that already exist is essential to continue the research that allows to innovate in various branches of the computing science, in this way many of the papers published in this volume contribute to analysis and improvement of algorithms like "*Capacitated P-Median and Tabu Search*" or "*Tuning the Parameters of a Convolutional Artificial Neural Network by Using Covering Arrays*".

Some of the selected papers implement bioinspired algorithms, the first of which implements an artificial neural network to identify fruit ripeness. Another paper uses a genetic algorithm in the optimization of deformation sequences in industrial welding structures. Others, for example, are looking for improvements in existing algorithms such as automatic tuning of parameters in neural networks. Also, another paper reports on the exploration of dynamic environments using stochastic search strategies such as optimal foraging theory.

In relation to automatic learning techniques some of the approaches used were the typical testors applied in the selection of subsets of characteristics, another one of the reported works implements data mining for oncological analysis of different types.

In the implementation of methodologies for the design and evaluation of industrial automation devices is developing a system of fuzzy logic to control the speed and torque servo system.

Another issue addressed in this volume is the design, creation and evaluation of vehicles of different characteristics: in the case of unmanned aerial vehicles, a multi-agent system was used to allow collaboration between devices. Another case is the design and identification of hydrodynamic parameters.

I would like to thank Mexican Society for Artificial Intelligence (Sociedad Mexicana de Inteligencia Artificial) for the help in preparation of this volume.

The entire submission, reviewing, and selection process, as well as preparation of the proceedings, were supported for free by the EasyChair system (www.easychair.org).

Obdulia Pichardo Lagunas
Guest Editor
Instituto Politécnico Nacional, UPIITA
Mexico

November 2016

Table of Contents

	Page
Using Conceptual Frames to Define a Representation for a Medical Expert System that Evaluates Visual Pathologies	9
<i>Eduardo Eloy Loza Pacheco, Miguel Jesús Torres Ruiz, Dulce Lourdes Loza Pacheco, Augusto Dobeslao Hernandez Lopez</i>	
An Elitism Based Genetic Algorithm for Welding Sequence Optimization to Reduce Deformation	17
<i>Jesus Romero-Hdz, Sinai Aranda, Gengis Toledo-Ramirez, Jose Segura, Baidya Saha</i>	
Finding Events in Background EEG in Rats in Early Posttraumatic Period	37
<i>Ivan A. Kershner, Yurii V. Obukhov, Ilya G. Komoltsev</i>	
Exploring Dynamic Environments Using Stochastic Search Strategies	43
<i>C. A. Piña-García, Dongbing Gu, Carlos Gershenson, J. Mario Siqueiros-Garca, E. Robles-Belmont</i>	
A Solution Proposal for the Capacitated P-Median Problem with Tabu Search	59
<i>Mauricio Romero Montoya, María Beatriz Bernábe Loranca, Rogelio González Velázquez, José Luis Martínez Flores, Horacio Bautista Santos, Abraham Sánchez Flores, Francisco Macías Santiesteban</i>	
Tuning the Parameters of a Convolutional Artificial Neural Network by Using Covering Arrays	69
<i>Humberto Pérez-Espinosa, Himer Avila-George, Josefina Rodriguez-Jacobo, Hector A. Cruz-Mendoza, Juan Martínez-Miranda, Ismael Espinosa-Curiel</i>	
A Meta-Heuristic Based on Genetic Algorithm for Selecting Bailiffs by Districts	83
<i>Ribamar Loura do Carmo, Omar Andres Carmona Cortes, Fernando Jorge Cutrim Demétrio</i>	
Artificial Vision System Using Mobile Devices for Detection of Fusarium Fungus in Corn	95
<i>Pedro Salazar, Saul Ortiz, Talhia Hernández, Nestor Velasco</i>	

Determination of the Ripeness State of Guavas Using an Artificial Neural Network	105
<i>Edwin M. Lara-Espinoza, Monica Trejo-Duran, Rocio A. Lizarraga-Morales, Eduardo Cabal-Yeppez, Noe Saldana-Robles</i>	
A BDI Agent System for the Collaboration of the Unmanned Aerial Vehicle.....	113
<i>Mario Hernandez Dominguez, Jose-Isidro Hernández-Vega, Dolores Gabriela Palomares Gorham, C. Hernández-Santos, Jonam L. Sánchez Cuevas</i>	
CAD design and Identification of Hydrodynamic Parameters of an Underwater Glider Vehicle	125
<i>Jorge Díaz Moreno, Reynaldo Ortiz Pérez, Eduardo Campos Mercado, Luis Fidel Cerecero Natale</i>	
Oncological Analysis Using Data Mining	139
<i>Doricela Gutiérrez Cruz, Ricardo Rico Molina, Liliana Rodríguez Páez, Karla Vilchis Hernández, Bernardo Soto Rivera, Yaroslaf Albarrán Fernández, Alma Gutierrez Cruz, Mónica Ortega</i>	
Feature Subset Selection and Typical Testors Applied to Breast Cancer Cells	151
<i>Alexis Gallegos, Dolores Torres, Francisco Álvarez, Aurora Torres</i>	
Fuzzy Logic Controller for Speed and Torque in AC Servo System.....	165
<i>L. Rodrigo Silva Sánchez, Antonio Hernández Zavala, Jorge A. Huerta Ruelas</i>	

Using Conceptual Frames to Define a Representation for a Medical Expert System that Evaluates Visual Pathologies

Eduardo Eloy Loza Pacheco¹, Miguel Jesús Torrez Ruiz²,
Dulce Lourdes Loza Pacheco³, Augusto Dobeslao Hernandez Lopez¹

¹ Universidad Nacional Autónoma de México, Facultad de Estudios Superiores Acatlán,
Mexico

² Centro de Investigación en Computación, Instituto Politécnico Nacional,
Ciudad de Mexico, Mexico

³ Centro de Investigación y Estudios Avanzados, Instituto Politécnico Nacional,
Ciudad de Mexico, Mexico

eduardo.loza@apolo.acatlan.unam.mx, dobeslao@gmail.com,
mtorres@cic.ipn.mx, dloza@cinvestav.mx

Abstract. This Works propose the benefits of developing an expert system, specialized to evaluate visual diseases. The pathologies of interest in this work are: Diabetic retinopathy, macular degeneration, retinitis pigmentosa and glaucoma. These visual impairments are common in Mexico. The purpose of develop a medical expert system is to evaluate visual diseases with the aim of help people who have no resources or live in a distant town from the major cities in Mexico. We found that the majority of people affected are: in a productive age, have chronic conditions and misinformed about those problems. The number of ophthalmologist is reduced and the often they live in cities. Additionally, we show the type of reasoning methods are used to develop medical expert systems. And we conclude that it is necessary a knowledge representation to store the knowledge of the experts.

Keywords: Expert systems, knowledge representation, reasoning, visual impairments.

1 Introduction

Expert System (ES) has been contributing to the solution of complex problems. One of the first systems was DENDRAL, developed in 1965. This ES had the ability to deduce information about biochemical structures. Later Macsyma were born with the ability to perform complex mathematical analysis. Then HearSay which performs the early attempts of Natural Language interpretation [1]. The evolution of these systems

reaches their zenith in the eighties with the LISP machines. Enterprise applications like XCon from the DEC Company [2]. Since then we can see great variety of applications such as: interpretation, prediction, diagnosis, planning, monitoring, reparation, control, intelligent tutors [3].

In the case of a medical expert system one of the first attempts was MYCIN. The system was design to assist doctors. MYCIN gave a description of treatments for blood infections. Thanks to this specialist in microbiology were capable to provide expertise to other specialist, with less experience in the field. MYCIN asked a series of questions with the aim to recommend a treatment [4].

In Mexico there is a great demand of medical experts. Especially in areas like ophthalmology [5]. There are several advantages of capture the expert knowledge into an Expert System. For example we can have a system available all the time. We can translate it o remote regions of the country. The implementation cost is less than using a human expert. Finally we can have a formal representation of expert knowledge [4].

The following section describes some recent examples of SE used clinical support systems. Section 3 describes the conceptual frames designed to represent knowledge from visual pathologies.

2 Medical Expert Systems

This section reviews the different types of ES. Where we can find that the most used reasoning methods are: production rules [6], Framework for eliciting knowledge for a medical laboratory diagnostic expert system], Bayesian networks [7], pattern recognition. It was found that the common characteristic of medical expert systems they have a validation from an expert in a specific area [6,7] For example as it is shown in [el de la diabetes], a review of several systems developed for diabetes diagnosis. In this case, the majority of the reasoning methods are: production rules, fuzzy reasoning and case based reasoning. In this section we have found that a medical expert system is a very common kind of intelligent systems. Additionally, the knowledge of a system usually is limited to a particular domain. An expert is defined as a person whose knowledge is obtained gradually through a period of time. His learning and experiences shapes his procedural, analytic, social, cognitive, judgement and creative behavior [8]. To become an expert is necessary at least seven years of experience in academy or industry. Normally an expert occupation is classified as academic or industrial [9].

In [6] it shows an ES that helps to determine the age of a hand using an X-ray image. One of the main motivations of this work is to develop a system to detect malformations in children early. This can be a helpful tool to pediatricians. The common method used by specialist is to identify regions of a hand, denominated regions of special interest and then give a diagnosis. To build the body of knowledge were necessary to interview radiologist and endocrinologist pediatricians. After the interviews rules were obtained. Then the rules were modeled from the expert knowledge.

The article emphasizes that experts usually have different criteria to evaluate the bone age. So as a consequence every expert has its own set of rules and evaluation criteria. Because of that it was necessary to classify and combine every rule from every expert. Finally bone age determination algorithm is developed which fuses all the rules from the experts.

In [7] it develops a clinic system to perform decisions. With the purpose of identifying the probability of suffering from a heart failure angina. These sufferings have increased because of factors like stress and poor alimentation. The main problem identified is that in a hospital there are not suitable tools for its diagnosis. That leads that patient with the characteristics of an angina to wait, and be observed. And the patient has to wait several hours.

The proposed solution is a web application, filled by a clinician. The system output is the probability the patient can suffer from these conditions. The system gives the answers: low, medium and serious. According with the response of the system the patient feedbacks, the patient evaluates the result as correct or incorrect. Allowing the system to update it believes. The constructions of the network were developed with the MATLAB library BNT.

The system uses Bayesian networks to evaluate 17 variables. The project took place in Spain in a Valencian Hospital. The reasoning process is performed in language C using the NETICA API for Bayesian networks and the front end were using PHP, HTML and JavaScript.

A framework is proposed in [10], for the elicitation of a medical expert system. The aim is to elicit knowledge from expert, because of the shortage of medical experts. The work is divided in three stages: The selection of an expert, the elicitation part and a fuzzy evaluation.

In the first stage, the framework proposed a selection of an expert. Many factors in the selection of an expert were identified. First be aware that the knowledge of an expert is affected for his personal experiences, perspectives and goals. Then the conditions where the expert gains his knowledge can be gained at the industry or in the academic field. It is also important to consider the number of publications and public debates.

The elicitation part of the framework, are described as follows: The positioning phase allows the knowledge engineer to “explain the structure of the system” that need to be described. Then a description phase permits to know the set of inferences by the expert. We also know the set of variables and a range of variables used by them. The work generates a form to obtain the first description of the knowledge. The aim of discussion phase is to validate, validate and improve the description obtained. The results are compared and analyzed to clarify the differences in results from one expert to another.

3 Conceptual Frames

We propose a set of frames divided in: diseases, symptoms and risk factors. The frames are divided in three to have the possibility to ask an expert for each case

individually [4, 11]. The frame developed for eye diseases. We expose the proposal for the frames, the following are the proposal for the diseases.

3.1 Frames for Diseases

In table 1 it is shown the diseases for the different visual impairments, In the frame the synonyms are written for further explanation. In the image section. Human expert will provide information about how a patient visualized an image. For example, in diabetic retinopathy patients usually see a black hole in the center of their vision. Finally, in the risk factor play an important role. In order to relate other information, like the clinical history of the patient.

Table 1. Diseases.

Frame	Slot	Slot value
Diabetic retinopathy		
	Synonym	Diabetic eye disease
	Symptoms	Visual acuity, Blurred vision
	Images	Black hole in the center image
	Risk factors	Diabetes
	Inheritance	Yes, No
Macular degeneration		
	Synonym	Age-related macular degeneration
	Symptoms	Visual acuity, Blurred vision
	Image	Distorted vision, Missing of vision areas, shadows, Do not identify colors.
	Risk factors	Hypertension, age, atherosclerosis High cholesterol, obesity
	Inheritance	Yes, No
Retinitis pigmentosa		
	Synonym	Degenerative eye
	Symptoms	Visual acuity, Blurred vision
	Image	No central vision, Night blindness, Tunnel vision, Photophobia, Poor color separation, Slow adjustment to light, Head ache, Latticework vision.
Glaucoma		
	Symptoms	Visual acuity, Blurred vision
	Image analysis	Angle vision
	Risk factors	Hypertension
	Family History	Yes, No

3.2 Frames for Symptoms

The more common symptoms are discretized according to the level of importance. In table 2 it is shown some examples of them. In the case of the slot value for the frame visual acuity were classified from normal to no vision. Then we can see an example of the variables that the system will take into account, named as image analysis.

Table 2. Symptoms.

Frame	Slot	Slot value
Symptoms		
	Visual acuity	Over, Normal, Low, No vision
	Blurred vision	
Image analysis	Angle vision	Wide, central, reduced, none
	No central vision,	Yes, No
	Night blindness	Yes, No
	Tunnel vision	Yes, No
	Photophobia,	Yes, No
	Poor color separation,	Yes, No
	Slow adjustment to light	Yes, No
	Head ache	Yes, No
	Latticework vision.	Yes, No
	Distorted vision	Yes, No
	Missing of vision areas	Yes, No
	Do not identify colors	Yes, No
	shadows	Yes, No
	Black hole in the center image	Yes, No

3.3 Frames for risk factors

The frame risk factor has the intention to describe the elements that can affect directly or indirect the vision of a person. According with the specialist obesity and hypertension have a significant impact as an indirect factor. When you sum this factor can derive into a serial of important diseases. For example, high cholesterol combined with a hypertension can arise serious problems to a person. Especially if the person has 60 to 70 years old. Finally exert can decide which factor are more relevant in the analysis of vision. So the frames are deemed according their utility to the study of visual acuity. See table 3.

Table 3. Risk Factors.

Frames	Slot	Value
Risk factors		
	Hypertension	Yes, No
	Age	1,2,3
	Atherosclerosis	Yes, No
	High cholesterol	Yes, No
	Obesity	Yes, No
	Diabetes	Yes, No

4 Conclusions

According to expert we have found that the majority of the expert prefers divide visual impairment problems into three main categories: Diseases, Symptoms and Risk Factors. The elicitation process gives the necessity to ask further question in order to obtain more information about the diabetic problems since there so many factors related to the affection. Finally, the technology propose to the implementation is Python and Django framework.

References

1. Quintanar, T.: *Sistemas expertos y sus aplicaciones*. Universidad Autónoma de Hidalgo (2007)
2. Coppin, B.: *Artificial intelligence illuminated*. Jones & Bartlett Learning (2004)
3. Boden, M.: *Artificial Intelligence*. Academic Press (1996)
4. Liebowitz, J.: *The Handbook of Expert Systems*. Academic Press (1999)
5. World Health Organization.: *Ceguera y deficiencias ópticas en el mundo pueden prevenirse con un poco de visión*. Press Report (2006)
6. Jinwoo, S., Kasa-Vubu, J., DiPietro, M., Girard, A.: Expert system for automated bone age determination. *Expert System with Applications*, Elsevier, Vol. 50, pp. 75–88 (2016)
7. Vila-Frances, J.: Expert system for predicting unstable angina based on Bayesian networks. *Expert Systems with Applications*, Elsevier, Vol. 40, pp. 5004–5010 (2013)
8. Osuagwu, C., Okafor, E.: Framework for eliciting knowledge for a medical laboratory diagnostic expert system. *Expert Systems with Applications*, Elsevier, Vol. 37, pp. 5009–5016 (2010)
9. Quintana-Amate, S., Bermell-Garcia, P., Tiwari, A.: Transforming expertise into Knowledge-Based Engineering tools: A survey of knowledge sourcing in the context of engineering design. *Knowledge-Based Systems*, Elsevier, Vol.84, pp. 89–97 (2015)
10. Osuagwu, C., Okafor, E.: Framework for eliciting knowledge for a medical laboratory diagnostic expert system. *Expert Systems with Applications*, Elsevier, Vol. 36, pp. 2009–5016 (2010)
11. Quintanar, T.: *Sistemas Expertos y sus aplicaciones*. Universidad Autónoma de Hidalgo (2007)

Using Conceptual Frames to Define a Representation for a Medical Expert System that Evaluates ...

12. Coppin, B.: Artificial intelligence illuminated. Jones & Bartlett Learning (2004)
13. Boden, M.: Artificial Intelligence. Academic Press (1996)

An Elitism Based Genetic Algorithm for Welding Sequence Optimization to Reduce Deformation

Jesus Romero-Hdz¹, Sinai Aranda², Gengis Toledo-Ramirez¹, Jose Segura¹,
Baidya Saha³

¹ Centro de Ingeniería y Desarrollo Industrial (CIDESI), Mexico

² Universidad Tecnológica de Nayarit (UTN), Mexico

³ Centro de Investigación en Matemáticas (CIMAT), Mexico

{jaromero,gengis.toledo,jose.segura}@cidesi.edu.mx,
sinaivoz@gmail.com, baidya.saha@cimat.mx

Abstract. This paper reports the development and implementation of a Genetic Algorithm (GA) based on welding sequence optimization in which a structural deformation is computed as a fitness function. Moreover, a thermo-mechanical finite element analysis (FEA) was used to predict deformation. Elitism selection approach has been used to ensure that the three best individuals are copied over once into the next generation to expedite convergence by preserving qualified individuals having the potential of generating optimal solution. We exploited a sequential string searching algorithm into single point crossover method to avoid the repetition of single beads into the sequence. We utilized a bit string mutation algorithm by changing the direction of the welding from one bead chosen randomly from the sequence to avoid the repetition of the weld seams in the sequence. We computed the minimum number of iterations required for elitism GA based on the general Markov chain model of GA. Welding simulation experiments were conducted on a typical widely used mounting bracket which has eight seams using well-known software Simufact[®]. Simulation results were validated through a experiment and a fair amount of agreement was achieved in terms of deformation pattern. This algorithm allowed the reduction up to (~80%). Finally elitism-based GA effectively reduces the computational complexity over exhaustive search.

Keywords: Genetic algorithm, welding deformation, AI application, welding sequence, welding optimization.

1 Introduction

Welding is the most common metal joining process [7]. It is widely used in various industries such as automotive, shipbuilding, aerospace, construction, gas and oil trucking, nuclear, pressure vessels, heavy and earth-moving equipment [18,11]. Nevertheless, welding deformation plays a negative role in the process having high impacts in several ways, such as constraints in the design phase, reworks, quality cost and overall capital

expenditure. Welding sequence optimization significantly reduces welding deformation. The conventional approach is to select the best sequence by experience using a simplified design of experiments which often does not offer an optimal sequence [15]. Welding deformation can be numerically computed through finite element analysis (FEA) where thermo-mechanical models are commonly used. FEA offers reasonable solutions for various welding conditions and geometric configurations. However, under certain circumstances it can be computationally very expensive and time consuming.

The optimal welding sequence is only guaranteed using a full factorial design procedure. In this sense, the total number of welding configurations (N) are computed by $N = n^r \times r!$, where n and r are the number of welding directions and beads (seams) respectively. These possible configurations grows exponentially with the number of welding segments. For example, in this research we have used eight weld seams and two welding directions, hence the number of welding configurations for exhaustive search is 10,321,920. Considering a practical scenario, a complex weldment like an aero-engine assembly might have between 52 and 64 weld segments [12]. Therefore, full factorial design is often practically infeasible even using FEA.

In this paper, we implement a GA for welding sequence optimization. We make the following technical contributions. First, deformation based GA significantly reduces the computational complexity over extensive search. In the study case proposed in this paper, we achieved the optimal solution through GA after executing 72 welding configurations. In addition, this is the minimum number of iterations necessary to find the pseudo-optimal solution, which was found based on the general Markov chain model of GA. Second, we exploited a fitness function consisting of the inverse of the maximum structural deformation for welding sequence optimization. Third, we facilitated the convergence of the GA through the elitism selection approach in which we copied the three best individuals into the next generation and preserved the qualified individuals which possess high probability of providing an optimal solution. Fourth, we adjusted the single point crossover method for welding sequence optimization to avoid the repetition of single beads in the welding sequence by blending a sequential string searching algorithm into the single point crossover method. Finally, we implemented the bit string mutation algorithm by altering only the direction of welding instead of changing the bead itself to avoid seam repetition. One bead is selected randomly.

Gas Metal Arc Welding (GMAW) simulation experiments were conducted through the well-known simulation software Simufact Welding[®]. The average execution time for each welding configuration is 30 minutes using a workstation with two Intel[®] Xeon[®] @2.40 GHz, 48G GB of RAM and 4 GB of dedicated video memory. The study case in this paper is a mounting bracket which is widely used in telescopic jib [5] and automotive industries [21,10] among others. Simulation results were validated through real welding experiment. There exists a high agreement among the results of simulation and experiment in terms deformation pattern. Experimental results demonstrate that best welding sequence can reduce significant amount of structural deformation (~80%) over worst sequence.

The organization of the paper is as follows. Section 2 presents literature review. Section 3 discusses the thermal and mechanical analysis of finite element based welding simulation method. Proposed deformation based GA for welding sequence optimization

and its convergence analysis is presented in Section 4. Results are demonstrated in Section 5. Section 6 concludes this work. Relevant references are listed at the end of the paper.

2 Literature Review

Concerning the welding deformation problem this section overviews five relevant papers published in the last decade. Chapple *et al.* [4] have developed a GA approach for welding distortion optimization from two perspectives: (i) weld removal optimization and (ii) a combination of weld removal and welding sequence optimization. They proposed a fitness function in terms of total distortion in a critical region as shown in Equation 1. However, constraints on stress and stiffness were added in weld removal optimization to prevent removing many weld seams. A simplified FEA was used for fitness function evaluation:

$$F = \text{Min}(\text{Max}(D_i)) \text{ if } S_i > T, \quad (1)$$

$$i = 1, 2, 3 \dots N \quad i \in R_c,$$

where D_i is the total deformation for all nodes i in the critical region R_c , S_i is the stiffness of the structure and T is the minimum stiffness defined value. Total deformation is computed by the following equation:

$$D_i = \sqrt{d_{x_i}^2 + d_{y_i}^2 + d_{z_i}^2}, \quad (2)$$

where d_{x_i} , d_{y_i} , and d_{z_i} are the deformations of node i along x , y , and z axis respectively.

Islam *et al.* [11] have implemented GA in order to minimize the distortion in welded structures. They exploited a fitness function in terms of the maximum distortion on the overall structure. They have a conditional that includes a penalty term which is proportional to the number of nodes on the weld seam that have temperature less than melting value Equation 3. The penalty term determines upper and lower bounds for welding process parameters such as current, voltage and speed. They also defined six variables for possible welding direction. A thermo-mechanical FEA was carried out on a specimen as well as an automotive part. Experimental tryouts were done on a specimen using GMAW process:

$$F = \begin{cases} g & \text{IF } Q = 0 \\ g + M_1 & \text{IF } Q > 0 \end{cases}, \quad (3)$$

where

$$g = \text{Min}(\text{Max}(D_i)), \quad (4)$$

$$M_1 = 100Q. \quad (5)$$

D_i is the total deformation given by Equation 2, Q are the number of nodes in the weld seam that are below the melting point; M_1 is a penalty term that is proportional to Q .

Mohammed *et al.* [19] present an optimization procedure where GA and FEA minimize the welding induced distortion. The fitness function (Equation 6) used in their work is in terms of displacements along Z geometrical axis. This fitness function was developed for the simplified model of an aero-engine part where the distortion on Z axis dominates the other ones:

$$\begin{aligned} \text{Min } F &= \text{Max}(|(d_z)_i|), \\ i &= 1, 2, 3, \dots, N, \end{aligned} \quad (6)$$

where d_z is the deformation on z axis and N the total amount of nodes.

Liao [16] presents an implementation of GA for searching the optimal weld pattern in a spot welding process. The proposed fitness function is computed in two ways, first, in a deterministic mode which means the future states depend from the previous ones. Second, in a stochastic mode where the future states do not depend from the previous ones. FEA was used to compute the fitness function. The fitness function for the deterministic mode is shown in Equation 7:

$$\begin{aligned} F &= \sum_{i=1}^n w_{1i}(D_i)^2, \\ i &= 1, 2, 3, \dots, N, \end{aligned} \quad (7)$$

where w_{1i} is a weight factor that determines the importance of each node; D_i is the total deformation on all the nodes N . The fitness function for the stochastic mode is shown in equation 8:

$$\begin{aligned} F &= \sum_{i=1}^n w_{1i}(U_i)^2 + w_{2i}(V_i), \\ i &= 1, 2, 3, \dots, N, \end{aligned} \quad (8)$$

where w_{1i} and w_{2i} are weights, U_i is the average deformation on every single node and V_i is the variance of the deformation.

Xie and Hsieh [22] have implemented GA for finding a combined clamping and welding sequence. A multi-objective fitness function is taken into account to minimize cycle time (gun travel path) and assembly deformation as shown in Equation 9. FEA was used to evaluate the fitness function on automotive parts joined by spot welding process:

$$\begin{aligned} \text{Min } F &= w_1 \frac{D_i}{D_{0i}} + w_2 \frac{C}{C_0}, \\ i &= 1, 2, 3, \dots, N, \end{aligned} \quad (9)$$

where w_1 and w_2 are weights that define the importance of each sub-function; D_i is the total deformation on all nodes for the actual generation. D_{0i} is the total deformation on all nodes for the initial generation; C is the cycle time for the actual generation and C_0 is the cycle time for the initial generation. Notice that $\frac{D_i}{D_{0i}}$ and $\frac{C}{C_0}$ are considered as normalized functions because the units of deformation and cycle time are different.

3 Welding Simulation Framework

In order to present our approach we overview the welding simulation framework. This is important because the fitness function is computed using FEA.

3.1 Thermal Analysis

Weld process modeling (WPM) is quite complex task because of the physics of heat generation, specially for fusion processes like GMAW. The fundamental principle that defines the heat source is the law of conservation of energy [7]. Typically, the complexity of heat generation physics in the weld puddle is simplified by using a heat input model. The classical approach in Computational Welding Mechanics (CWM) is to ignore fluid flow and use a heat input model where heat distribution is prescribed. The given heat input replaces the details of the heat generation process and focus on larger scales. Moreover, the modeling of fluid flow and pertaining convective heat transfer may be integrated with a CWM model. The most common used model for fusion welding processes is the well-known Goldak double ellipsoidal heat distribution [7]. This heat input model combines two ellipsoidal heat sources to achieve the expected steeper temperature gradient in front of the heat source and a less steep gradient at the trailing edge of molten pool. This two heat sources are defined as follow:

Front heat distribution:

$$Q(x', y', z', t) = \frac{6\sqrt{3}f_f Q_w}{\pi\sqrt{\pi abc_f}} e^{\left(\frac{-3x'^2}{a^2}\right)} e^{\left(\frac{-3y'^2}{b^2}\right)} e^{\left(\frac{-3z'^2}{c_f^2}\right)}. \quad (10)$$

Rear heat distribution:

$$Q(x', y', z', t) = \frac{6\sqrt{3}f_r Q_w}{\pi\sqrt{\pi abc_r}} e^{\left(\frac{-3x'^2}{a^2}\right)} e^{\left(\frac{-3y'^2}{b^2}\right)} e^{\left(\frac{-3z'^2}{c_r^2}\right)}, \quad (11)$$

where f_f is the fraction factor of heat deposited in the front part, f_r is the fraction factor of heat deposited in the rear part. Those factors must satisfy the relation $f_f + f_r = 2$. a is the width, b is depth, c_f is the length of the front ellipsoid and c_r is the length of the rear ellipsoid Figure 1.

These parameters are physically related to the shape of the weld puddle. Width and depth are commonly taken from the cross section, the authors recommend to use a half of parameter a for the front fraction and two times a for the rear fraction. The heat available from the heat source is defined by:

$$Q_w = \eta IE, \quad (12)$$

where η is the heat source efficiency, I is the current (A), E is the voltage (V).

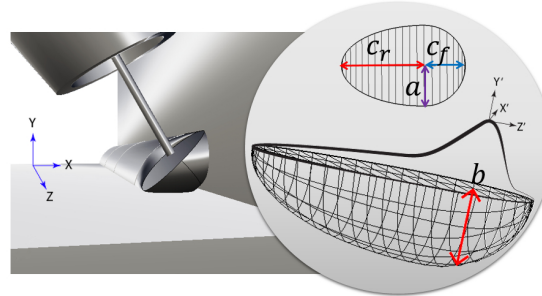


Fig. 1. Goldak double ellipsoidal model.

Thus the heat input model in CWM must be calibrated with respect to experiments. Therefore, the classical CWM models have some limitations in their predictive power to solve different engineering problems. For example, they cannot prescribe what penetration a given welding procedure will give. The appropriate procedure to determine the heat input model is therefore important in CWM [17].

FEA software solves this time dependent system of partial differential equations on a domain defined by the mesh used in FEA. The domain is dynamic because of it changes with each time step as filler metal is added to the weld pass. The initial condition is often assumed to be the ambient temperature, but the domain can be initialized to any initial temperature field. The heating effect of the arc is often modeled by a double ellipsoid power density distribution that approximates the weld pool as measured from macro-graphs of the cross-section of several weld passes. A convection boundary condition $q = h(T - T_{amb})$ with convection coefficient h and ambient temperature T_m usually is applied to external surfaces. The FEM formulation of the heat equation leads to a set of ordinary differential equations that are integrated in time using a backward Euler integration scheme.

3.2 Mechanical Analysis

The temperature history from the thermal analysis is used as a series of loads in the structural analysis. In this phase, the temperature history from the thermal cycle of each node is taken as an input and it is used as a node load with temperature dependent material properties. The mesh for the mechanical analysis was also used for the thermal analysis where each increment of weld deposition corresponded to one load step. The total strain ϵ^{total} (assuming negligible contribution from solid state phase transformation) can be decomposed into three components as follows: $\epsilon^{total} = \epsilon^e + \epsilon^p + \epsilon^{th}$, where ϵ^e , ϵ^p , and ϵ^{th} represent elastic, plastic and thermal strain respectively. In the welding process, changes in stress caused by deformation are assumed to travel slowly compared to the speed of sound. So, at any instant, an observed group of material particles is approximately in static equilibrium, i.e., inertial forces are neglected. In rate independent plasticity, viscosity is zero and viscous forces are zero. In either the Lagrangian or the Eulerian reference frame, the partial differential equation of equilibrium is, at any

moment given by the conservation of momentum equation that is mentioned below [6]:

Conservation of Momentum Equation

$$\begin{aligned} \nabla \sigma + f &= 0, \\ \sigma &= D\varepsilon, \\ \varepsilon &= (\nabla u + (\nabla u)^T + (\nabla u)^T \nabla u)/2, \end{aligned} \tag{13}$$

where $\nabla, \sigma, f, D, \varepsilon$ and u represent partial differential, Cauchy stress, total body force, temperature dependent material property (elastic matrix relevant to the modulus of elasticity and Poisson’s ratio), the Green-Lagrange strain and displacement vector respectively. ∇u represents the displacement gradient. The mechanical model is based on the solution of three partial differential equations of force equilibrium illustrated in Equation 13. In the FEM formulation, Equation 13 is transformed and integrated over the physical domain, or a reference domain with a unique mapping to the physical domain [7]. FEA software solves this partial differential equation for a viscothermo-elasto-plastic stress-strain relationship. The initial state often is assumed to be stress free. Dirichlet boundary conditions constrain the rigid body modes. The system is solved using a time marching scheme with time step lengths of approximately 0.1 second during welding and 5 second during cooling phase.

4 Welding sequence optimization framework

GA emulate natural selection of a set of individuals in order to search the best solution to a problem [8]. The genetic configuration of each individual is a possible solution. The algorithm starts with an initial population and those are submitted to an evolutionary process in such way that the best adapted individuals will continue to reproduce among them and over several generations the best adapted stands out. We tailor the GA for the welding sequence optimization: selection, cross-over and mutation to avoid the repetition of single bead.

4.1 String Representation of Welding Sequence

Being Q a welding application consisting of a set of welding beads and S a set of all possible sequences of Q , each sequence $s \in S$ represents a possible sequence which minimizes the overall structure deformation. Each sequence has N weld seams, here called genes $s = \{x^1, x^2, x^3, \dots, x^N\}$, these are a combination of real numbers $\forall n = 1, 2, 3, \dots, N$. In this approach every seam can be welded in two directions, so it can be represented by a positive sign $if \circlearrowleft$ or \uparrow or \leftarrow or with a negative sign $if \circlearrowright$ or \downarrow or \rightarrow .

4.2 Initialization of Welding Sequence

The algorithm starts with an initial population $P = \{s_j\}$, where elements of the set of sequences are called “individuals” $j = 1, 2, 3, \dots, J$. Their genes are generated randomly and special considerations are taken in order to avoid repeated seam in the same welding sequence.

4.3 Deformation Based Fitness Value

Within the scope of natural selection, the individual eligibility is regarded as the degree of adaptability. In this paper the fitness function (Equation 14) returns a real number (maximum deformation) $f(s_{j=1}^J) \Rightarrow \mathbb{R}$ that measures the adaptability of each sequence. Final deformation is computed by FEA:

$$f(s_j) = 1 / (\text{Max}(D_i) + \epsilon), \tag{14}$$

where D_i is the total deformation on all nodes defined by:

$$D_i = \sqrt{d_{x_i}^2 + d_{y_i}^2 + d_{z_i}^2}, \tag{15}$$

$$i = 1, 2, 3, \dots, N,$$

d_{x_i} , d_{y_i} , and d_{z_i} are deformations at the node i along x , y , and z axis respectively. ϵ is a very small number which was used to offer continuity to the fitness function when the value of the maximum deformation is zero.

4.4 Welding Sequence Selection Algorithm

Selection is an important sub-routine where individuals are chosen from the actual population for later procreation. Good selection algorithm expedites the convergence of the welding sequence. As a selection procedure, we first implemented a truncation procedure where the population is sorted by ascending fitness values, then a proportion μ of the individuals are taken based on fitness value. The proportion μ is computed by the fraction of the individual fitness value to the sum of the fitness values of all the samples as shown in Fig. 2.

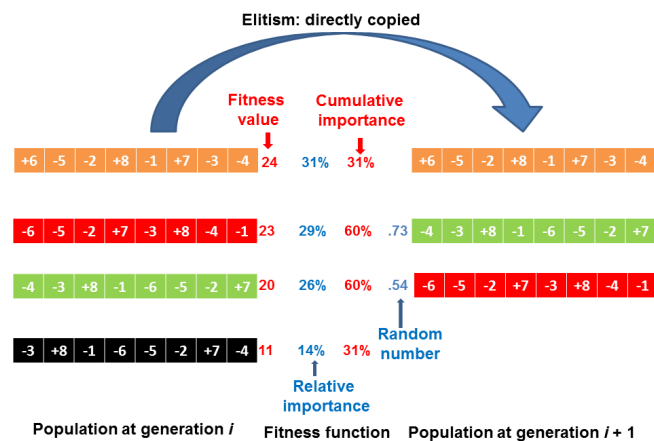


Fig. 2. Selection process using an elitism function.

4.5 Crossover for Generating New Welding Sequences

Crossover is analogous to reproduction, new individuals are created from the selected parents. Each couple of selected individuals s_1 and s_2 exchange their genes and make two new individuals, $s'_1 = s_1 \times s_2$ and $s'_2 = s_2 \times s_1$. Several methods for crossover are reported in literature such as arithmetic, heuristic, single or multi-point, uniform, cycle, partially mapped and order [13,9]. In this paper we implemented a single point crossover as demonstrated in Fig. 3 where a random number defines the cut point $a \in [1, N]$. Later, the descendants are defined by Equations 16 y 17 respectively:

$$s'_1 = \{[x_1^1, \dots, x_1^a], [x_2^{a+1}, \dots, x_2^N]\}, \quad (16)$$

$$s'_2 = \{[x_2^1, \dots, x_2^a], [x_1^{a+1}, \dots, x_1^N]\}. \quad (17)$$

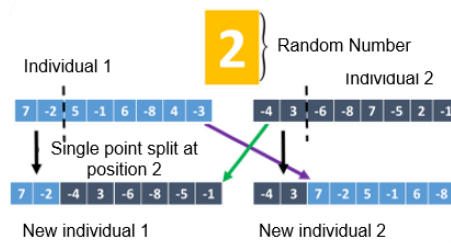


Fig. 3. Single point crossover process.

To avoid the repetition of the weld seam in the same welding sequence during crossover we implement a REPEATED STRING VALIDATION algorithm, the pseudo-code of which is illustrated below.

```

function REPEATED STRING VALIDATION
    random number  $a \in [1, N - 1]$ ;
     $s'_1 = \{x_1^1, \dots, x_1^a\}$ ;
     $s'_2 = \{x_2^{a+1}, \dots, x_2^N\}$ ;
    for  $i = 1 : N$  do
        if  $\Pi(\sqrt{s'_1} * s'_1) \neq \sqrt{s_2(i)' * s_2(i)'}$  then
             $s'_1 = \{[s'_1] \cup s_2(i)'\}$ ;
        end if
        if  $\Pi(\sqrt{s'_2} * s'_2) \neq \sqrt{s_1(i)' * s_1(i)'}$  then
             $s'_2 = \{[s'_2] \cup s_1(i)'\}$ ;
        end if
    end for
end function
    
```

4.6 Mutation for Generating New Welding Sequences

Mutation alters one or more genes in the individual from its actual configuration. It occurs during the evolution in a very low incidence according to a defined mutation

probability. Some of the operators found in literature are bit string, delta, invert and swap [20,1,14]. In our approach, we have used a bit string operator in order to change only the direction of welding, rather than the welding seam itself to avoid the repetition of the weld seam (Fig. 4).

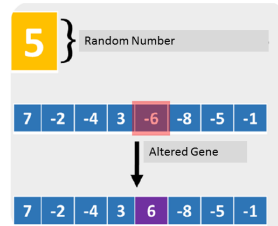


Fig. 4. Mutation using a bit string operator.

4.7 Elitism Based Welding Sequence Selection Algorithm

The *Elitism* function is a practical variant that ensures that the best individual in the current population $s_{best} \in P_t$ and current generation t is carry over to the next generation P_{t+1} (Fig. 2). Elitist based selection algorithm guarantees that the convergence obtained by the GA will follow monotone decreasing behavior over generations, $[s_{best} \in P_t] \rightarrow P_{t+1}$.

4.8 Pseudo-code and Flowchart of the Proposed Iterative GA for the Welding Sequence Optimization

This GA function is a repetitive process where the population is going to be changing over generations: $P_t = (s_1(t), s_2(t), \dots, s_J(t)) \in S$. The pseudo-code for the proposed GA based welding sequence optimization is given below.

function GA(*Min D* : *Q*)

Input: $P_0 = (s_1(t), s_2(t), \dots, s_J(t)) \in S$

Output: s_{best} , the best sequence that shows minimum deformation.

$t \leftarrow 0$;

initialize $P_t \in S$;

evaluate $f\left(s_{j=1}^J\right)$;

while !terminating condition **do**

$t++$;

Select P_t from P_{t-1} based on the relative importance of the value of the individual fitness function $f(s_j)$; /* Priority given to the welding sequences based on less deformation */

crossover $P_t \leftarrow P_t$; /* String searching based single point crossover */

```

mutation  $P_t \leftarrow P_t$ ; /* Change the direction of the welding of one seam */
evaluate  $f(s_{j=1}^J)$ ;
elitism  $P_t \leftarrow s_{best}$  from  $P_t$ ; /* Elitism based selection approach */
end while
return  $s_{best}$  from  $P_t$ .
end function
    
```

In Figure 5 we present a flowchart where we describe at detail our GA based welding sequence optimization approach.

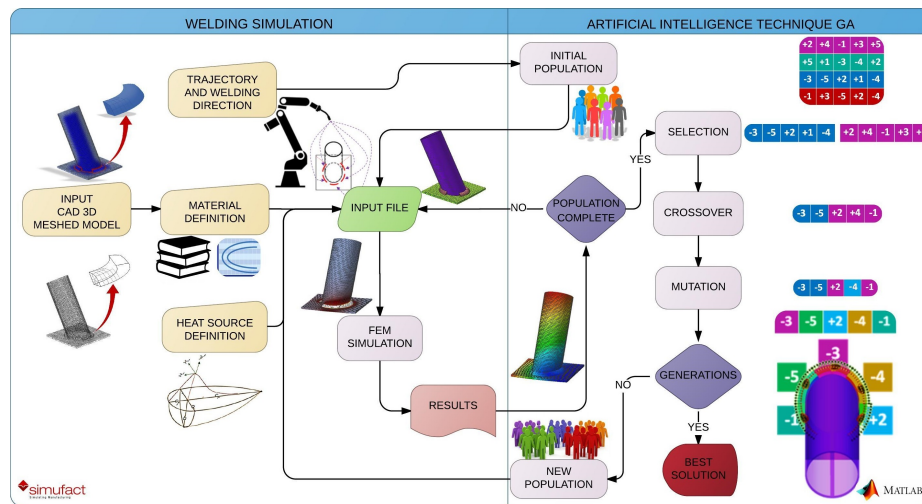


Fig. 5. GA based welding sequence optimization approach.

4.9 Convergence Analysis of the GA

For a general Markov chain model of GA with elitism, an upper bound for the number of iterations t is required to generate a population S^+ consisting of minimal solutions has been generated with probability $\alpha \in (0, 1)$ [2,3], is given by

$$t \geq \left\lceil \frac{\ln(1 - \alpha)}{n \ln(1 - \min\{\mu^l, (1 - \mu)^l\})} \right\rceil, \quad (18)$$

where l is the length of the chains that represent the individual, n is the population size and $\mu \in (0, 1)$ is the mutation rate. $\lceil x \rceil$ is the smallest integer greater than or equal to x . Equation 18 reaches to minimum when $\mu = 0.5$. For faster convergence, in our experiment we chose the value of $\mu = 0.5$ since the thermo-mechanical finite element analysis based welding simulation model is computationally very expensive.

5 Experimental Results

The organization of this section is as follows. First we introduce the study case. Second, we list the parameters used for this study. Third, we present convergence analysis of proposed GA. Fourth, we describe the effects of welding sequence on welding process optimization. Fifth, we show experimental validation of the simulation results. And finally, we show a comparative study: Simulation vs real experiment.

5.1 Study Case

We chose a study case of welding a mounting bracket shown in Fig. 6 and 7 which is typically used in telescopic jib [5], automotive industries [21], and cars [10]. We conducted a simulation experiment of GMAW process using popular FEA software. [11]. We implemented a GA algorithm for choosing the best welding sequence having minimum deformation and we demonstrated the effects of welding sequence on the weld quality (structural deformation) by analyzing the structural deformation caused by welding of the four sequences (the best two and worst two found by GA). We used the same parameters for all the sequences (Table 1). We divided the welding bead into eight segments as shown in Fig. 7. In Fig. 6 we show geometries of different mounting brackets that can be found frequently in heavy equipment, vehicles, ships. Fig. 7 illustrates the engineering drawing with all specifications of the mounting bracket used in this experiment.



Fig. 6. Different mounting brackets available in the market as an example of welded parts.

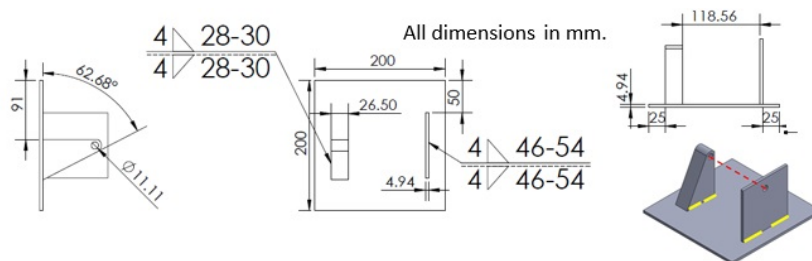


Fig. 7. Engineering drawing of the study case with 8 seams.

5.2 Parameters Used for this Study

Table 1 shows the GA parameters used in the simulation experiment. We considered 12 generations to converge the GA algorithm, initial population size as 6, crossover probability as 50%. We copy the three best candidates of the current generation to the next generation using elitism selection mechanism. We implemented single point crossover method for new sample reproduction. We also implemented single bit string mutation operator and changed the welding direction of a randomly selected welding seam instead of welding seam itself to avoid the repetition of the welding seam in the sequence.

Table 1. GA parameters for welding sequence optimization.

Parameter	Value
Initial population size	6
Generations	12
Elitism candidates	3
Crossover %	50%
Mutation operator	bit string
Crossover operator	single point
Qty of seams	8
Possible welding directions	2

We have validated the result of the simulation experiment. Since conducting the real welding experiment is costly, we have conducted the real experiment for only the best sequence found by the GA. Fig. 8 illustrates the flowchart of the real experiment.

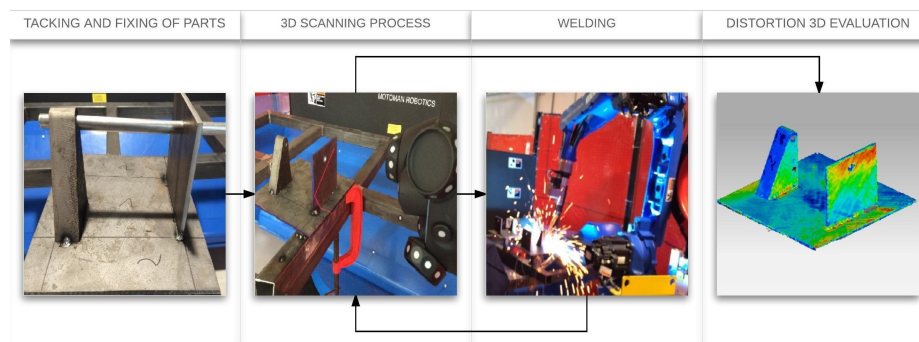


Fig. 8. Flowchart of the real experiment.

5.3 FEA Results and Convergence Analysis of the Proposed GA

The best, second best, worst and second worst sequences are $(+6, +5, -1, +8, -2, -3, +4, -7)$, $(+6, +5, -1, -8, -2, -3, +4, +7)$, $(-3, +4, -7, +6, +5, -1, +8, -2)$ and $(-3, +4, -7, +6, +5$

, -1, -8, -2) respectively (Fig. 9). Their maximum structural deformation values are 0.55mm., 0.57mm., 2.43mm., and 2.42mm. respectively (Fig. 10). We carried out the GA experiment for twelve generations and we conducted the convergence analysis that is shown in Fig. 11. Fig. 11(a) shows the behavior of the individual in terms of deformation over generations for four sequences (best, second best, worst and second worst). Elitism based selection method expedites the convergence of the GA. Fig. 11(b) shows the monotonically decreasing values of the deformation over twelve generations.

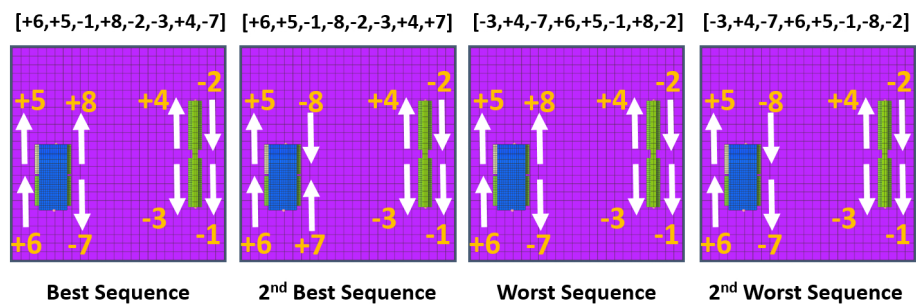


Fig. 9. Best, second best, worst and second worst sequences configuration.

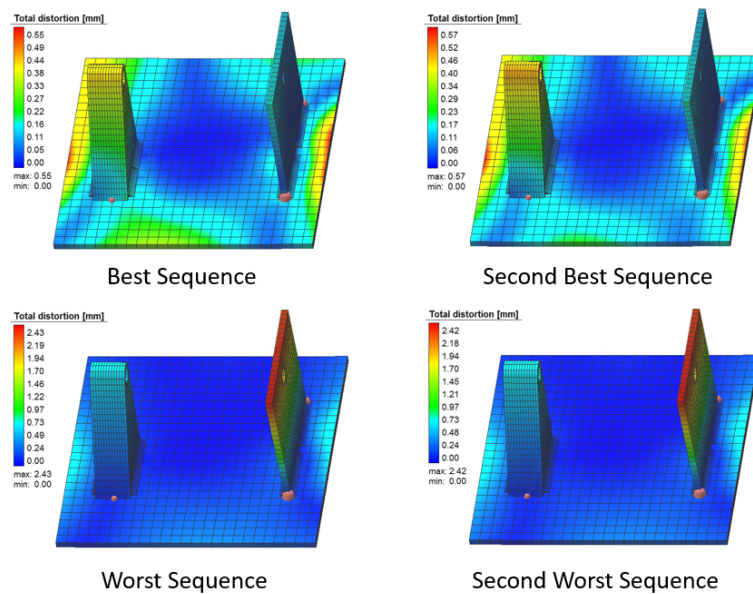
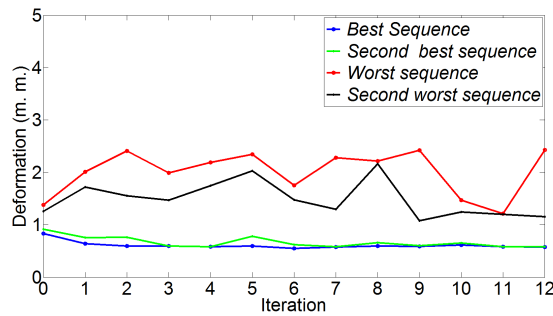
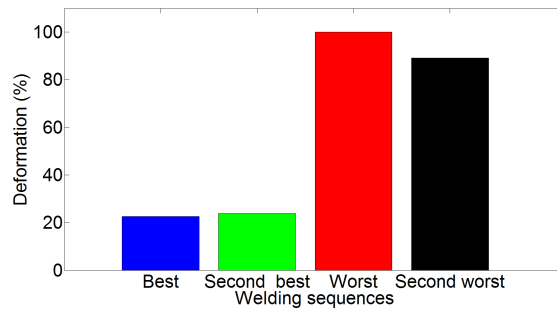


Fig. 10. Deformation pattern of best, second best, worst and second worst sequences.

To compute the minimum number of iterations necessary to ensure finding an optimal solution for GA with a prescribed probability $\alpha = 0.96$, mutation rate $\mu = 0.5$, number of bits required to represent an individual $l = 8$, number of individual $n = 72$ in equation 18, we get $t \geq \lceil 11.42 \rceil = 12$. We conduct the GA up to twelve iterations since the computational complexity of the finite element based thermo-mechanical welding simulation approach is computationally very expensive.



(a) Deformation over generations



(b) Deformation Reduction

Fig. 11. Convergence analysis of proposed GA.

5.4 Effects of Welding Sequence on Welding Process Optimization

Normalized frequency of the deformation and effective stress values are shown in Fig. 12(a) and 12(b). Fig. 11(b) shows the deformation values of the four sequences in terms of the percentage. If we consider the deformation value of the worst sequence (red color bar in Fig. 11(b)) as 100%. Fig. 11(b) shows that best sequence (blue color bar) achieves $\sim 80\%$ maximum structural deformation over worst sequence (red color bar). Fig. 11(b) also demonstrates that both best and second best sequences obtains substantial reduction of maximum structural deformation over worst and second worst sequences (red and black bars are much taller than blue and green bars). These results clearly demonstrates that welding sequence has significant effect on welding deformation.

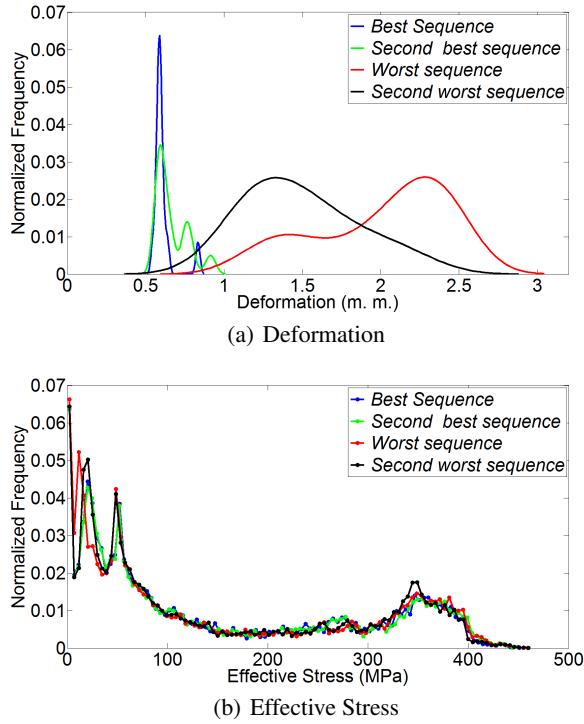


Fig. 12. Normal distribution of both experimental and simulation fitness values.

5.5 Experimental Validation of the Simulation Results

Thermal analysis was validated using thermocouples. In Figure. 13 we show the temperature curve acquired in one seam. It can be seen in the curve two peaks, the first one is the heat transferred from the other side of the plate over the time when the seam located there is being welded. On the other hand, the second peak is the temperature when the heat source reaches the thermocouple. It is observed that there is a good agreement between acquired temperatures of the welding simulation and thermocouples used in real experiment. Fig. 14 shows a three dimensional (3D) comparison between

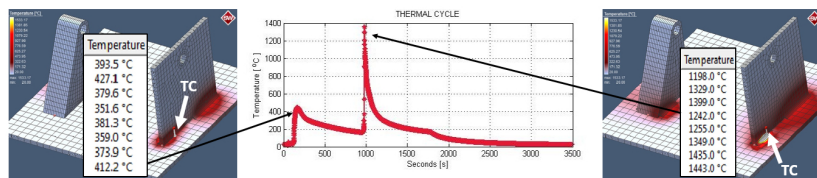


Fig. 13. Temperature acquired with thermocouples.

the structural deformation found in the real and simulation experiment for the best sequence (+6, +5, -1, +8, -2, -3, +4, -7). For 3D visualization of real experiment, we used Geomagic Control[®] software with a Creaform[®] optical scanner and for simulation experiment, we used simufact[®] FEA software [11]. Fig. 14 demonstrates a good agreement between the structural deformation found in real and simulation experiment.

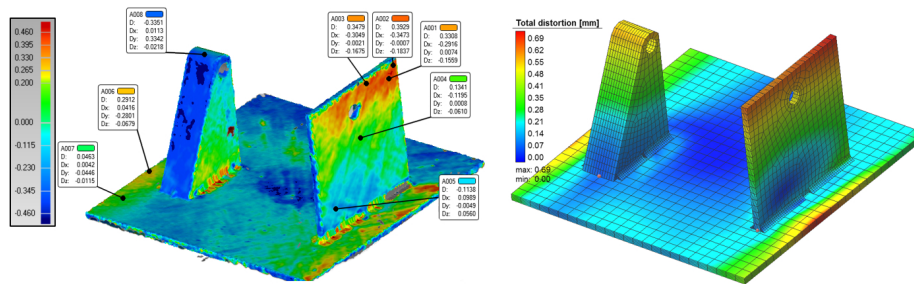


Fig. 14. Structural deformation comparison between real and simulated experiments.

5.6 Comparative Study: Simulation vs Real Experiment

Deformation values found in the experiment are below the predicted values found in the welding simulation. The difference between them is the cumulative error in the measurement process. 3D scanner has 0.085 mm. of error, welding positioner has 0.1 mm of error and typically welding simulation is around 20% error (0.13 mm in this case). Lindgren [17] and Islam [11] showed that the main driving force in the welding simulation is heat generation process. If the simulation can predict the weld pool boundary correctly then the temperature field outside the region will also be correct. Therefore, the heat source model of the welding simulation was validated with respect to the weld macroetch test as shown in Fig. 15 and a fairly good agreement was achieved in terms of weld pool boundary shape and size. The red and yellow line illustrates the weld pool boundary of real and simulation experiment respectively.

6 Conclusion and Future Work

Structural deformation is an important parameter to measure the quality of the welded structures. Welding sequence plays an important role on welding deformation. In this paper, the inverse of the maximum structural deformation was exploited as the fitness function of a proposed GA algorithm for welding sequence optimization. GA was used to reduce significantly the search space of the exhaustive search. A finite element based thermo-mechanical analysis was used to compute the deformation. An elitism selection approach was implemented by copying the three best individuals into the

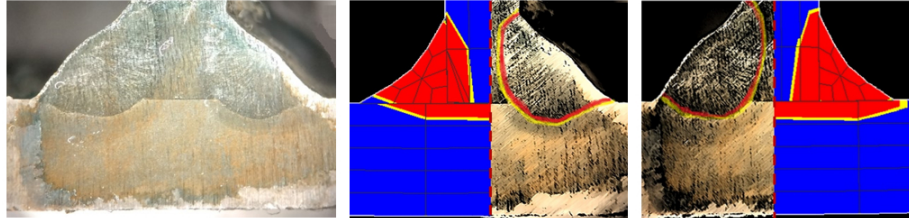


Fig. 15. Macroetch test and a comparison between real and simulation experiment.

next generation to expedite the convergence as well as not allowing to destroy the chromosomes which have high probability to offer optimal solution. We implemented a sequential string searching algorithm for a single point crossover method to avoid the repetition of single beads. We changed the welding direction of the bead, rather than the welding bead itself from the sequence into one bit string mutation algorithm to avoid the repetition of the weld seam. We conducted a simulation experiment on a mounting bracket which were widely used in vehicles and other applications. A experiment was conducted on eight weld seams. Results of simulations were validated through a real experiment by comparing the temperature recorded by thermocouples kept on different weld seams with the temperature computed by the thermo-mechanical FEA as well as comparing the structural deformation of real and simulation experiment. A reasonable agreement was achieved among the results of simulation and real experiment in terms of the temperature profile curve and the shape and size of the weld pool boundary. Elitism based GA algorithm discussed in this paper effectively reduces the computational complexity over extensive search with significant reduction of overall structure deformation. We computed and executed minimum number of iterations necessary for finding the optimal solution of the GA based on the general Markov chain model of GA.

The proposed research opens up different avenues for welding sequence optimization research. In the near future, we would like to develop a multi-objective GA to incorporate residual stress, temperature, robot time and robot path for welding sequence optimization. Information of the deformation after welding each seam in a sequence needs to be investigated for achieving better reduction of welding deformation.

Acknowledgments. The authors gratefully acknowledge the support provided by CONACYT (The National Council of Science and Technology) and CIDESI (Center for Engineering and Industrial Development) as well as their personnel that helped to realized this work.

References

1. Alexandrescu, A., Agavriloaei, I.: Determining the best mutation probabilities of a genetic algorithm for mapping tasks. *The Bulletin of The Polytechnic Institute from Iași LVII (LXI)(Lxi)*, 10 (2011)

2. Aytug, H., J., K.G.: Stopping criteria for finite length genetic algorithms. *INFORMS Journal on Computing* 8(2), 183–191 (1996)
3. Aytug, H., J., K.G.: New stopping criterion for genetic algorithms. *European Journal of Operational Research* 126(3), 662–674 (2000), <http://www.sciencedirect.com/science/article/pii/S0377221799003215>
4. Chapple, A., Tahir, Z., Jardine, F.: Weld Distortion Optimisation using HyperStudy. In: *The 8th UK Altair Technology Conference*. pp. 1–13 (2013)
5. Derlukiewicz, D., Przybyek, G.: Chosen aspects of FEM strength analysis of telescopic jib mounted on mobile platform. *Automation in Construction* 17(3), 278–283 (2008), <http://www.sciencedirect.com/science/article/pii/S0926580507000714>
6. Goldak, J.: PVP2010-25770 Challenges in verification of cwm software to compute residual pp. 1–9 (2010)
7. Goldak, J.A., Akhlaghi, M.: *Computational welding mechanics*. Springer (2005), <http://www.worldcat.org/isbn/9780387232874>
8. Goldberg, D.E.: *Genetic Algorithms in Search, Optimization and Machine Learning*. Addison-Wesley Longman Publishing Co., Inc., Boston, MA, USA, 1st edn. (1989)
9. Hasançebi, O., Erbatur, F.: Evaluation of crossover techniques in genetic algorithm based optimum structural design. *Computers & Structures* 78(13), 435–448 (2000), <http://www.sciencedirect.com/science/article/pii/S0045794900000894>
10. Hussain, M.: Study of the dynamic behavior of a car body for mounting the rear axle 25, 782 (2016), <http://link.springer.com/10.1007/978-3-319-27276-4>
11. Islam, M., Buijk, A., Rais-Rohani, M., Motoyama, K.: Simulation-based numerical optimization of arc welding process for reduced distortion in welded structures. *Finite Elements in Analysis and Design* 84, 54–64 (jul 2014), <http://linkinghub.elsevier.com/retrieve/pii/S0168874X14000201>
12. Jackson, K., Darlington, R.: Advanced engineering methods for assessing welding distortion in aero-engine assemblies. *IOP Conference Series: Materials Science and Engineering* 26, 012018 (2011)
13. Kaya, Y., Uyar, M., Tekin, R.: A novel crossover operator for genetic algorithms: Ring crossover. *CoRR abs/1105.0355* (2011), <http://dblp.uni-trier.de/db/journals/corr/corr1105.html#abs-1105-0355>
14. Koenig, A.: A Study of Mutation Methods for Evolutionary Algorithms. CS 447 - Advanced Topics in Artificial Intelligence pp. 1–8 (2002), <http://web.mst.edu/~tauritzd/courses/ec/fs2002/project/Koenig.pdf>
15. Kumar, D.A., Biswas, P., Mandal, N.R., Mahapatra, M.M.: A study on the effect of welding sequence in fabrication of large stiffened plate panels. *Journal of Marine Science and Application* 10(4), 429–436 (2011)
16. Liao, Y.G.: Optimal design of weld pattern in sheet metal assembly based on a genetic algorithm. *International Journal of Advanced Manufacturing Technology* 26(5-6), 512–516 (2005)
17. Lindgren, L.E.: Computational welding mechanics. In: Lindgren, L.E. (ed.) *Computational Welding Mechanics*, pp. 31–46. Woodhead Publishing Series in Welding and Other Joining Technologies, Woodhead Publishing (2007), <http://www.sciencedirect.com/science/article/pii/B9781845692216500045>
18. Masubuchi, K.: *Analysis of Welded Structures*, vol. 3. Pergamon Press Ltd. (1980)
19. Mohammed, M.B., Sun, W., Hyde, T.H.: Welding sequence optimization of plasma arc for welded thin structures. In: *WIT Transactions on The Built Environment*. vol. 125, pp. 231–242 (2012), <http://library.witpress.com/viewpaper.asp?pcode=OP12-020-1>
20. Soni, N., Kumar, T.: Study of Various Mutation Operators in Genetic Algorithms. *International Journal of Computer Science and Information Technologies* 5, 4519–4521 (2014)

Jesus Romero-Hdz, Sinai Aranda, Gengis Toledo-Ramirez, Jose Segura, Baidya Saha

21. Subbiah, S., Singh, O., Mohan, S.K., Jeyaraj, A.P.: Effect of muffler mounting bracket designs on durability. *Engineering Failure Analysis* 18(3), 1094–1107 (2011)
22. Xie, L.S., Hsieh, C.: Clamping and welding sequence optimization for minimizing cycle time and assembly deformation. *International Journal of Materials & Product Technology* 17(5/6), 389–399 (2002)

Finding Events in Background EEG in Rats in Early Posttraumatic Period

Ivan A. Kershner¹, Yuri V. Obukhov¹, Ilya G. Komoltsev²

¹ Kotel'nikov Institute of Radio Engineering and Electronics of RAS,
Moscow, Russia

² Institute of Higher Nervous Activity and Neurophysiology of RAS,
Moscow, Russia

Abstract. Processing of a big experimental data is a problem in neurophysiologic researches. Epileptiform discharges (ED) detection in long EEG-records requires an algorithm for recognition of ED and sleep spindles (SS). Electroencephalogram recordings were performed in rats using implanted electrodes before and after traumatic brain injury (TBI). Intervals about 10 second with typical ED and typical SS have been manually selected from these records by experts. The algorithm for the allocation of events from background activity was developed. Parameters founded by the algorithm can serve as criteria for the recognition of ED and SS events.

Keywords: EEG, rats, event detection.

1 Introduction

Posttraumatic epilepsy (PE) is a serious medical and social problem. It develops in 2–17% of patients after traumatic brain injury (TBI) [1]. It takes years for a posttraumatic epileptogenesis to develop and its mechanisms are poorly understood. At the same time, prediction of PE in clinical practice is the unsolved problem [9]. Animal models [11,6] are widely used to study neurobiological mechanisms of epileptogenesis to detect biomarkers for PE development and to find new targets for drugs to prevent PE.

PE induced by lateral fluid percussion (LFP). Head trauma reproduces clinical signs and, most likely, pathogenesis of PE [10]. Silent period of epileptogenesis from TBI to first unprovoked seizure in rats takes weeks. Many groups using this model are focused on delayed consequences appearing weeks and months after TBI [3]. However, appearance of early epileptiform discharges (ED) on electroencephalograms (EEG) and its dynamics are possible biomarkers of PE development [4].

So, it has been suggested that the appearance and dynamics of development of ED in early posttraumatic period can predict the development of PE. To verify this hypothesis a detailed analysis of long EEG-records is needed. Total duration of EEG-records from one experimental group, which consists of 12 experimental

and 12 sham-operated animals with 2 weeks EEG length per animal, is one year and it is not the limit. Therefore, automatic detection of ED is essential for processing big data and we focused on this problem.

TBI was modeled on Wistar rats using lateral fluid percussion of 3 atm. [7]. To detect ED four stainless steel epidural electrodes were implanted. One week prior to and one week after TBI the video-electrocorticograms were recorded.

2 Method of Detection

Long EEG-records include all phases of wake-sleep cycle of the animals. Sleep spindles (SS) are a normal physiological EEG-pattern of sleep. One sign of ED is the increase of amplitude, which is also present in SS that make difficult to automatically recognize ED. Figure 1 shows example of ED and of SS, respectively, on the day following TBI.

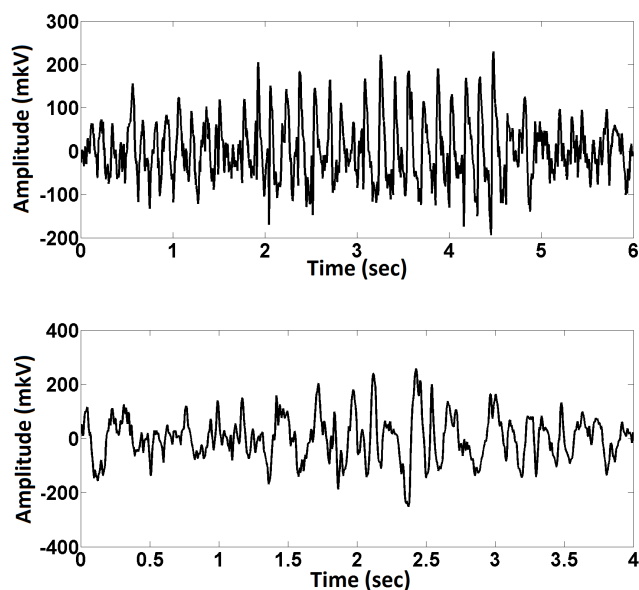


Fig. 1. Upper plot: epileptic discharge; lower plot: sleep spindles.

Algorithm of finding ED has to recognize SS and separate it from ED to avoid wrong positives results. To solve this problem, fragments of the EEG lasting from 3 to 10 seconds was allocated from daily record by neurophysiologists. They contain ED or SS. 36 SS and 39 ED were selected to be compared.

All fragments were processed by the 8th order bandpass Butterworth filter 2–124 Hz and a set of notch filters were applied for removing a power line noise

at 50 and 100 Hz from signals recorded with a sampling rate 250 Hz. After that, the complex Morlet wavelet was used [5]:

$$S_x = |W(\tau, f)|^2, \quad (1)$$

$$W(\tau, f) = \frac{1}{f} \int x(t) \psi * \left(\frac{t - \tau}{f}\right), \quad (2)$$

$$\psi(\eta) = \frac{1}{\sqrt{\pi F_b}} e^{2\pi i F_c \eta} e^{-\frac{\eta^2}{F_b}}. \quad (3)$$

The equation (1) describes the power spectral density (PSD). The wavelet transform (2) is based on the Morlet wavelet (3). The coefficients F_b and F_c equal to 1.

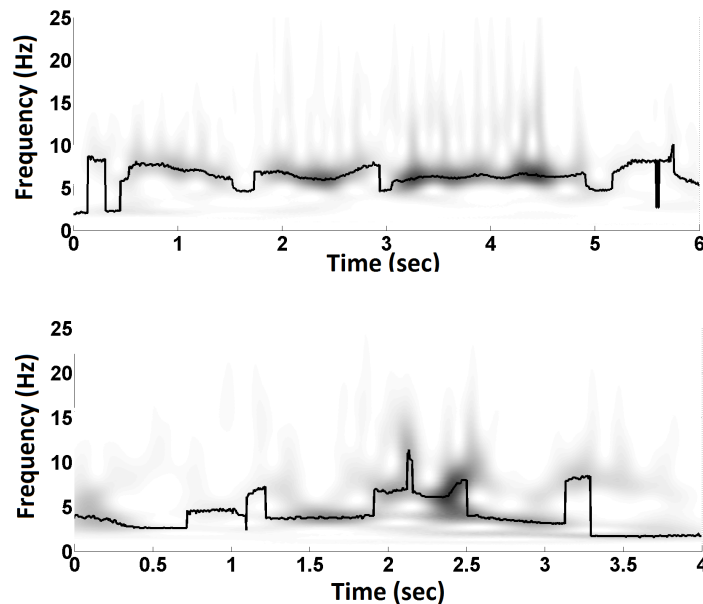


Fig. 2. Ridges (bold lines) of the wavelet spectrograms of epileptic discharge (upper plot) and sleep spindles (lower plot).

Previously the time-frequency segmentation (detection) method of the SS was studied in [8]. In [2] the time-frequency properties of the spike-wave discharges in absence epilepsy with wavelet spectrograms ridges analysis were studied. Start positions of these discharges were selected manually. An approach to automatic detection of SS and ED in PE, based on the analysis of the ridges of the wavelet spectrograms, was developed. Each point of the ridge is the maximum value of

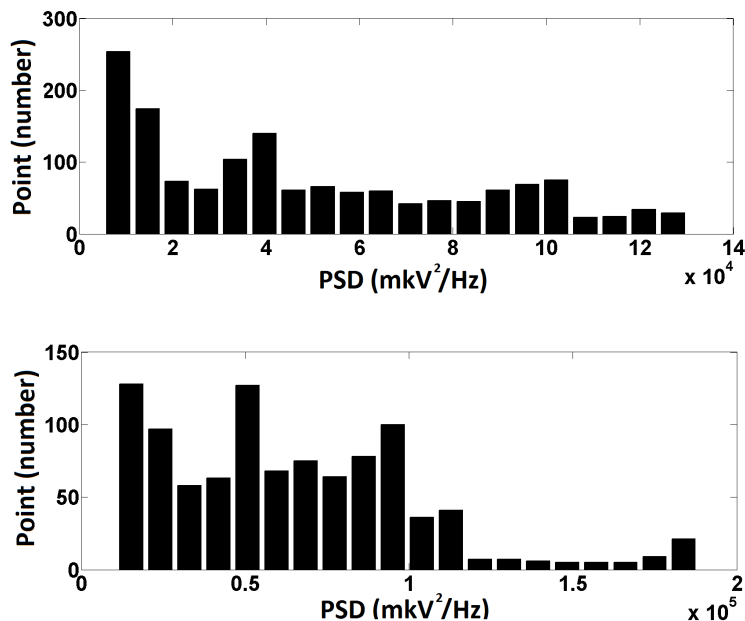


Fig. 3. PSD histograms for the epileptic discharge (upper plot) and sleep spindles (lower plot).

power spectral density in this time point. Examples of wavelet spectrograms and their ridges for ED and SS are shown in figure 2.

SS and ED are characterized by a higher value of the power spectral density in comparison with the background. For the segmentation of SS and ED from background activity, it is advised to analyze histogram of power spectral density at the points of ridge (figure 3).

The histograms have a sharp decline in the region of small values of the power spectral density (with $2 * 10^4$ in the left graph and $0.4 * 10^5$ in the right graph). Therefore, these values of power spectral density can be selected as an adaptive threshold for segmentation of the ED and SS. Areas of the ridge of ED and of SS where the spectral power density is above the PSD threshold value were selected (figure 4).

The following parameters were calculated in selected fragments: frequency range, duration, and the maximum value of power spectral density. These data can be used to classify SS and ED on long EEG-records.

3 Conclusion

The following results were obtained:

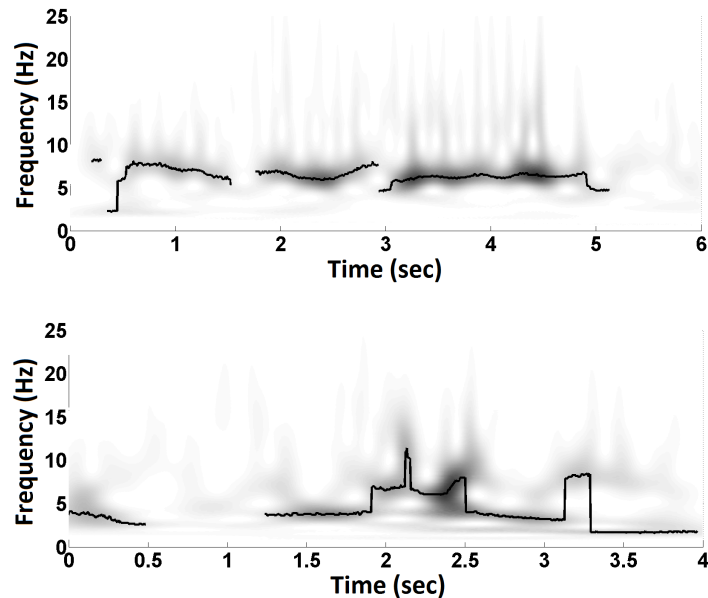


Fig. 4. Wavelet spectrogram with the segmented ridges of epileptiform discharges (upper plot) and sleep spindles (lower plot).

- The algorithm for detection of ED and SS on the background activity was developed.
- 36 EEG records with SS and 39 EEG records with ED were processed using this algorithm.
- Ridge parameters of the processed EEG records were calculated.

Results of this research will help to detect and to separate ED and SS from background activity on long EEG records.

Acknowledgments. This research was done at the expense of the grant of the Russian Scientific Fund (project 16-11-10258)

References

1. Annegers, J., Hauser, W.A., Coan, S., Rocca, W.: A population-based study of seizures after traumatic brain injuries. *NEJM* 338, 20–24 (1998)
2. Bosnyakova, D., Obukhov, Y.: Extraction of dominant feature in biomedical signals. *Pattern Recognition and Image Analysis* 15(3), 513–515 (2005)
3. D’Ambrosio, R., Fender, J., Fairbanks, J., Simon, E., Born, D., Doyle, D., Miller, J.: Progression from frontal-parietal to mesial-temporal epilepsy after fluid percussion injury in the rat. *Brain* 128(1), 174–188 (2004)

4. D'Ambrosio, R., Hakimian, S., Stewart, T., Verley, D., Fender, J., Eastman, C., Sheerin, A., Gupta, P., Diaz-Arrastia, R., Ojemann, J., Miller, J.: Functional definition of seizure provides new insight into post-traumatic epileptogenesis. *Brain* 132(10), 2805–2821 (2009)
5. Goupilland, P., Grossman, A., Morlet, J.: Cycle-octave and related transforms in seismic signal analysis. *Geoexploration* 23(1), 85–102 (1984)
6. I.Kharatishvili, Pitkanen, A.: Association of the severity of cortical damage with the occurrence of spontaneous seizures and hyperexcitability in an animal model of posttraumatic epilepsy. *Epilepsy Research* 90(1-2), 47–59 (2010)
7. Kabadi, S., Hilton, G., Stoica, B., Zapple, D., Faden, A.: Fluid-percussion-induced traumatic brain injury model in rats. *Nature Protocols* 5(9), 1552–1563 (2010)
8. Parekh, A., Selesnick, I., Rapoport, D., Ayappa, I.: Sleep spindle detection using time-frequency sparsity. In: *IEEE Signal Processing in Medicine and Biology Symposium (SPMB)*, 2014 IEEE. pp. 1–6. IEEE, Philadelphia, PA: IEEE. (Dec 2014)
9. Pitkanen, A., Engel, J.: Past and present definitions of epileptogenesis and its biomarkers. *Neurotherapeutics* 11(2), 231–241 (2014)
10. Pitkanen, A., Immonen, R., Grohn, O., Kharatishvili, I.: From traumatic brain injury to posttraumatic epilepsy: what animal models tell us about the process and treatment options. *Epilepsia* 50(2), 21–29 (2009)
11. Pitkanen, A., Kharatishvili, I., Karhunen, H., Lukasiuk, K., Immonen, R., Nairismagi, J., Grohn, O., Nissinen, J.: Epileptogenesis in experimental models. *Epilepsia* 48(2), 13–20 (2007)

Exploring Dynamic Environments Using Stochastic Search Strategies

C. A. Piña-García¹, Dongbing Gu², Carlos Gershenson¹,
J. Mario Siqueiros-García¹, E. Robles-Belmont¹

¹ Universidad Nacional Autónoma de México,
Instituto de Investigaciones en Matemáticas Aplicadas y en Sistemas, México, D.F.,
Mexico

² University of Essex, School of Computer Science and Electronic Engineering,
Colchester, UK

carlos.pgarcia@iimas.unam.mx

Abstract. In this paper, we conduct a literature review of laws of motion based on stochastic search strategies which are mainly focused on exploring highly dynamic environments. In this regard, stochastic search strategies represent an interesting alternative to cope with uncertainty and reduced perceptual capabilities. This study aims to present an introductory overview of research in terms of directional rules and searching methods mainly based on bio-inspired approaches. This study critically examines the role of animal searching behavior applied to random walk models using stochastic rules and *kinesis* or *taxis*. The aim of this study is to examine existing techniques and to select relevant work on random walks and analyze their actual contributions. In this regard, we cover a wide range of displacement events with an orientation mechanism given by a reactive behavior or a source-seeking behavior. Finally, we conclude with a discussion concerning the usefulness of using optimal foraging strategies as a reliable methodology.

Keywords: Search strategies, random walks.

1 Introduction

Stochastic search strategies plays an important role in terms of facing environmental uncertainty. Therefore, the present paper pretends to uncover the most insightful directional rules inspired by stochastic methods, statistical physics and random walks. Likewise, we consider these strategies as an emergent phenomenon (formation of global patterns from solely local interactions) which is a frequent and fascinating theme in the scientific literature both popular and academic [10].

The aim of this paper is to examine existing techniques and do a comprehensive analysis to understand state-of-the-art, trends and research gaps. It is important to mention that these strategies can be used in the field of robotics

as exploration and discovery algorithms with the aim to speeding up searching tasks.

Stochastic search strategies are mainly inspired by optimal foraging theory which involves animal search behavior as an alternative for facing highly dynamic environments. Thus, these strategies can be viewed as a correlated process which may consists of displacements only broken by successive reorientation events. Strategies such as: Lévy walk, ballistic motion and correlated random walk are well known examples of foraging strategies, which are subject to statistical properties derived from Lévy stochastic processes [4,25].

A considerable amount of literature has been published on stochastic search strategies. These studies have been most extensively applied in the field of biology, particularly, in movement ecology [16]. However, an expressed interest has been shown by robotics researchers for adopting or mimicking specific behaviors belonging to optimal foraging theory [25].

Recent evidence suggests that search strategies are mainly related to availability, quality and quantity of publicly accessible data on animal movement and Artificial Intelligence techniques. Recently, synthetic experiments have shown that what really matters is where the explorer diffuses, not the manner by which the explorer gets there [25]. We therefore, decided to concentrate on what we considered to be some of the more significant developments in stochastic search models. It is important to mention that for organization purposes, we have split in two categories as follows: stochastic rules and directional rules (*taxes*).

2 Stochastic Rules

In this section, we will explain a group of strategies related to biological foraging. In this regard, the traditional concept of random search plays an important role introduced by the optimal foraging theory [25]. Central to the entire discipline of optimal foraging is the concept of stochastic cause-effect response, which is determined by what we could call a “complex environment³” [12].

One of the most significant current hypothesis in the biological field states that natural mechanisms should drive foraging organisms to maximize their energy intake. This model is well known as *optimal foraging theory* [25]. Thus, a organism is either a searcher, e.g., forager, predator, parasite, pollinator or it is a target, e.g., prey or food. It is necessary here to clarify exactly what is meant by a searcher. In this study, the term searcher will be used as a computational or embodied agent. Throughout this paper the term uncorrelated refers to the direction of movement which is completely independent of the previous direction and unbiased refers to that there is no preferred direction, i.e., the direction moved at each step is completely random.

³ This term refers to a highly dynamic environment, and it will be used indistinguishably in this paper.

2.1 Brownian Motion as a Random Walk

The Brownian motion is one of the most widely used random walks and have been extensively applied for locating resources. Previous studies [6] have shown that this type of random walk presents explorations over short distances which can be made in much shorter times than explorations over long distances. In addition, the random walker tends to explore a given region of space and after that, it tends to return to the same point many times before finally wandering away. Therefore, it can be say that the random walker chooses new regions to explore blindly and it has no any tendency to move toward regions that it has not occupied before. In general, a Brownian walk has a normal diffusion where the mean square displacement increases in a linear way [18]. Fig. 1 presents a plot of simple Brownian walk.

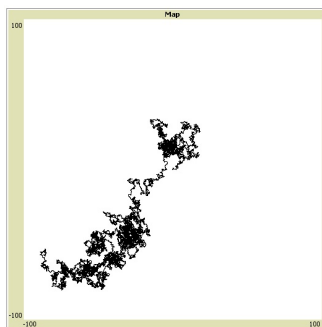


Fig. 1. A two dimensional random walk showing a random walker using Brownian motion to explore a given region. The random walker chooses new regions to explore blindly and it has no any tendency to move toward regions that it has not occupied before.

An important point to note is that extensions to the Brownian model would include variable speed and/or turning frequency, waiting times between steps, temporally dependent parameters, interactions between individual walkers, and allowing movement in three dimensions rather than restricting the model to two dimensions (See Fig. 2).

2.2 Lattice Model as Random Walk

A lattice model can be considered as an arrangement of points or objects in a regular periodic pattern in two or three dimensions [26]. The lattice space between successive steps of the random walk is constant, with every end point of the random walk being chosen as a grid node. It requires all walking steps to exactly conform to the lattice of regular grid nodes and each move is restricted only to one of the adjacent nodes (see Fig. 3).

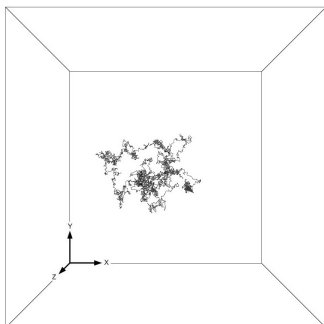


Fig. 2. Plot of a Brownian motion in three dimensions after 15000 time steps.

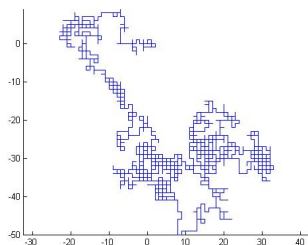


Fig. 3. Plot of a two-dimensional lattice random walk. It requires all walking steps to exactly conform to the lattice of regular grid nodes and each move is restricted only to one of the adjacent nodes.

A first serious discussion of lattice models can be described from the Chapman-Kolmogorov equations. This approach can be applied to describe a random walk on a lattice [25,9]. Similarly, the Pauli master equation describing a random walker jumping between sites on a lattice is given by

$$\frac{d}{dt}P_k = \sum_{\ell} (W_{k,\ell}P_{\ell} - W_{\ell,k}P_k), \quad (1)$$

where $P_k(t)$ represents the probability of being in state k at time t and $W_{k,\ell}$ are the transition rates to go from site ℓ to site k . Thus, normal diffusion arises in the long time limit provided that (1) there is stochasticity (nondeterministic kinematics) and that (2) the transition rates have a range with finite variance [25].

2.3 Spiral Searching

There is a considerable amount of literature describing the role of systematic search rules that provide a set of alternative strategies to random walks. These studies point out that the classic example of a systematic search strategy is

moving in the same direction. However, it is possible to find more complicated rules such as: the *Archimedean* spiral, also known as circular searches.

An important feature of this approach is the fact that under real conditions is very unlikely to obtain an almost perfect Archimedean spiral. A plot showing a spiral strategy is depicted in Fig. 4.

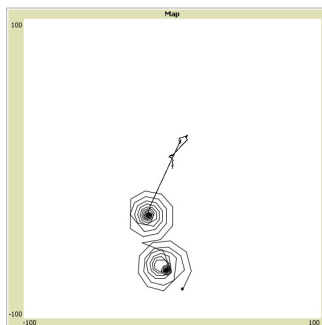


Fig. 4. Plot of an Archimedean spiral showing a series of outwardly concentric circles connected by linear segments. A searcher returns repeatedly to the starting point of the search (homing behavior).

Similarly, according to [4] the Archimedean spiral represents one of the most common searching rules in homing behaviors. In this case, a searcher is able to follow a spiral pattern during an initial phase, then systematically extends its range and moves in broad loops returning repeatedly to the starting point of the search as can be seen in Fig. 4. What is interesting in the results presented in [28], is that spiral searching paths may work well in clumped landscapes.

In a controlled study of spiral searching, Reynolds in [21], reported that a spiral search can work in some cases where the navigation of the searcher were precise enough, and their visual detection ability were reliable enough to ensure that all areas are explored. However, in some cases targets could be missed without any chance of encountering them in a second round due to the path is an ever expanding spiral. Thus, relying on a spiral search pattern would be disastrous where navigational and detection systems are less than ideal. This method could be used for short searches, before the inevitable cumulative navigational error became too large, to allow a true spiral to be maintained [20].

2.4 Lévy Walks

There is a consensus among scientists that the search efficiency depends on the probability distribution of flight lengths taken by a searcher. These studies have reported that when the target sites are sparse, an inverse square power-law distribution of flight lengths corresponding to a Lévy flight, which can be considered as an optimal strategy.

Lévy walks are characterized by a distribution function $P(l_j) \sim l_j^{-\mu}$ with $1 < \mu \leq 3$ where l_j is the flight length and the symbol \sim refers to the asymptotic limiting behavior as the relevant quantity goes to infinity or zero [24]. For the special case when $\mu \geq 3$ a Gaussian or normal distribution arises due to the central limit theorem [1].

The exponent of the power-law is named the Lévy index (μ) and controls the range of correlations in the movement, introducing a family of distributions, ranging from Brownian motion ($\mu > 3$) to straight-line paths ($\mu \rightarrow 1$) [4]. In this regard, a random explorer can present an optimal strategy by selecting the Lévy index as follows: $\mu_{opt} = 2$. Thus, $\mu \approx 2$ is the optimal value for a search in any dimension. Fig. 5 provides an example of a Lévy walk using the probability distribution $P(l_j) \sim l_j^{-\mu}$ and $\mu \approx 2$.

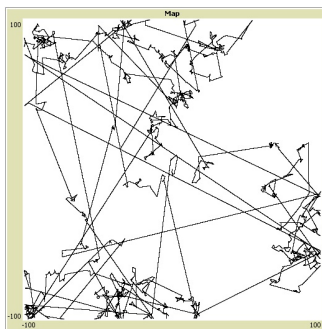


Fig. 5. Plot of a Lévy walk where Lévy index: $\mu \approx 2$.

An idealized model which captures some of the essential dynamics of foraging was developed by Viswanathan in [24], where target sites are distributed randomly and the random walker behaves as follows:

1. If a target site lies within a “direct vision” distance r_v , then the random walker moves on a straight line to the nearest target site.
2. If there is no target site within a distance r_v , then the random walker chooses a direction at random and a distance l_j from the probability distribution $P(l_j) \sim l_j^{-\mu}$. It then incrementally moves to the new point, constantly looking for a target within a radius r_v along its way. If it does not detect a target, it stops after traversing the distance l_j and chooses a new direction and a new distance l_{j+1} ; otherwise, it proceeds to the target as in rule (1).

Detailed examination of the mechanistic links between animal behavior, statistical patterns of movement and the role of randomness (stochasticity) in animal movement showed that temporal patterns can emerge at higher levels in terms of animal movement [2]. Thus, two important lessons can be learned from the model developed in [24]: (i) a search process of the Lévy-type may be optimal whenever the searcher have no information at all on the behavior

of the target (e.g. location, velocity of movement, type of motion, etc.) even if targets are not uniformly distributed, and (ii) high directional persistence in the movement may not necessarily be related to cues persecution.

According to Bartumeus in [5] points out that the key advantage of a Lévy walk over other types of walks is restricted to prey density, mobility and size of the predator relative to the prey. In addition, a Lévy walk can be more efficient than the classic Brownian motion [24,25]. A comparison of the two walks reveals that Lévy walks do not consist simply in adding long walks to a Brownian motion i.e., these two types of motion differ in the whole flight-time probability distribution. Therefore, it is possible to claim that Lévy walks are better than Brownian walks when resources are scarce. However, it should be noted that Brownian motion is not necessarily a null model, it can be considered as a different searching strategy that is optimal under certain conditions. Fig. 6 compares two paths obtained from a Brownian motion and a Lévy walk.

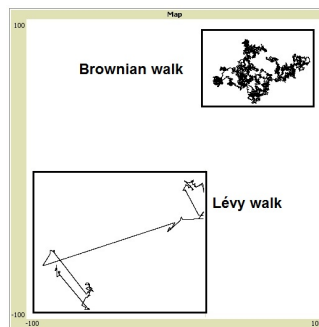


Fig. 6. A Brownian walker returns many times to previously visited locations. In contrast, the Lévy walker frequently takes long jumps to unexplored territory.

2.5 Correlated Random Walk

The simplest way to incorporate directional persistence into a random walk model is introducing correlations (i.e., memory effects) between successive random walk steps [25]. Thus, the trajectories generated by correlated random walk models appear more similar to the empirical data than those generated by uncorrelated random walks. The correlated random walks (CRWs) appeared in the study of ecology when short and medium scaled animal movement was analyzed.

These CRWs have a correlation length or time that can be quantified via sinuosity and introduced into the random walk as follows: in two dimensions, typically two random walk step vectors differ only in their angular directions. The turning angles θ_j between successive step vectors \mathbf{r}_j and \mathbf{r}_{j+1} are usually

chosen from a symmetric distribution. Thus, we can define the mean resultant as

$$\rho = \langle \cos(\theta) \rangle. \quad (2)$$

It is important to note that CRW models have been studied in the context of biological mechanisms that link information processing directly to the sinuosity parameter ρ . In this regard, the correlation function for CRWs decay exponentially and hence the memory effects have a finite range. Consequently, beyond certain spatial and temporal scales CRWs become uncorrelated random walks and correlations are not strong enough, resulting in a loss of directional persistence at large spatial and temporal scales.

In another major study an explanatory theory which defines a correlated random walk is presented in [4]. This research argues that a CRW can be seen as a model that combines a Gaussian distribution of move lengths (i.e., displacement events) with a nonuniform angular distribution of turning angles (i.e., reorientation events). Likewise, it suggests that the optimization of random searches mainly depends on the optimal temporal execution of reorientation events.

These CRW models are able to control directional persistence (i.e., the degree of correlation in the random walk) via the probability distribution of turning angles. Preliminary results using a wrapped Cauchy distribution (WCD) for the turning angles are reported in [13]. See equation 3:

$$\theta = \left[2 \times \arctan \left(\frac{(1 - \rho) \times \tan(\pi \times (r - 0.5))}{1 + \rho} \right) \right], \quad (3)$$

where ρ is the shape parameter ($0 \leq \rho \leq 1$) and r is a uniformly distributed random variable $r \in [0, 1]$. Directional persistence is controlled by changing the shape parameter of the WCD (ρ). Thus, for $\rho = 0$ we obtain a uniform distribution with no correlation between successive steps (Brownian motion), and for $\rho = 1$, we get a delta distribution at 0° , leading to straight-line searches (see Fig. 7).

It is also important to note that the simplicity of random walks is methodologically attractive. However, these type of random searches result in redundant paths and may not be applicable to behaviorally sophisticated searchers. Therefore, many simulations tend to apply correlated random walks to reduce these redundancies and simulate more realistic movements.

3 Directional Rules

Recent developments in random walks have heightened the need for a better approach in terms of searching methods. In this regard, it has been suggested a suitable framework in terms of biological inspired motion e.g., birds, insects, mammals and parasites [3,2,4]. Likewise, a set of important features need to be taken into account, for example: external factors (such as cues, obstacles and targets), information availability (full or partial) [12].

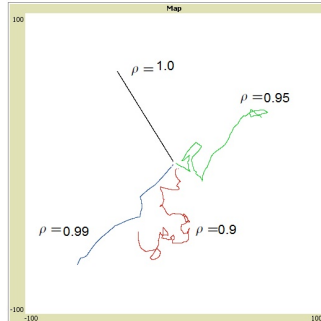


Fig. 7. Plots showing various degrees of correlation generated by the shape parameter ($0 \leq \rho \leq 1$).

A large and growing body of literature has investigated a deterministic cause-effect strategies using an action-reaction behavior e.g., kinesis or taxis [22].

In this section we will focus on examine a group of strategies that depend on attractants or repellents. Thus, random searchers tend to move according to certain chemicals attractants in their environment or towards the highest concentration of resources (biased movement and taxis). In addition, these rules can be successfully combined with stochastic rules with the aim to improve the performance of the searching task. It is important to note that these strategies are in principle based on a chemotactic phenomenon.

3.1 Run-and-tumble Chemotaxis

Chemotaxis can be defined as a biased random walk mainly composed of two phases. The “run phase” allows the cells to move with a constant velocity; and the “tumble phase” allows to reorient the cells to a new (random) direction [25].

Recent evidence suggests that Monte Carlo simulations represents a suitable approach, for determining the effect of directional memory on the efficiency of “run-and-tumble” in environments with different attractant gradients [17]. Thus, to evaluate and compare results the authors designed a simple simulation as follows. First, n bacteria were initially placed (and oriented) at random positions in a 2D simulation space. Then, attractant concentration was placed in this space with a linear gradient at point (x, y) , which is provided by

$$C(x, y) = \max \left\{ C_{max} - k\sqrt{(x - x_0)^2 + (y - y_0)^2}, 0 \right\}, \quad (4)$$

where k is the gradient, (x_0, y_0) is the origin and C_{max} is the concentration of attractant at the peak of the gradient. In the presence of a gradient of attractant (or repellent), the bacteria use temporal comparisons of the attractant concentration over the preceding above 3–4 seconds to determine if conditions are improving or deteriorating. The cells compare their average receptor occupancy, approximated by the values of C , between 1 and 4 seconds (s) in the past, $\langle C \rangle_{1-4}$, to the average receptor occupancy during the past 1 s, $\langle C \rangle_{0-1}$, to produce the biaser $b = \langle C \rangle_{0-1} - \langle C \rangle_{1-4}$. If $b > 0$, the cell reduces

the tumbling rate Γ_{tumble} from the ambient value Γ_0 by an amount dependent on b : $\Gamma_{tumble} = \Gamma_0 - \gamma f(b)$, where $f(b)$ is a monotonically increasing function of b and γ is a sensitivity coefficient that is positive for positive chemotaxis and negative for negative chemotaxis. The authors in [17] set γ , the sensitivity of the response of the bacterium to changes in attractant concentration, to 1. Thus, If $b < 0$, Γ_{tumble} is retained at the ambient value Γ_0 . And if a bacterium i is in a “run phase”, its orientation θ_i and position p_i are updated according to the system of equations

$$\theta_i(t + 1) = \theta_i(t) + \eta D_{rot}, \tag{5}$$

$$p_i(t + 1) = p_i(t) + v \begin{pmatrix} \cos \theta_i \\ \sin \theta_i \end{pmatrix}, \tag{6}$$

where D_{rot} is the rotational diffusion coefficient (set to $0.15 \text{ rad}^2/s$), $\eta = \mathcal{N}(0, 1)$ (\mathcal{N} stands for normal distribution) and v is the mean velocity of the bacterium. Consequently, t is incremented by δt ($0.1s$) and then, a random number r between 0 and 1 is compared to $1/\Gamma_{tumble}$, if $r < 1/\Gamma_{tumble}$ then the cell tumbles and chooses a new direction

$$\theta_i(t + 1) = \theta_i(t) + \vartheta_{tumble} D_{rot}, \tag{7}$$

where ϑ_{tumble} is the directional persistence parameter. If $\vartheta_{tumble} = 0$ then the new direction is identical to the previous direction (no reorientation). Large values of ϑ_{tumble} result in the new direction being independent of the old direction (perfect reorientation). Fig. 8 illustrates an example of the “run-and-tumble” chemotaxis strategy.

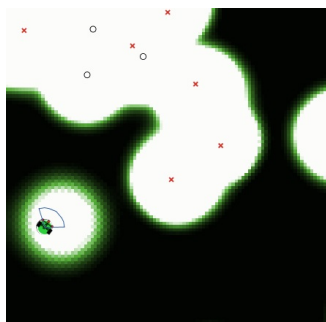


Fig. 8. In this “run-and-tumble” model, a group of bacterial cells drift towards spatial regions with high nutrient concentration for growth and survival.

3.2 Infotaxis

Infotaxis is focused on finding sources of particles transported in a random environment [14]. The main issue is whether a source of particles can be located when the only clues of its presence are rare detections? An good attempt to answer the question is a study carried out by Vergassola in [23].

It is possible to define the infotaxis strategy as a searching algorithm designed to work under an environment with sporadic cues and partial information; the process can

be thought of as acquisition of information on source location, so that information plays an important role similar to concentration in chemotaxis. Consequently, the infotaxis strategy locally maximizes the expected rate of information gain. In general terms, the infotaxis can be considered as a strategy for searching without gradients. Thus, two main aspects must be taken into account. On one hand, new actions should be tried and the available phase space must be explored (“exploration”). On the other hand, this should not be done blindly, e.g., the searcher in this case needs to minimize the searching time (“exploitation”). Therefore, infotaxis can be applied more broadly in the context of searching with sparse information.

In [23] is argued that given a probability distribution $P(\mathbf{r}_0)$ for the location of the source, it is possible to show that the expected search time $\langle T \rangle$ is bounded by $\langle T \rangle \geq e^{S-1}$, where S is the entropy of Shannon for the distribution $S \equiv - \int dx P(x) \ln P(x)$. The latter quantifies how spread-out the distribution is and goes to zero when the position of the source is localized to one site that is known. The rate of acquisition of information is quantified by the rate of reduction of entropy. Consequently, the main problem for the searcher is that the real probability distribution is unknown (to it) and must be estimated from the available data. As information accumulates, the entropy of the estimated distribution decreases and with it the expected time to locate the source. The searcher is faced with conflicting choices of either proceeding with its current information, or alternatively pausing to gather more information and obtain a more reliable estimate of the source distribution.

An important point to note is that in the search context, “exploitation” of the currently estimated $P_t(\mathbf{r}_0)$ by chasing locations of maximal estimated probability is very risky, because it can lead off the track. On the other hand, the most conservative “exploration” approach is to accumulate information before taking any step. This strategy is safe but not productive and is inferior to more active exploration, for example, systematic search in a particular sector. Hence, to balance exploration and exploitation, the searching algorithm needs to be redefined as follows: at each time step, the searcher chooses the direction that locally maximizes the expected rate of information acquisition. Specifically, the searcher chooses among the neighboring sites on a lattice and standing still, the move that maximizes the expected reduction in entropy of the posterior probability field. The intuitive idea is that entropy decreases (and thus information accumulates) faster close to the source because cues arrive at a higher rate. Consequently, tracking the maximum rate of information acquisition will guide the searcher to the source (see Fig. 9).

The authors in [23], estimate the variation of entropy expected upon moving to one of the neighboring points \mathbf{r}_j (or standing still) as:

$$\overline{\Delta S}(\mathbf{r} \mapsto \mathbf{r}_j) = P_t(\mathbf{r}_j) [-S] + [1 - P_t(\mathbf{r}_j)][\rho_0(\mathbf{r}_j)\Delta S_0 + \rho_1(\mathbf{r}_j)\Delta S_1 + \dots]. \quad (8)$$

The first term on the right-hand side corresponds to finding the source, that is, P_{t+1} becoming a δ function and entropy becoming zero. The second term on the right-hand side refers to the alternative case when the source is not found at \mathbf{r}_j . Symbols $\rho_k(\mathbf{r}_j)$ denote the probability that k detections be made at \mathbf{r}_j during a time-step Δt . The symbols ΔS_k in the equation denote the change of entropy between the fields $P_{t+1}(\mathbf{r}_0)$ and $P_t(\mathbf{r}_0)$. The first term on the right-hand side of the equation is the exploitative term, weighing only the event that the source is found at the point \mathbf{r}_j and favoring motion to maximum likelihood points. The second term on the right-hand side of the equation is the information gain from receiving additional cues. Thus, infotaxis naturally combines exploitative and exploratory tendencies [23].

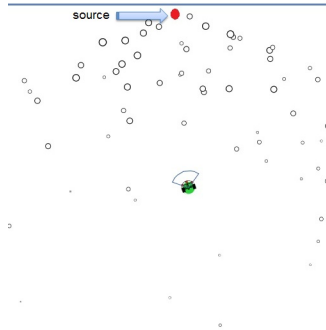


Fig. 9. A computer simulation showing a searcher pausing to gather more information. Thus, it can obtain a more reliable estimate of the source distribution.

As discussed previously, the gain mostly arises when the searcher is close to the source and its wandering is slightly reduced. Fig. 10 provides an infotactic trajectory toward an emitting source.

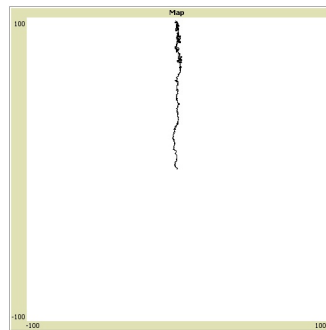


Fig. 10. A plot showing an infotactic trajectory toward an emitting source. When the searcher is close to the source it starts to wander. The starting point was set to (0,0).

An important point to note is that having multiple sources can generate conflicts and ambiguities. In this case, the searcher may get stuck by contradictory clues making its task more difficult [14].

4 Discussion

The main problem encountered with all these strategies is that it is not possible to find a general methodology to cope with different environments, so that a searcher is highly sensitive to its sensing and orientating abilities. In this regard, research in the area of random walks is far from complete [9]. There remains a wealth of exploration problems relating to random walks and searching strategies that have yet to be solved

(for example, how to select the best strategy for exploring a complex environment) and, of course, an almost endless supply of biological systems that are amenable to modeling using exploration techniques.

Similarly, according to the No Free Lunch Theorem of Optimization (NFLT) [27], which states that there is no one model that works best for every problem. The assumptions of a great model for one problem may not hold for another problem, so it is common in this searching context to try multiple strategies or models and find one that works best for a particular problem or environment.

Fig. 11 presents an overview of some existing techniques based on stochastic search strategies. These strategies are divided into two categories: stochastic rules and directional rules. It is important to note that we have added a set of extra *taxis* rules such as: Lévy taxis [19], Optimotaxis [15], Extremotaxis [7] and Rheotaxis [8].

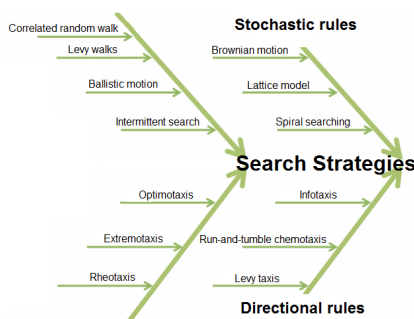


Fig. 11. A diagram showing search strategies divided into two categories: stochastic rules and directional rules.

5 Conclusions

In this paper, we have conducted an introductory overview of research of some existing techniques related to laws of motion based on stochastic search strategies. We have classified this study in two main categories: stochastic rules and directional rules, similarly, this survey has presented a variety of computer algorithms that have been assessed in terms of simulation. This manuscript has explained the central importance of using bio-inspired strategies with the aim to enhance our understanding of stochastic search strategies.

This work contributes to existing knowledge by adding and updating with current literature that provide with several practical applications. A number of caveats need to be noted regarding the present study. For instance, the random searcher is highly sensitive to its sensing and orientating abilities. Small changes in the environment can have a critical impact on the probability of success. In such case, the variability in the environment cannot be ignored.

Finally, We are well aware that there are many other techniques that we have not mentioned in this work. However, we consider that this introductory review is a good start point. Please refer to[11] for an in depth analysis about searching strategies.

Acknowledgements. This work has been supported in part by “Programa de Apoyo a Proyectos de Investigación e Innovación Tecnológica” (grant no. PAPIIT IA301016, and grant no. PAPIIT IA300916). Carlos Gershenson was partially supported by SNI membership 47907. J. Mario Siqueiros-García was partially supported by SNI membership 54027. We also acknowledge the support of projects 212802, 221341, 260021 and 222220 of CONACyT. Carlos Piña-García acknowledges UNAM for post-doctoral fellowship.

References

1. Anderson, D., Sweeney, D., Williams, T.: Introduction to statistics: concepts and applications. West Publishing Co., St. Paul, MN, USA (1994)
2. Bartumeus, F.: Behavioral intermittence, Lévy patterns, and randomness in animal movement. *Oikos* 118(4), 488–494 (2009)
3. Bartumeus, F., Catalan, J.: Optimal search behavior and classic foraging theory. *Journal of Physics A: Mathematical and Theoretical* 42, 434002 (2009)
4. Bartumeus, F., Da Luz, M., Viswanathan, G., Catalan, J.: Animal search strategies: a quantitative random-walk analysis. *Ecology* 86(11), 3078–3087 (2005)
5. Bartumeus, F., Peters, F., Pueyo, S., Marrasé, C., Catalan, J.: Helical Lévy walks: adjusting searching statistics to resource availability in microzooplankton. *Proceedings of the National Academy of Sciences of the United States of America* 100(22), 12771 (2003)
6. Berg, H.: Random walks in biology. Princeton Univ Pr (1993)
7. Burrage, K., Nicolau, D., Maini, P.: ‘extremotaxis’: Computing with a bacterial-inspired algorithm. *Biosystems* 94(1-2), 47–54 (2008)
8. Carton, A., Montgomery, J.: Evidence of a rheotactic component in the odour search behaviour of freshwater eels. *Journal of fish biology* 62(3), 501–516 (2003)
9. Codling, E.: Biased random walks in biology. Ph.D. thesis, The University of Leeds (2003)
10. Downing, K.L.: Intelligence Emerging: Adaptivity and Search in Evolving Neural Systems. MIT Press (2015)
11. García, C.A.P.: Sampling online social networks through random walks. <http://bit.ly/1ZZxGPV> (2014), accessed: 2016-01-01
12. Giuggioli, L., Bartumeus, F.: Animal movement, search strategies and behavioural ecology: a cross-disciplinary way forward. *Journal of Animal Ecology* 79(4), 906–909 (2010)
13. Kent, J., Tyler, D.: Maximum likelihood estimation for the wrapped cauchy distribution. *Journal of Applied Statistics* 15(2), 247–254 (1988)
14. Masson, J., Bechet, M., Vergassola, M.: Chasing information to search in random environments. *Journal of Physics A: Mathematical and Theoretical* 42, 434009 (2009)
15. Mesquita, A., Hespanha, J., Åström, K.: Optimotaxis: A stochastic multi-agent optimization procedure with point measurements. *Hybrid Systems: Computation and Control* pp. 358–371 (2008)
16. Morales, J., Haydon, D., Frair, J., Holsinger, K., Fryxell, J.: Extracting more out of relocation data: building movement models as mixtures of random walks. *Ecology* 85(9), 2436–2445 (2004)
17. Nicolau Jr, D., Armitage, J., Maini, P.: Directional persistence and the optimality of run-and-tumble chemotaxis. *Computational Biology and Chemistry* 33(4), 269–274 (2009)

18. Nurzaman, S., Matsumoto, Y., Nakamura, Y., Shirai, K., Koizumi, S., Ishiguro, H.: An adaptive switching behavior between levy and Brownian random search in a mobile robot based on biological fluctuation. In: Intelligent Robots and Systems (IROS), 2010 IEEE/RSJ International Conference on. pp. 1927–1934. IEEE (2010)
19. Pasternak, Z., Bartumeus, F., Grasso, F.: Lévy-taxis: a novel search strategy for finding odor plumes in turbulent flow-dominated environments. *Journal of Physics A: Mathematical and Theoretical* 42, 434010 (2009)
20. Press, W., Flannery, B., Teukolsky, S., Vetterling, W., et al.: Numerical recipes, vol. 3. Cambridge Univ Press (2007)
21. Reynolds, A., Smith, A., Menzel, R., Greggers, U., Reynolds, D., Riley, J.: Displaced honey bees perform optimal scale-free search flights. *Ecology* 88(8), 1955–1961 (2007)
22. Torney, C., Neufeld, Z., Couzin, I.: Context-dependent interaction leads to emergent search behavior in social aggregates. *Proceedings of the National Academy of Sciences* 106(52), 22055 (2009)
23. Vergassola, M., Villermaux, E., Shraiman, B.: Infotaxis as a strategy for searching without gradients. *Nature* 445(7126), 406–409 (2007)
24. Viswanathan, G., Buldyrev, S., Havlin, S., Da Luz, M., Raposo, E., Stanley, H.: Optimizing the success of random searches. *Nature* 401(6756), 911–914 (1999)
25. Viswanathan, G., da Luz, M., Raposo, E., Stanley, H.: *The Physics of Foraging: An Introduction to Random Searches and Biological Encounters*. Cambridge Univ Pr (2011)
26. Wang, J., Wang, X., Ren, C.: 2D conditional simulation of channels on wells using a random walk approach. *Computers & Geosciences* 35(3), 429–437 (2009)
27. Wolpert, D.H., Macready, W.G.: No free lunch theorems for optimization. *Evolutionary Computation, IEEE Transactions on* 1(1), 67–82 (1997)
28. Zollner, P., Lima, S.: Search strategies for landscape-level interpatch movements. *Ecology* 80(3), 1019–1030 (1999)

A Solution Proposal for the Capacitated P-Median Problem with Tabu Search

Mauricio Romero Montoya¹, María Beatríz Bernábe Loranca²,
Rogelio González Velázquez², José Luis Martínez Flores¹, Horacio Bautista Santos³,
Abraham Sánchez Flores², Francisco Macias Santiesteban²

¹ Universidad Popular Autónoma del Estado de Puebla,
Mexico

² Benemérita Universidad Autónoma de Puebla (BUAP),
Facultad de Ciencias de la Computación,
Puebla, Mexico

³ Instituto Tecnológico Superior de Tantoyuca,
Mexico

Abstract. This work presents the Capacitated P-Median problem, which seeks to solve the optimal location of p distributors. In understanding the computational complexity of this problem, partitioning principles are applied in the process of associating a distribution center with customers to be serviced. These are treated as clusters containing each distribution center and its customers. The optimization of the implicit cost function within the partitioning (distance minimization) is performed using Tabu Search with a diversified search. A series of computational experiences is performed aided by the OR-Library test instances, where in most cases an optimal solution is reached in reasonable computing time. As Tabu Search does not obtain all expected optima, OR-Library test instances are solved with the help of Lingo 16.0 and the obtained results are compared with those resulting from Tabu Search.

Keywords: Tabu Search, capacited P-median, NP-hard.

1 Introduction

The location of facilities deals mainly with choosing the physical location for a set of facilities in such a way that, given a set of restrictions, the demands from a set of customers are optimally met for some target function, from some set of candidate places. Facilities are to be understood in a broader sense, as they could be entities such as hospitals, factories, schools, ports, etc.

In this area, the P-Median and Capacitated P-Median (CPMP) problems are noteworthy due to their popularity in several areas. Here, the Capacitated P-Median problem is dealt with, as it was treated in previous work without reaching all optima.

Here, Tabu Search (TS) is introduced as an approximation tool, thus reaching the optima established in OR-Library.

This work is organized as follows: this introduction is section 1. Section 2 shows general aspects of related works. Section 3 shows the modeling leading to Section 4, which presents the approximation method and associated algorithm, section 5 shows the results of the computational experiences. Lastly, in section 7 results and conclusions are presented.

2 Related Works: P-Median and Capacitated Facility Location Problems

Location models are applied for specific cases, thus their structure (objectives, restrictions and variables) are case-dependent, therefore there are no generic models appropriate for all problems, and models with different objectives may provide different solutions for the same case study.

Facility location, also known as location analysis or location science, is concerned with the siting of facilities on a plane or within a network. These locations are dependent upon various attributes such as customers' demand on a facility, the cost of supplying those customers and the costs of opening facilities at potential locations.

A general description of location problems may be found in [1]. The problem dates back to Euclid and Pythagoras, due to their proposals of geometric models for distances; however literature suggests that it was emperor Constantine who pioneered its formal expression, as the location in a network was solved by means of discrete coordinates that placed the roman legions. Later, Fermat and Torricelli formulated the three node problem, which led to the Weber problem we know today (the infinite solution space Euclidian distance minimum single site location problem). In the 19th century Sylvester posed the problem of minimizing the maximum Euclidean distance in the infinite solution space.

In the 20th century Steiner's problem is generalized and formalized. Other contributions appear in the field of logistics (Hoover and Pallander [2]), but it was Wersan, Quon and Charnes [3] who placed the problem within the framework of mathematical optimization and programming, leading to the work of Daskin [4]. Location decisions may well be the most difficult for the efficient design of a supply chain, due to their strategic nature, for it is a long-term decision, which means it should consider facility cost, which may be quite steep as happens in manufacturing facilities. Therefore, it must be concluded that it is an inflexible decision. For a deeper discussion on the relevance of location decisions the reader is advised to refer to Daskin [5].

The quality of the location decision may make the difference in the efficiency of a supply chain, affecting customer satisfaction. Let us not forget that location decisions investigates the siting of a set of facilities in order to best satisfy the needs of a set of customers (Hale and Moberg, 2003) [6] thus, a poor location decision would hinder this purpose, contradicting the definition of supply chain as proposed by Chopra and Meindl (2001) [7]. Brandeau and Chiu (1989) [8] reviewed 50 location problems that had been studied, indicating their formulations, classification and relationships, thus showing a

series of optimization objectives that models may follow. Discrete models for the location in networks may be classified according to distance (Current et al. 2001) [9], distinguishing models based on maximum distance, and models based on total or average distance.

Daskin (2008) and ReVelle et al. (2008) [10, 11] reviewed and categorized the models for location problems into four classes: analytical, continuous, network and discrete. Analytical models refer to simple contrived problems. They have analytical value and are solved using classical mathematical optimization techniques but are of limited use in practice, due to their simplicity. While customer demand is most often restricted to fixed points or nodes within a region or a plane, continuous problems allow for the location of facilities anywhere within the region. These problems are known as Weber-type problems, and are often solved by means of analytical techniques. The applications and algorithmic techniques for these problems were reviewed by Drezner et al. (2001) [12, 13].

2.1 P-Median

The P-median problem, credited to Hakimi (1964) is an adaption of the classical Weber problem. It is particularly difficult to solve when considering problems of a more practical size where the number of variables may run in the hundreds or even thousands. Hence heuristic solution methods are often employed, as the complete enumeration time component increases exponentially with the number of binary variables to be considered (facilities and customers) [13]. The combinatorial nature of the p-median problem caused advances in solution techniques to be often made using combinations of mathematical programming and heuristic search techniques such as branch and bound and Lagrangean relaxation. This significant work, along with its results, is still often cited today by many authors. Reese (2006) [14], provides an annotated bibliography for the p-median problem which indicates that since the late 1980s there has been a significant shift from using traditional mathematical programming relaxation techniques, such as Lagrangean and surrogate relaxation, towards the use of more modern metaheuristics techniques (Bernabé 2012) [15].

2.2 Capacitated Facility Location Problem

The p-median and uncapacitated location problems both consider facilities with more than enough capacity or supply to provide for all their assigned customers. However, as facilities have only a finite supply or capacity, in practice this may not be the case. While most customers may be assigned to their nearest facility, when supply runs out, some customers may need to be directed –or at least partially directed – to the nearest available facility. Thus, there are two cases: first, the assignment of customers to facilities is determined via a binary constraint, to ensure a customer is served from a single facility, and second, the demand constrained may be fractional, to allow for the demand to be satisfied from one or more facilities. As a direct consequence, the capacitated p-median and the capacitated facility problems have been the interest of studies. The capacity constraints result in greater theoretical difficulty for the solution

of these problems, and are generally NP-hard. The contributions to solving the capacitated p-median problem are primarily metaheuristic or hybrid based.

The capacitated facility location problem may be regarded as either deriving from the the p-median problem by including fixed opening costs for facilities or, even better, as extending the uncapacitated facility location problem by considering each facility to have a limited supply or capacity constraint. It is referred to be NP-hard, and Kariv and Hakimi (1979) [16, 17] and Garey and Johnson (1979) [18] are often cited, even though neither considered this problem. However, the problem is modeled on a network, and is therefore likely to be at least as hard as the p-median problem. Heuristic algorithms are often presented as solution techniques. ReVelle and Eislet (2005) [19] pointed out that the introduction of capacity constraints effectively eliminates the property that all demand from a given customer is to be assigned to a single facility, and thus makes the problem much more difficult to solve.

3 Metaheuristics for Capacitated P-Median CPMP

Many attempts have been made to solve both capacitated and uncapacitated P-median. Two articles are of interest regarding Tabu Search, as this approximation to the capacitated p-median problem is solved by means of TS.

A Tabu Search procedure for the CPMP was developed by Sörensen (2008) [20], which managed to produce optimal solutions for all the small to medium sized OR-Library test problems, save two. Even though their paper does not identify said instances, relative errors were reported to be less than 0.1%, which represents an improvement over any previous work for CPMP. This work both backs up the conclusions by Arostegui et al. (2006) [21] and suggests that Tabu Search may well be a dominant methodology to use when solving the CPMP.

3.1 Capacitated P-Median Model

The CPMP, also known as the Capacitated Clustering Problem, the Capacitated Warehouse Location Problem, the Sum-of-Stars Clustering Problem and some others, is a classical location problem that finds applications in many practical situations. It may be described as: given a set of n points (customers), each of them with a known demand, it is required to find p medians (centers) and assign each point to exactly one median such that the total distance of assigned points to their corresponding medians is minimized, and the capacity limit on the medians may not be exceeded. Several heuristics and metaheuristics have been proposed for these problems, known to be NP-hard [18]. Osman and Christofides [22] propose a simulated annealing and tabu search method. Maniezzo [7] present a bionomic algorithm for the solution of this problem. Lorena and Senne [6] explore local search heuristics based on location-allocation procedures and Lorena and Senne [25] use column generation to CPMP.

The CPMP considered in this paper is modeled as the following binary integer programming problem:

$$z = \min \sum_{i \in N} \sum_{j \in N} d_{ij} x_{ij} \quad (1)$$

$$\text{subject to } \sum_{j \in N} x_{ij} = 1, \forall i \in N, \quad (2)$$

$$\sum_{j \in N} x_{jj} = p, \quad (3)$$

$$\sum_{i \in N} q_i x_{ij} \leq Q x_{jj}, \forall j \in N, \quad (4)$$

$$x_{ij} \in \{0,1\}, \forall i \in N, \forall j \in N, \quad (5)$$

where: $N = \{1, \dots, n\}$ is the index set of points to allocate and also of possible medians, where p medians will be located; q_i is the demand of each point and Q the capacity of each possible median; d_{ij} is a distance matrix; x_{ij} is the allocation matrix, with $x_{ij} = 1$ if point i is allocated to median j , and $x_{ij} = 0$, otherwise; $x_{jj} = 1$ if median j is selected and $x_{jj} = 0$, otherwise.

Target function (1) minimizes the sum of distances between all demand nodes. Constraint (2) ensures each node is assigned to exactly one facility. Constraint (3) sets the number of medians to be located. Constraint (4) imposes that a total median capacity must be respected, and (5) provides the integer conditions.

Clustering Search Partitioning (CSP) was used to assign clients to suppliers. This uses clustering to detect promising areas in the search space. It is of particular interest to find out these areas as soon as possible, in order to change the search strategy over them. In CSP, a clustering process is executed simultaneously with the Tabu Search algorithm, identifying groups of individuals that call for special interest.

The CS tries to locate promising search areas by framing them by clusters. Clusters may be defined as $G = \{c; r; s\}$ where c is the center, r the radius of the area, and s is a search strategy associated with the cluster.

The center c is a solution that represents the cluster, identifying the location of the cluster inside of the search space. The radius r establishes the maximum or minimum distance, starting from the center, that a solution can be associated to the cluster. The search strategy s is a systematic search intensification, in which solutions of a cluster interact among themselves along the clustering process, generating new solutions.

4 Tabu Search for Capacitated P-Median

This approximation relies on traditional Tabu Search, which generates a random initial solution. The parameters here have been defined as: 1) numberOfIterations (global iterations to be performed by the algorithm) 2) perturbationIterations, (determines the number of times a solution may be accepted according to the solution of the previous iteration. When the counter perturbationCounter crosses this limit, a new random solution is generated, and search is restarted).

The module parameter determines the frequency with which in Vicinity 1 (Algorithm 2) is to be used instead of Vicinity 2 (Algorithm 3), as can be seen in the first conditional within the main while loop. When the cost given by the vicinity functions improves on the best known cost (bestCost), this will be replaced, along with the solution configuration (bestSolution). The last step updates the tabu lists and global iteration counter.

Algorithm 1. Tabu Search (PSEUDOCODE):

```
READ numberOfIterations
READ perturbationIterations
READ module
SET iterationCounter and perturbationCounter to 0
SET initialSolution and bestSolution to currentSolution

WHILE iterationCounter < numberOfIterations
  SET currentCost to cost of currentSolution
  IF iterationCounter % module = 0
    CALL Neighbor1 with currentSolution RETURNING newCost
  ELSE
    CALL Neighbor2 with currentSolution RETURNING newCost
  END IF
  IF newCost > currentCost
    INCREMENT perturbationCounter
  END IF
  IF newCost < bestCost
    SET bestSolution to newSolution
    SET bestCost to newCost
  END IF
  SET currentSolution to newSolution
  SET currentCost to newCost
  IF perturbationCounter > perturbationIterations
    CALL RestartSolution RETURNING newSolution
    SET currentSolution to newSolution
    SET perturbationCounter to 0
  END IF
  CALL UpdateTabuLists RETURNING updatedTabuLists
  INCREMENT iterationCounter
END WHILE
RETURN bestSolution
```

CPMP is a problem in combinatorial optimization, classified as NP-Hard, and the tabu search metaheuristic has proven efficient in searching for solutions for a wide variety of problems of this kind, such as the quadratic assignment problem, the traveling salesman problem, or p-median search, among others. The tabu search metaheuristic uses different intelligent search schemes, like the short and long term memory use, keeps a list of tabu solutions that should not be visited because they lead to trajectories

that have proven not to be good solutions; these are tools in the search for artificial intelligence.

5 Computational Experience

Table 1 gathers the attained results for two kinds of tests with the Tabu Search approach: 1) varying parameters (random) and 2) using default set parameters and, on the other hand, the results obtained by the Branch & Bound method in Lingo 16 are presented.

It can be seen that varying parameters gives better results, and the OR-Library [26] demanded optima are approached. On the other hand, the results obtained are better than those reached in previous work [27].

Table 1. Results for Capacited P-Median with TS.

I	Capacited Q=120 Random						Default			Lingo 16	
	BV	C	P	RC	T	GAP	DC	T	GAP	OPT	T OPT
1	713	50	5	717	48340	0.56	722	10040	1.26	713	7.77
2	740	50	5	740	50933	0	740	9950	0	740	1.05
3	751	50	5	752	72445	0.13	772	9810	2.8	751	2.34
4	651	50	5	653	53402	0.31	654	10030	0.46	651	1.18
5	664	50	5	664	50073	0	664	9950	0	664	2.80
6	778	50	5	778	24426	0	778	9930	0	778	1.55
7	787	50	5	796	52371	1.14	810	9820	2.92	787	63.02
8	820	50	5	826	54607	0.73	851	9690	3.78	820	236.96
9	715	50	5	718	23938	0.42	721	9840	0.84	715	9.95
10	829	50	5	844	47455	1.81	844	9810	1.81	829	129.25
11	1006	100	10	1054	3E+05	4.77	1074	11900	6.76	1006	119.65
12	966	100	10	978	2E+05	1.24	983	11900	1.76	966	219.48
13	1026	100	10	1032	1E+05	0.58	1055	12050	2.83	1026	27.22
14	982	100	10	1012	3E+05	3.05	1027	12110	4.58	982	1190.93
15	1091	100	10	1133	7E+05	3.85	1160	12010	6.32	1091	711.64
16	954	100	10	975	2E+05	2.2	985	12120	3.25	954	108.53
17	1034	100	10	1077	64331	4.16	1072	11960	3.68	1034	112.21
18	1043	100	10	1086	67329	4.12	1088	12040	4.31	1043	543.21
19	1031	100	10	1057	63633	2.52	1049	11780	1.75	1031	380.67
20	1005	100	10	1133	66159	12.7	1146	11850	14.03	1005	48439.28

In the table 1, the notation is the next: I=Instance, BV is the best known value published in the OR-Library, C are the n Customers, P are the medians, RC are the values in the experiment when we were varying parameters (random), T (sec), is the execution time for each test, The GAP is the difference between the best cost and the obtained value by the approximation method, DC are the default parameters by default with TS, OPT are the values obtained with optimization software Lingo 16, T OPT is

the run time for each instance in Lingo 16. Tests were performed on a PC with 6GB RAM and a second generation i5 processor.

6 Conclusions

Throughout this work the extensive literature, efforts and applications surrounding the Capacitated P-Median problem have been confirmed.

Our objective is to obtain all optima dictated by the OR-Library, and at this point in the computational experience, it is assumed that satisfaction of optima is possible by adjusting the parameters in Tabu Search in such a way that the design of factorial statistical experiments becomes necessary.

In this work the robustness of the tabu search performed on the 20 OR-Library instances has been proven and compared with the results from Lingo, with an acceptable GAP, as shown in table 1.

The contribution from this work is the design of a sequential program based in object oriented programming and a data structure that allows for covering trajectories that partially explore the set of feasible solutions, known to have a combinatory explosion as the size of the problem increases even in moderate cases. This Tabu Search proposal is competitive even with the implementation of Lingo 16, a professional version without restrictions that is recommended for large scale testing.

Lastly, the capacitated P-median is part of the localization-assignment problems which define the strategy of an organization, that is, they are long-term decisions, and a good decision in the distribution and location of facilities has positive implications in the efficiency of the supply chain and the cost competitiveness of products and services reaching the customer, thus in general being benefic for the population sector that demands said product or service. In this point, as a future development from this work, a series of applications with both TS and Lingo 16 is to be developed, in particular for the meat industry.

References

1. Revelle, C.: A perspective of location Science. *Location Science*, 5, pp. 3–13 (1997)
2. Hoover, E.: *The location of Economic Activity*. New York (1948)
3. Wersan S. J., Quon J. E., Charnes, A.: System Analysis of refuses collection and disposable practice. *Yearbook American Public Works Association*, 14, pp. 195–211 (1962)
4. Daskin, M.S.: *Network and Discrete Location: Models, Algorithms, and Applications*. New York, John Willey & Sons, Inc., pp. 201–203 (1995)
5. Shen, Z. J., Coullard, C., Daskin, M. S.: A joint location-inventory model *Transportation science*. 37(1), pp. 40–55 (2003)
6. Hale, T., Moberg, C.: Location science research: A review. *Annals of Operations Research*, 123(1), pp. 21–35 (2003)
7. Chopra, S., Meindl, P.: *Supply Chain Management: Strategy, Planning, and Operation*. 2 Edition, New Jersey: Pearson Prentice Hall (2001)
8. Brandeau, M., Chiu, S.: An Overview of Representative Problems in Location Research. *Management Science*, 35(6), pp. 645–674 (1989)

9. Kaufman, L., Current, J., Daskin, M., Schilling, D.: Discrete Network Location Models. In: Facility Location Theory: Applications and Methods, Berlin: Z. Drezner and H. Hamacher Eds., pp. 85–112 (2001)
10. Daskin, M.: What you should know about location modelling. *Naval Res Logis*, 55, pp. 283–294 (2008)
11. Reville, C., Eislet, H., Daskin, M.: A bibliography for some fundamental problem categories in discrete location science. *European Journal of Operational Research*, 184, pp. 817–848 (2008)
12. Drezner, Z., Klamroth, K., Schobel, A., Wesolowsky, G.: *The Weber Problem*. Berlin, Germany: Springer-Verlag, pp. 1–36 (2001)
13. Venables, H.: Ant Colony Optimization: A Proposed Solution Framework for the Capacitated Facility Location Problem. <http://sure.sunderland.ac.uk/policies.html> (2011)
14. Reese, J.: Methods for solving the p-median problem: An annotated bibliography. *Networks*, 48(3), pp. 125–142 (2006)
15. Diaz, J. A., Bernabe, M. B., Luna, D., Olivares, E., Martínez, J. L.: Lagrangean relaxation for the geographical partitioning problem. *Rev. Mate. Teor. Aplic.*, 19(2), pp. 169–181 (2012)
16. Hakimi, S.: An algorithmic approach to network location problems. part i: The p-centres, *SIAM Journal of Applied Mathematics*, 37, pp. 513–538 (1979)
17. Kariv, O., Hakimi, S.: An algorithmic approach to network location problems. part ii: The p-median, *SIAM Journal of Applied Mathematics*, 37, pp. 539–560 (1979)
18. Garey, M. R., Johnson, D. S.: *Computers and Intractability: A Guide to the Theory of NP-Completeness*. W. H. Freeman (1979)
19. Reville, C., Eislet, H.: Location analysis: A synthesis and survey. *European Journal of Operational Research*, 165, pp. 1–19 (2005)
20. Sörensen, K.: Investigation of practical, robust and flexible decisions for facility location problems using tabu search and simulation. *J Operations Research Society*, 59(5), pp. 624–636 (2008)
21. Arostegui, M. J., Kadipasaogul, S., Khumawala, B.: An empirical comparison of tabu search, simulated annealing and genetic algorithms for facilities location problems. *International Journal of Production Economics*, 103, pp. 742–754 (2006)
22. Osman, I. H., Christofides, N.: Capacitated clustering problems by hybrid simulated annealing and tabu search. *Intern. Trans. in Operational Research*, Vol.1 (3), pp. 317–336 (1994)
23. Maniezzo, V., Mingozzi, A., Baldacci, R.: A bionomic approach to the capacitated p-median problem. *J Heuristics*, (4), pp. 263–280 (1998)
24. Lorena, L. A., Senne, E. L.: Local search heuristics for capacitated p-median problems. *Networks and Spatial Economics*, 3(4), pp. 407–419 (2003)
25. Lorena, L. A., Senne, E. L.: A column generation approach to capacitated p-median problems. *Computers and Operational Research*, Vol.31, pp. 863–876 (1994)
26. Bernábe, B., González, R., Estrada, M.: Adaptación de Particionamiento sobre Medoides a PMediana Capacitado. En: 5° Congreso Internacional de computación, México – Colombia, XV Jornada Académica en Inteligencia Artificial Cicom, pp. 2462-9588 (2015)
27. OR-library: <http://people.brunel.ac.uk/~mastjib/jeb/orlib/pmedinfo.html>, Retrieved (2014)

Tuning the Parameters of a Convolutional Artificial Neural Network by Using Covering Arrays

Humberto Pérez-Espinosa^{1,2}, Himer Avila-George^{1,2},
Josefina Rodriguez-Jacobo¹, Hector A. Cruz-Mendoza¹,
Juan Martínez-Miranda^{1,2}, Ismael Espinosa-Curiel¹

¹ CICESE-UT³, Tepic, Nay.,
Mexico

² CONACYT - CICESE-UT³, Tepic, Nay.,
Mexico

hperez@cicese.mx, himerag@cicese.mx
<http://idi.cicese.mx/ut3/>

Abstract. Artificial Neural Networks have proven to be a very powerful machine learning algorithm which can be adequate to learn successfully a variety of tasks. Currently, very complex classification problems on different kind of data (images, video, sound, text, DNA) have been solved using neural networks. This kind of algorithms usually has many parameters that need to be fine-tuned in order to have good results. Usually, this tuning is made by trial and error. However, this procedure does not guarantee the optimal performance of the training process. In this work, we study the use of mixed-level covering arrays to design experiments that help us to find the best combinations of parameters. We tested this approach by tuning a convolutional neural network for an audio classification task. For the implementation, we took advantage of the flexibility of the open source software library for machine learning TensorFlow.

Keywords: Artificial neural networks; covering arrays; artificial neural networks tuning; ConvNet architectures.

1 Introduction

Currently, artificial neural networks are used for solving a variety of machine learning tasks. The use of deep architectures has allowed going beyond the limits reached with other architectures in certain tasks such as speech recognition and image classification. This new revival of neural networks has even resulted in the successful creation of mass consumption products and services with a very high added value. For example, products for the classification of image, video, text, written language, speech and audio. Services for product recommendation, relational data and social networks mining. Deep learning methods aim at learning

feature hierarchies. The features from higher levels of the hierarchy are formed by the composition of lower level features [4]. Despite the great potential of deep neural networks, it is not easy to tune them. The problem of identifying the parameters for a specific structure of a neural network is an important research topic.

There have been several research efforts focused on the tuning of artificial neural networks (ANN). Some researchers have applied genetic algorithms for tuning the parameters of the network [3] and some others for tuning the parameters and also the structure of the network [13] [9]. Bashiri *et al.* [3] used central composite to design experiments and also to analyze the behavior of the neural network according to some identified parameters by using an overall desirability function. The genetic algorithm was applied to find optimal parameter status. They varied three parameters to evaluate the performance of the ANN: the percentage of trained data, the number of neuron in the first layer and the number of neuron in the second layer. Central composite was applied to extract the relationship between responses and controllable factors. To validate the proposed method, they compared their results versus the obtained applying the Taguchi methodology. Taguchi methodology is considered an important tool for robust design, i.e. for optimizing the product of process conditions which are minimally sensitive to the various causes of variation. This methodology has been used in several works for tuning ANN. In the work done by Tsai *et al.* [13] the authors used a hybrid Taguchi-genetic algorithm to tune the network structure and also the parameters of a feed-forward neural network. The numbers of hidden nodes and the links are chosen by increasing them from small numbers until the learning performance is good enough. A similar approach was proposed by Leung *et al.* [9], the method tunes the structure and parameters of an ANN by using an improved genetic algorithm. The neural network is able to learn both, the input-output relationships of an application and the network structure using the improved genetic algorithm. The authors propose the use of an ANN with link switches and its particularity is a unit step function introduced to each link. They observed that the weights of the links govern the input-output relationship of the ANN, while the switches of the links govern its structure. Tortum *et al.* [12] also applied the Taguchi method in the optimization of the design parameters of an ANN.

Besides genetic algorithms, other evolutionary approaches have been tested to solve the ANN tuning problem. Xiao *et al.* [14] applied a good point set-evolutionary strategy for tuning both, the network structure and parameters of a feed-forward neural network. The good point set is incorporated to enhance the crossover operator of the evolutionary strategy. The numbers of hidden nodes and the links of the feed-forward neural networks were chosen by increasing from small number of both until the learning performance is good enough. Zhao *et al.* [15] applied a cooperative binary-real particle swarm optimization to find compact structures and optimal parameters of an ANN with link switches which define the structure of the network. The works found in the literature have several points in common:

- The optimization of feed-forward neural networks [14], [15], [13], [9],
- The use of evolutionary strategies [14], [15], [13], [9], [3],
- The optimization of the number of hidden nodes and links [14], [15], [13], [9],
- The structure of the ANN is chosen by increasing the number of nodes and links until the learning performance is good enough [14], [15], [13], [9],
- The combination of an optimization technique with an experiment design method [14], [13], [3], [12].

In recent years, some combinatorial objects called covering arrays (CAs) have become very important in the design of experiments [7,8,10]. CAs are a generalization of orthogonal arrays (OAs). In the 80s, G. Taguchi [11] promoted the use of OAs as templates for developing experimental plans. The problem is that not OAs exist for certain configurations of variables, levels, and interaction degrees. Therefore, it is often difficult to choose a suitable OA to a specific problem. A CA is a combinatorial object that does not need to be balanced (not all t -tuples need to appear the same number of times) to open the possibility of create CAs with different configurations of variables, levels, and interaction degrees. A mixed-level covering array denoted by $MCA(N; t, k, (v_1, \dots, v_k))$ is a $N \times k$ matrix in which the entries of the i th column arise from an alphabet of size v_i ; additionally, each column i ($1 \leq i \leq k$) contains only elements from a set S_i with $|S_i| = v_i$, and the rows of each $N \times t$ subarray cover all t -tuples of values from the t columns at least once.

In this work, we propose the use of an experiment design method, based on mixed-level covering arrays (MCA), for tuning parameters of a Convolutional Neural Network (ConvNet). The characteristics of our approach, in contrast with the related works found in the literature, are:

- Optimization of a deep architecture neural network (ConvNet),
- The use of an experimental design instead of evolutionary strategies,
- The tuning of a relatively large number of parameters, some for tuning neural networks in general and some for tuning ConvNet architectures in particular,
- The structure of the ANN (number and type of layers) is fixed. We only change the parametrization,
- We do not apply any optimization technique.

The experiments presented in this work are based on two research questions:

1. Are mixed-level covering arrays a good option to fine tune the performance of an ANN?
2. How much significant is the improvement obtained using this approach?

2 Methodology

In order to answer the research questions posed in the previous section, we conducted an experiment in which we implemented a convolutional neural network

using an open source tool. We identified the set of parameters that need to be tuned and determined their possible range of values. Using MCA, we obtained a list of parameter combinations to test. We run the testing cases on an audio classification task. In the following subsections, we explain the details of the proposed method.

2.1 TensorFlow

For the implementation of the convolutional neural network, we used the software TensorFlow [1]. It was originally developed by researchers and engineers from the Google's Brain Team with the objective of conducting machine learning and deep neural networks research. This software is currently used for both, research and production by different teams in several of the commercial Google products, such as speech recognition, Gmail, Google Photos, and Search. An important characteristic of this tool is its flexible architecture which allows deploying computation to one or more CPUs or GPUs in a desktop, server, or mobile device using the same API. Google released TensorFlow under the Apache 2.0 open source license in November 2015.

2.2 ConvNets

ConvNets are a type of neural networks inspired by the visual system's structure. In these networks, the weights are shared across time or space. Neurons with the same weights are applied on input patches of the previous layer at different segments of the input data. In this way, it is obtained a *translational invariance* that allows the networks learning patterns and reuse them on different space or time context. Therefore, ConvNets are useful when the inputs samples are statistical invariants, that is, the input samples contain the same kind of information and it does not change on average across time or space. In a ConvNet, instead of having stacks of matrix multiply layers, there are stacks of convolutions. When the size of the patch is the same size than the whole feature vector, it is just a regular layer of a neural network. But when the patch is smaller than the whole feature vector, there are fewer weights and they are shared along the sequence of input features. Currently, pattern recognition systems based on convolutional networks are among the best performing systems. This type of network architecture typically have five, six or seven layers, a number of layers which makes fully connected neural networks almost impossible to train properly when initialized randomly [4].

2.3 ConvNet Structure

ConvNets are usually structured by stacking up convolution layers. At the top of the structure, there are fully connected layers. And finally, there is a classifier. Stride is the number of features that are shifted each time the filter moves. The strides between layers are used to reduce the dimensionality and to increase the

depth of the neural network. A stride of one makes the output the same size as the input. A stride of 2 means that output is half the size as the input. Each layer in the structure is called a feature map. There could be more than one feature map, for instance, if an image has the channels R,G, and B, these three channels (K-size = 3) can be handled as individual features maps. In our particular case, we are handling only one channel because the audio recording are mono-channel. When the shifting filter does not go beyond the edge of the feature vector, it is called valid padding. If the filter goes off the edge of the feature vector and therefore the output map size is exactly the same size than the input map, it is called same padding.

One possible improvement to this configuration of a ConvNet is to reduce the extent of the feature maps in the convolutional stack. Striding to shift the filters by a few features each time removes important information and produce less accurate models. The pooling layers take all the convolutions in a neighborhood and combine them instead of skipping one in every two convolutions. Max pooling take a small neighborhood around every point in the feature map and compute the maximum of all the responses around it. Given that the convolutions are done on lower stride, the structure becomes more expensive to compute and there are more parameters to tune. Average pooling instead of taking the max, just take an average over the window of features around a specific location.

For our implementation, we are using a typical architecture for ConvNet. It has two alternated layers of convolution and pooling, followed by a fully connected layer and a classification layer at the end. The Fig. 1 shows the network structure.

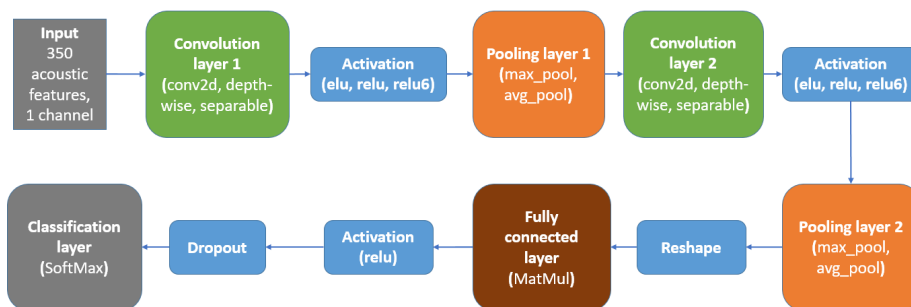


Fig.1: Convolutional neural network architecture used for the experiments presented in this paper. The different options that we tested at each layer are shown in parentheses.

2.4 ConvNet Parametrization

We identified three types of parameters. General: that are common in the training of any artificial neural network (e.g., number of epochs, learning rate).

Convolutional: that are particular parameters of a basic ConvNet (e.g., the stride to slide the filter, type of padding). Improvement: that are parameters of operations used to improve the performance of a ConvNet (e.g., pooling region size, pooling stride).

General:

- v1 - Num_epochs:** a positive integer that limits the number of steps that validation set is evaluated.
- v2 - Learning_rate:** a float that represents the magnitude of the update per each training step. Decay once per epoch.
- v3 - Batch_size:** a positive integer that indicates the percentage of the training data that are feed in each iteration.
- v4 - Eval_batch_size:** a positive integer that indicates the percentage of the validation data that is feed in each iteration.
- v5 - Loss:** Operation to measure the error of a network. The possible values for the parameter are `reduce_max` and `reduce_min`.
- v6 - Optimizer:** functions to compute gradients for a loss measure and apply gradients to variables. The four possible values of this parameter are *MomentumOptimizer*, *GradientDescentOptimizer*, *AdamOptimizer* and *RMSPropOptimizer*.
- v7 - Activation:** functions that provide nonlinearities. This parameter takes three possible values. One function for smooth nonlinearities (*elu*) and two continuous but not everywhere differentiable functions (*relu*, *relu6*).
- v8 - Classification:** operations to perform classification. In our case, *softmax* activations.

Convolutional:

- v9 - K-size** an integer that represents the size of the dimension of the input.
- v10 - Strides** a list of integers that represents the number of features that are shifted by the sliding window for each dimension of the input vector each time the filter moves.
- v11 - Convolution** functions to sweep a filter over a batch of input data, applying the filter to each window of each input vector of the appropriate size. This parameter takes three possible values *conv2d*, *depth-wise_conv2d* and *separable_conv2d*.
- v12 - Padding** If the filter goes off the edge of the feature map or not. The two possible values for this parameter are `same` and `valid`.
- v13 - Patch_size** a positive integer that indicates the size of the window that slides across the feature vector. It could be also bidimensional, in our case it is unidimensional.
- v14 - Depth1** a positive integer that represents the depth of the first convolution layer.

v15 - Depth2 a positive integer that represents the depth of the second convolution layer.

Improvement:

v16 - Pool function to reduce the extent of the feature maps sweeping a rectangular window over the input. The two possible values for this parameters are *max_pool* and *avg_pool*.

In Table 1??, the sixteen main variables and their levels/values are shown.

2.5 Criteria to Evaluate the ConvNet Parametrization

The criteria that we used to select the best parametrization of the ConvNet was a measurement of the classification performance. The results tables show the performance of the classification experiments in terms of precision, recall and F-measure. The F-measure is a classification performance metric that is calculated as the harmonic mean of precision and recall. The F-measure score reaches its best value at 1 when precision and recall are 1, and worst at 0 when precision or recall is 0. This is, the closest to 1, the most accurate is the classification. To measure the performance we use three data subsets: training, validation, and testing. The results showed in the tables are the ones obtained with the test set.

2.6 Design of Experiments based on MCA

The methodology for setting the values of the parameters of an ANN is based on the study of the effect on the quality of the solution, which is caused by the interaction between the variables of the experiment. The tuning process of the parameters of the ANN was done using an $MCA(49; 2, 7^4 5^1 4^3 3^4 2^3)$, this MCA represents the experimental plan. The MCA was constructed using the simulated annealing algorithm reported in [2]. The experimental plan is composed of fifty-two experiments, see Table 1??. In the construction of the experimental design, only fifteen parameters were used, because the parameter *Classification* only has one level.

2.7 Used Data

To find out which is the best configuration of the ConvNet, we used data from a dog barks database created by the Haramara TIC Lab at CICESE-UT³ in Nayarit, Mexico. The recorded barks of this database were induced applying four stimuli, three of them were related to negative emotions (aggression to unfamiliar people), and the fourth with a positive emotion (playfulness). The dogs were recorded in their habitual environment.

Aggression to unfamiliar people:

We divided this procedure into three parts:

Table 1: The design of experiment based on a MCA. ?? Variables and their levels. ?? The experimental plan.

(a)																(b)																
Variables																Variables																
Levels	v1	v2	v3	v4	v5	v6	v7	v8	v9	v10	v11	v12	v13	v14	v15	v16	Experiment #	v1	v2	v3	v4	v5	v6	v7	v9	v10	v11	v12	v13	v14	v15	v16
0	20	0.0001	8	8	tf.reduce.max	Momentum	relu	softmax	1	1	tf.nn	same	3	8	32	max	exp01	3	3	3	5	0	0	1	0	1	1	0	1	1	0	1
1	30	0.0006	20	20	tf.reduce.mean	GradientDescent	relu6	softmax	2	2	tf.nn.depthwise	valid	4	16	64	avg	exp02	1	1	1	0	0	1	1	1	1	0	0	1	1	3	1
2	40	0.0011	32	32	Adam	RMSProp	elu	softmax	3	3	tf.nn.separable		5	32	96		exp03	1	1	1	5	0	2	0	0	2	1	0	3	1	1	1
3	50	0.0016	44	44									6	64	128		exp04	2	2	2	4	1	0	0	2	0	0	1	1	0	1	0
4	60	0.0020	56	56									7				exp05	0	0	0	1	1	0	1	1	1	0	0	0	1	0	1
5	70	0.0025	68	68													exp06	0	0	0	5	0	1	2	0	2	2	1	4	1	1	1
6	80	0.0030	80	80													exp07	4	4	4	6	0	2	0	2	0	1	0	1	0	3	0
																	exp08	1	1	1	4	1	0	1	1	1	0	1	2	3	2	1
																	exp09	2	2	2	0	1	3	2	2	2	0	1	0	0	3	0
																	exp10	4	4	4	3	0	0	0	0	0	0	0	4	1	2	1
																	exp11	4	4	4	1	0	1	1	1	1	0	1	2	1	0	1
																	exp12	5	5	5	3	1	3	2	2	2	2	1	1	3	0	1
																	exp13	5	5	5	5	0	3	0	1	1	0	0	0	3	3	0
																	exp14	2	2	2	6	1	3	1	2	0	2	1	4	2	1	1
																	exp15	0	0	0	2	1	3	2	2	1	2	0	3	0	2	1
																	exp16	4	4	4	2	0	3	0	2	0	2	1	0	1	0	0
																	exp17	2	2	2	3	0	0	1	1	1	0	0	3	0	0	0
																	exp18	0	0	0	3	1	1	2	0	2	1	1	2	2	3	1
																	exp19	6	6	6	4	0	2	0	0	0	0	0	4	2	2	1
																	exp20	4	4	4	0	1	3	1	1	1	2	1	4	3	3	0
																	exp21	5	5	5	6	0	1	2	2	2	2	1	2	0	2	0
																	exp22	0	0	0	4	1	0	0	0	0	0	0	1	1	2	1
																	exp23	3	3	3	2	0	2	1	1	1	0	4	0	2	0	
																	exp24	1	1	1	2	1	2	2	2	2	1	1	3	0	1	
																	exp25	6	6	6	2	0	2	0	0	0	0	1	2	0	0	
																	exp26	1	1	1	5	1	1	1	1	1	1	2	0	0	1	
																	exp27	5	5	5	1	0	2	2	2	2	2	0	4	0	3	0
																	exp28	1	1	1	6	1	3	2	0	1	0	1	0	1	1	
																	exp29	0	0	0	6	0	0	1	1	0	2	1	4	1	0	0
																	exp30	6	6	6	3	1	0	2	2	2	1	0	1	1	3	1
																	exp31	1	1	1	3	0	2	0	2	0	2	0	2	2	0	
																	exp32	6	6	6	1	1	3	1	2	1	1	2	1	3	1	
																	exp33	4	4	4	4	0	3	2	1	2	1	0	3	0	0	1
																	exp34	6	6	6	6	1	1	0	0	0	1	1	3	3	1	0
																	exp35	2	2	2	1	0	2	1	1	2	1	0	0	3	2	0
																	exp36	5	5	5	4	1	0	2	0	1	2	1	3	2	3	1
																	exp37	1	1	1	1	0	1	0	0	2	0	0	4	3	0	0
																	exp38	6	6	6	1	1	1	1	0	0	1	1	3	2	1	1
																	exp39	3	3	3	6	1	3	2	2	0	0	1	3	1	2	0
																	exp40	3	3	3	4	0	1	0	0	1	0	0	3	1	1	1
																	exp41	5	5	5	0	0	2	1	1	0	1	0	3	0	0	0
																	exp42	6	6	6	5	1	0	2	2	1	2	1	0	1	2	1
																	exp43	3	3	3	0	1	2	0	2	0	1	1	2	2	2	1
																	exp44	0	0	0	0	0	2	1	0	1	0	0	0	3	1	0
																	exp45	6	6	6	0	0	0	2	1	2	2	1	3	0	0	1
																	exp46	3	3	3	1	1	0	0	0	2	1	0	1	3	3	0
																	exp47	2	2	2	5	0	1	1	1	0	0	0	2	1	2	0
																	exp48	5	5	5	2	1	1	2	2	2	0	1	2	1	1	1
																	exp49	3	3	3	3	0	3	0	0	0	2	0	3	2	1	0
																	exp50	4	4	4	5	1	1	0	1	0	1	1	2	2	1	1
																	exp51	1	1	1	0	0	2	2	2	2	0	4	2	2	0	
																	exp52	2	2	2	2	1	0	0	0	0	0	1	1	2	3	1

- Aggr1: The dog started barking when it realized the presence of a stranger at the door. After the door was open, the experimenter stimulated aggressive barks by doing some threatening movements in front of the dog and kept recording until the dog stop barking.
- Aggr2: The experimenter moved away from the owner house for ten minutes and then returned. The experimenter pretended to be a thief, hit the door and tried to force it to open. In this case, the barks were more intense.
- Aggr3: Again the experimenter moved away from the owner house and then

returned and he looked out through the window or above the wall of the house.

Playfulness:

The experimenter asked the owner to play with the dog using a toy or its favorite object. The experimenter, then, recorded the interaction between the owner and the dog.

From these inductions we obtained four categories of barks that we will try to classify using a neural network:

- **Aggressive-bark:** bark occurred due to the presence of a stranger.
- **Very-Aggressive-bark:** bark occurred due to the presence of a stranger and imminent threat.
- **Play-bark:** bark occurred while the dog is playing.
- **Other-bark:** bark that was not produced by some of the planned stimuli.

2.8 Audio Characterization

We characterized acoustically the audio data from this database using the software openSMILE [5]. This software allowed us to extract the following Low-Level Descriptors (LLDs): Melspec, MFCC, Energy, Spectral Bands, Spectral Roll Off, Spectral flux, Spectral centroid, Spectral MaxPos, Spectral MinPos, Voice prob, F0Env, F0 envelope, F0 and zero crossing rate. We computed these acoustic features using a frame size of 25 ms and a frame step of 10 ms. We applied a moving average filter for smoothing data contours. We calculated the delta and double delta regression coefficients for the values of LLDS in each frame. We calculated 39 statistical functions over the values of the LLDS, its deltas, and its double deltas coefficients in each frame of the sample.

We obtained a total of 6,552 attributes for each single audio sample. After an experimentation stage we decided to use the *Relief Attribute* evaluation method as implemented in Weka [6]. The method showed the best accuracy rates when we took the 350 best-ranked attributes. We selected these features from the original feature set of 6,552 attributes to obtain the best attributes and reduce the dimensionality of the attributes vector.

3 Results

For the experiment implementation, we used the TensorFlow framework installed in a Linux server called Harvest. Harvest is part of the computing infrastructure of the Center for Scientific Research and Higher Education at Ensenada, Technology Transfer Unit at Tecip (CICESE-UT3). Harvest is equipped with 72 Intel Xeon processors, 64GB RAM, and a Tesla K20 GPU accelerator. The Linux distribution for this server is CentOS.

Fifty-two experiments were run (see Table 2). We observed a diversity of classification performances. From very bad results (F-Measure below 0.30) to

very good results (F-Measure above 0.90). We identified some parameters that have a more evident effect on the results, for example, learning rate, convolution, and batch size. Other parameters do not have an evident effect on the results, for example, patch size, depth, and activation. We found that the best configuration is **exp39**, this experiment reaches a *F-Measure* = 0.94.

Three combinations were not possible because when the convolution is a *depth-wise* the variable depth must be the divisor of *num_hidden*. And when the convolution is separable the variable depth must be less than *num_hidden*. Those three cases did not satisfy this condition (*exp12*, *exp24* and *exp35*).

Table 2: Experimental design results.

<i>Experiment #</i>	<i>Results</i>		
	<i>Precision</i>	<i>Recall</i>	<i>F-Measure</i>
exp01	0.32	0.57	0.41
exp02	0.62	0.63	0.59
exp03	0.55	0.58	0.55
exp04	0.78	0.76	0.73
exp05	0.32	0.57	0.41
exp06	0.45	0.56	0.45
exp07	0.00	0.06	0.01
exp08	0.73	0.72	0.70
exp09	0.90	0.90	0.90
exp10	0.79	0.79	0.79
exp11	0.47	0.52	0.49
exp12			
exp13	0.71	0.61	0.61
exp14	0.32	0.57	0.41
exp15	0.00	0.05	0.00
exp16	0.59	0.32	0.16
exp17	0.57	0.58	0.56
exp18	0.32	0.57	0.41
exp19	0.74	0.70	0.70
exp20	0.32	0.57	0.41
exp21	0.32	0.57	0.41
exp22	0.32	0.57	0.41
exp23	0.16	0.05	0.01
exp24			
exp25	0.92	0.92	0.92
exp26	0.32	0.57	0.41
exp27	0.10	0.32	0.16
exp28	0.88	0.88	0.87
exp29	0.10	0.32	0.16
exp30	0.32	0.57	0.41
exp31	0.10	0.32	0.16
exp32	0.32	0.57	0.41
exp33	0.44	0.57	0.41
exp34	0.32	0.57	0.41
exp35			
exp36	0.32	0.57	0.41
exp37	0.59	0.58	0.58
exp38	0.32	0.57	0.41
exp39	0.94	0.94	0.94
exp40	0.67	0.67	0.67
exp41	0.40	0.41	0.37
exp42	0.32	0.57	0.41
exp43	0.34	0.56	0.43
exp44	0.74	0.54	0.50
exp45	0.32	0.57	0.41
exp46	0.32	0.57	0.41
exp47	0.60	0.60	0.60
exp48	0.32	0.57	0.41
exp49	0.32	0.57	0.41
exp50	0.32	0.57	0.41
exp51	0.00	0.06	0.01
exp52	0.86	0.86	0.86

The Table 3 shows the classification performance metrics of the best parameters combination obtained by the MCA. This result is compared with the classification results obtained with some widely used machine learning algorithms. We used the software Weka [6] to run the training algorithms. We used the default parametrization of this tool for all the algorithms. The evaluation was done using the same data subsets for all the classifiers. The samples were randomly distributed in the three subsets, 2,246 samples in the testing set, 642 in the validation set and 321 samples in the test set. Features vectors consist of 350 acoustic features.

We observed a marked difference in the classification performance between the ConvNet with tuned parametrization and the rest of classifiers. This comparison shows that by applying the proposed method for parametrization of ConvNets, we can obtain very accurate classification models. Random Forest and Support Vector Machines showed good results (F -Measure = 0.79 and 0.78 respectively) but there is a significant difference in the results showed by the ConvNet (0.94). Eight of the configurations obtained an F -Measure above the results obtained with Random Forest and Support Vector Machines.

Table 3: Comparison between the best result of the experiment and other classifiers.

<i>Classifier</i>	<i>Precision</i>	<i>Recall</i>	<i>F-measure</i>
Tuned ConvNet	0.94	0.94	0.94
Naive Bayes	0.70	0.67	0.68
Support Vector Machines	0.78	0.79	0.78
C4.5	0.69	0.69	0.69
Random Forest	0.79	0.79	0.78

4 Conclusions and Future Work

In this work, we applied MCA to design an experiment with the objective of finding good combinations of parameters for a ConvNet. We found out that running the experiments resulted in a variation of classification performance from very bad to very good. Given the best classification result from the experiment, we can conclude that this method for tuning the parameters of a ConvNet is a good option. We compared the best result obtained with the proposed method against the results obtained with other classifiers. We observed a significant improvement in relation with the other classifiers.

The results obtained in this work are very encouraging to keep exploring the use of MCA for tuning deep ANN architectures. As future work, we are planning to do a more exhaustive and formal evaluation of the classification performance and benefits of the proposed method. In that evaluation, we plan to test the following aspects:

- Testing of other audio, image and text databases.
- Testing with regression tasks.
- Testing of other deep structure variants such as auto-encoders, inceptions, and long short-term memory.
- Comparison with other ANN fine-tuning methods.
- Tuning of the structure of the deep architecture number, type and order of the layers stack.

Acknowledgements. This research work has been carried out in the context of the “Cátedras CONACyT” programme funded by the Mexican National Research Council.

References

1. Abadi, M., Agarwal, A., Barham, P., Brevdo, E., Chen, Z., Citro, C., Corrado, G.S., Davis, A., Dean, J., Devin, M., et al.: Tensorflow: Large-scale machine learning on heterogeneous systems, 2015. Software available from tensorflow.org 1 (2015)
2. Avila-George, H., Torres-Jimenez, J., Gonzalez-Hernandez, L., Hernández, V.: Metaheuristic approach for constructing functional test-suites. *IET Software* 7(2), 104–117 (2013)
3. Bashiri, M., Geranmayeh, A.F.: Tuning the parameters of an artificial neural network using central composite design and genetic algorithm. *Scientia Iranica* 18(6), 1600–1608 (2011)
4. Bengio, Y.: Learning deep architectures for ai. *Foundations and trends® in Machine Learning* 2(1), 1–127 (2009)
5. Eyben, F., Wöllmer, M., Schuller, B.: Opensmile: the munich versatile and fast open-source audio feature extractor. In: *Proceedings of the international conference on Multimedia*. pp. 1459–1462. ACM (2010)
6. Hall, M., Frank, E., Holmes, G., Pfahringer, B., Reutemann, P., Witten, I.H.: The weka data mining software: an update. *ACM SIGKDD explorations newsletter* 11(1), 10–18 (2009)
7. Kacker, R.N., Kuhn, D.R., Lei, Y., Lawrence, J.F.: Combinatorial testing for software: An adaptation of design of experiments. *Measurement* 46(9), 3745 – 3752 (2013)
8. Kuhn, D.R., Kacker, R.N., Lei, Y.: Measuring and specifying combinatorial coverage of test input configurations. *Innovations in Systems and Software Engineering* pp. 1–13 (2015)
9. Leung, F.H., Lam, H.K., Ling, S.H., Tam, P.K.: Tuning of the structure and parameters of a neural network using an improved genetic algorithm. *Neural Networks, IEEE Transactions on* 14(1), 79–88 (2003)
10. Proust, M.: *Design of Experiments Guide, Version 12*. JMP, A Business Unit of SAS, SAS Campus Drive, Cary, NC27513 (2015)
11. Taguchi, G.: *Introduction to quality engineering: designing quality into products and processes*. ARRB Group (1986)
12. Tortum, A., Yayla, N., Çelik, C., Gökdağ, M.: The investigation of model selection criteria in artificial neural networks by the taguchi method. *Physica A: Statistical Mechanics and its Applications* 386(1), 446–468 (2007)

13. Tsai, J.T., Chou, J.H., Liu, T.K.: Tuning the structure and parameters of a neural network by using hybrid taguchi-genetic algorithm. *Neural Networks, IEEE Transactions on* 17(1), 69–80 (2006)
14. Xiao, C., Cai, Z., Wang, Y., Liu, X.: Tuning of the structure and parameters of a neural network using a good points set evolutionary strategy. In: *Young Computer Scientists, 2008. ICYCS 2008. The 9th International Conference for*. pp. 1749–1754. IEEE (2008)
15. Zhao, L., Qian, F.: Tuning the structure and parameters of a neural network using cooperative binary-real particle swarm optimization. *Expert Systems with Applications* 38(5), 4972–4977 (2011)

A Meta-Heuristic Based on Genetic Algorithm for Selecting Bailiffs by Districts

Ribamar Louira do Carmo¹, Omar Andres Carmona Cortes²,
Fernando Jorge Cutrim Demétrio¹

¹ Universidade Estadual do Maranhão, Computer Engineer Department,
São Luis, MA, Brazil

² Instituto Federal do Maranhão, Informatics Department,
São Luis, MA, Brazil

ctrinfo.ribamar@gmail.com, fdemetrio@uema.br, omar@ifma.edu.br

Abstract. This paper presents a proposal for solving the Problem of Selecting Bailiffs by Districts (PSB/D) in the central of warrants in Maranhão-Brazil using Genetic Algorithm (GA). The complete solution to the PSB/D problem is a Web-based software called GAPSB/D. We conducted several experiments to prove its applicability considering two scenarios. The first scenario represents the central of warrants in the city of Imperatriz. The second one depicts the city of São Luís. The GA results are compared against two approaches: the manual selection currently in use and Simulated Annealing (SA). Results have proved GA could create solutions as good as the manual process, and it is more stable than SA, especially in the second scenario, in which the search space can reach a size of $\approx 10^{71}$ possibilities of solutions.

Keywords: Bailiff, np-hard, metaheuristic, genetic algorithm, simulated annealing.

1 Introduction

Real world problems are usually complex and, in most cases, enumerative algorithms are impossible to be applied due to constraints and the size of search space. A real-world problem we have faced is the selection of bailiffs by Districts (PSB/D), which is ruled by the Provision 18/2011 of General Internal Affairs of Justice of State of Maranhão (CGJ-MA in Portuguese) [7]. The 2nd Art. of that provision says the allocation of bailiffs in their respective areas (districts) will be done quarterly and electronically by the information technology stall of the Court of Justice.

Currently, the selection and distribution is done manually by a Microsoft Excel spreadsheet, and all constraints are also met manually in a trial-error based; this process takes about two days and, at least, two employees to perform the four distributions of 1 year. Also, the search space is too large, about 10^{22}

possibilities of solutions for the first scenario (Imperatriz) and 10^{71} for the second one (São Luis). In fact, that problem size becomes attractive the use of meta-heuristics such as Genetic Algorithms.

In this context, this paper proposes an optimization model for the PSB/D problem. Thus, it can be solved by any binary meta-heuristic. At the best of our knowledge, there is no other way to solve this problem in the literature neither using a meta-heuristic nor a simplified enumerative algorithm. In fact, the works [2,5,8,12,16,18,19,20] solve problems in the legal area, but they are entirely different problems. In other words, there are no applications related to our problem. Thereby, our proposal is to solve the problem using a Genetic Algorithm (GA) [4,13,14]. Indeed, we used a specific GA called selection-mutation GA [1]. The final application is a Web-based one called GAPSB/D, which was developed using a combination of open source tools, techniques, models, and patterns. In fact, the solution will be available via the Web for using in different cities including those one mentioned in both test scenarios. Furthermore, we have compared the GAPSB/D with both the manual process and Simulated Annealing. Results have shown GAPSB/D produces reliable solutions with high quality.

The remainder of this paper is divided as follows: Section 2 presents some important concepts about the distribution problem. Section 3 details our proposal presenting how individuals are modeled and how to compute the fitness function; Section 4 shows all experiments; finally, Section 5 presents the conclusions and future work.

2 Distributing Bailiffs

Some concepts are necessary to understand how bailiffs are distributed. The first one is the concept of a district, which is composed by one or more neighborhoods. A Central is a place where writs and court orders are managed. A bailiff is an officer who belongs to a district and is responsible for delivering writs and court orders. Figure 1 shows the relationship between these concepts.

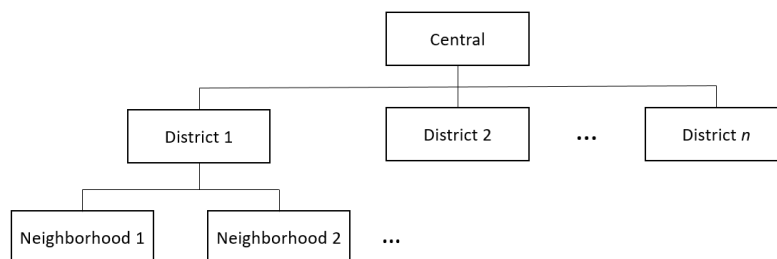


Fig. 1. Relationship between concepts.

In this work, we deal with two different scenarios. The first one is the Central of Imperatriz, which is devised by 27 bailiffs and 6 districts. The second scenario is the Central of São Luís that is composed of 16 districts and 84 bailiffs. Thus, the problem is how to distribute all bailiffs in order to deliver all writs and court orders.

This process is round-robin based and done quarterly; however, some rules must be obeyed. In the first one, none of the bailiffs can be allocated in the same district sequentially, *i.e.*, a bailiff can not be assigned to the same district in contiguous quarters. Further, there is a constraint that imposes that a district has an exact number of bailiffs. The distribution must select exactly the amount of available bailiffs on each district; in other words, none of the bailiffs can be idle.

3 Our Proposal: GAPSB/D

The Genetic Algorithm for Selecting Bailiffs by Districts (GAPSB/D) is a selection-mutation genetic algorithm for solving the PSB/D. The main characteristic of this approach is the unusual method of creating the initial population, which uses a constructive algorithm to try to select the best individuals. Similar operators can be seen in the works [9] and [6]. Furthermore, the GAPSB/D adds two different fitness functions: the population fitness and the genes fitness. Both are set using a minimum value, and both are used as stop criteria.

Because the GAPSB/D is a selection-mutation GA, the crossover operator is not used. Moreover, tests indicated the crossover operator created many invalid individuals that had to be submitted to repairing method in this particular application, increasing the computational time considerably. In other words, the benefit of the crossover operator does not pay-off the required processing. Algorithm 1 shows the pseudocode of the GAPSB/D.

Algorithm 1: The Genetic Algorithm GAPSB/D.

```
1 begin
2   Create initial population
3   Repair invalid individuals
4   Evaluate initial population
5   while stop criteria not achieved do
6     Run genetic mutation
7     Repair invalid individuals
8     Evaluate new population
9     Update population
10  end
11 end
12 return Best Population
```

The initial population is created using a constructive algorithm [9] that keeps individuals feasible by repairing the invalid ones. The stop criterion obeys one of the following conditions: (i) when the algorithm reaches the minimum of the population fitness, and all genes of the population met the gene fitness; or, (ii) when the algorithm reaches the maximum number of iterations.

While the stop criterion is not reached, the population undergoes mutation. Any invalid individual goes to the repairing function, which runs for 100 iterations trying to repair it. If the repairing process fails, the individual is added to the population nevertheless. Then, the population is evaluated, and the updating process only occurs if the new population (population fitness) is better than the previous one. Next sections give details about the representation and explain each step of the GAPS/D algorithm.

3.1 Individual Representation

The chromosome representation is fundamental to the AG. It is a way of transforming the information of the problem into a solution that a computer can deal with. In this context, each chromosome or individual is binary and has embedded into itself the following information:

- An individual represents a district;
- A gene represents a bailiff;
- The number of genes is the number of bailiffs involved in the distribution;
- A gene equals one indicates that the bailiff was selected to that particular district;
- The population represents the complete distribution of the available bailiffs throughout the districts;
- The population size is the number of districts used in the distribution;
- The chromosome size is the number of bailiffs used in the distribution;
- Capacity is the maximum amount of genes equal to 1 that each chromosome must possess. It is a constraint that the algorithm tries to obey because individuals out of the capacity are unfeasible solutions;
- Distribution is the activity of selecting bailiffs and assigning them to the districts.

Table 1 presents an instance of the population in the GAPS/D. In this particular example, we have six districts, 20 bailiffs, and a population size equals to 6. Moreover, the table shows the gene capacity, which is the maximum number of bailiffs that can be selected by a district. For example, the individual 6 depicts a district with five bailiffs being selected to that district. Furthermore, we can notice that all population is valid in this example.

3.2 Initial Population

The GAPS/D tries to select only the best genes for each individual when the initial population is created. If the capacity of each chromosome is violated, the

Table 1. Representation of the PSB/D in GA.

Individual	Capacity of genes	Chromosome
Individual 1	3	10000000110000000000
Individual 2	3	00010000000101000000
Individual 3	3	00000000000010110000
Individual 4	3	00001000001000000010
Individual 5	3	00000000000000001101
Individual 6	5	01100111000000000000
Total:	20	

repair method is executed to transform the infeasible solution into a valid one [9]. The process is iterative, and if after 100 iterations of repairing an individual is still invalid, it is added to the population nevertheless.

3.3 Evaluations: Fitness Functions

The fitness function must represent the quality of each individual in a particular problem to be solved [4], [14]. However, as previously mentioned, our approach introduces two more fitness functions: the population and gene fitnesses. As one can imagine, the gene fitness is used to calculate the individual fitness, which is used to compute the population fitness. The gene fitness is calculated using the historical selection of recent districts, *i.e.*; we consider the historical information of which bailiff was selected to which district in chronological order according to Equation 1:

$$ag = \begin{cases} p \times * \frac{100}{ps}, & \text{if } p > 0 \\ 100, & \text{otherwise} \end{cases}, \quad (1)$$

in which p is the position of the district in the history list of the last n districts, n is the number of districts participating in the distribution, and ps is the population size. An $ag = 100$ when $p = 0$ indicates the bailiff has not been selected by the district in the last n distributions. In the end, ag is a vector containing all genes evaluations. Afterward, the individual is evaluated by the lower fitness of its genes. If any chromosome has a gene with zero fitness, then zero will be the individual fitness. Finally the population is evaluated by Equation 2, in which p is the amount of genes with best fitness, *i.e.*, with fitness equals to 100, and cl is the chromosome length:

$$qg = p \times \frac{100}{cl}. \quad (2)$$

3.4 Updating Population and Elitism

Updating the population is a small modification in the population that almost not changes the processing time, but it assures that the performance of the AG always enhances over the generations. A good practice is to choose an individual

randomly combined with an elitist strategy, which ensures that the best solution never perishes while the algorithm tries to avoid the genetic convergence [14].

Replacing the old population by the new population based on the population fitness in GAPS/D does not guarantee the best individual will belong to the new population because the population fitness is a mean fitness. Thus, if the new population is better than the current one, one or two individuals (the best ones) from the current population are selected to go to the next generations. The choice is made randomly between all individuals with fitness equals to 100%. Only one individual is selected in the first scenario and two in the second one.

3.5 Genetic Mutation

The genetic mutation is applied to each individual of the population based on a mutation rate, excepting on those ones that have been selected by the elitism in the previous generation [3], [10]. After several tests, we could notice that a rate of 50% can explore the diversity of individuals and produces quality solutions in both scenarios. On the other hand, this high rate can also produce invalid chromosomes, which are repaired as previously stated.

4 Experiments

The experiments were conducted on a notebook with 4th generation processor, Intel Core i7-4500U, 08 GB of RAM, and 1 TB SATA hard drive (5400 RPM), running the Windows operating System 8.1, 64bits. Furthermore, as previously mentioned, the experiments were performed in two different scenarios using the parameter shown in Table 2 for GA and SA algorithms [17,11], respectively. Ten distributions of Bailiffs were performed for both scenarios. The results represent the mean of the fitness, runtime and standard deviation corresponding to 30 executions.

Table 2. Inputs parameter GAPS/D and SA per scenario.

GA		
Inputs parameter	scenario 1	scenario 2
Mutation rate	50%	50%
Generations number	10.000	30.000
Percentage of best fitness	100.00%	100.00%
Percentage of minimal fitness	100.00%	100.00%
SA		
Inputs parameter	scenario 1	scenario 2
Evaluations number	10.000	30.000
Percentage of best fitness	100.00%	100.00%
Percentage of minimal fitness	100.00%	100.00%

Regarding the comparison against SA, a solution is formed by a chromosome with 120 genes for the first scenario and 1344 genes for the second one. This modification is necessary for two reasons. The first one is for making the comparison fair in terms of evaluations. The second one is for having a full solution, which involves all bailiffs and districts.

In order to claim if the GAPSB/D is better than SA, we performed a bi-caudal t-test with $\alpha = 0.95$ considering H_0 as being “all means are the same”; therefore, any value without the interval $[-2.0452, 2.0452]$ is considered as a rejection of H_0 . A t-test is possible because of the central limit theorem, which states that any sample greater than 30 instances tends to present a normal distribution [15].

4.1 Scenario 1: 6 Individuals x 20 Genes

Table 3 illustrates the problem size of the Central of Warrants of Imperatriz, which has 6 districts and 20 bailiffs. Thus, combining all possibilities of the problem size we obtain a search space of something around 2.9×10^{22} .

Table 3. Scenario 1: illustrates the problem of the Central of Warrants of Imperatriz.

Individual	Genes capacity	Combinations
Individual 1	3	1.140
Individual 2	3	1.140
Individual 3	3	1.140
Individual 4	3	1.140
Individual 5	3	1.140
Individual 6	5	15.504
Total:	20	$\approx 10^{22}$

Figure 2 shows the comparison of the average fitness of 10 distributions for scenario 1, proving that the GAPSB/D presents, in general, better solutions than SA because SA obtained the best fitness only up to the second distribution. It is important to notice as we increase the number of distributions, we also increment the difficulty on solving the problem because it affects the historical of each bailiff.

Table 4 shows a t-test comparing GAPSB/D versus SA. As we can see, after the second distribution we start rejecting H_0 , which means that difference between algorithms starts being meaningful, *i.e.*, GAPSB/D starts presenting better solutions from the third distribution to the last one.

4.2 Scenario 2: 16 Individuals x 84 Genes

The second scenario represents the problem of the distribution of bailiffs in the central of warrants of São Luís. The information presented in Table 5 were extracted from the database of the System of process accompanying, called Themis

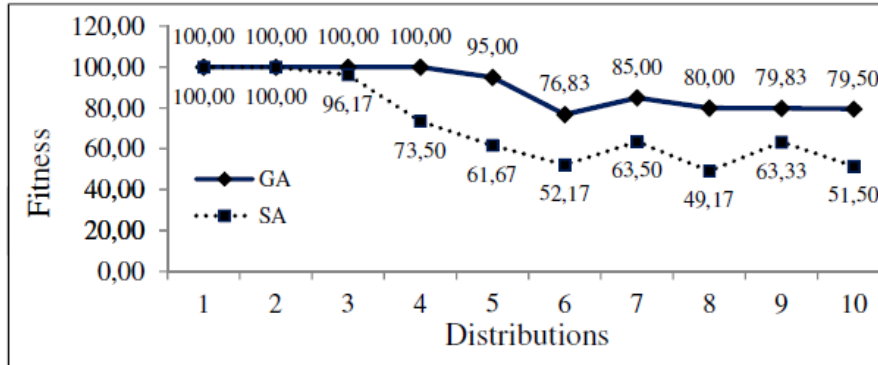


Fig. 2. Scenario 1: Average Fitness.

Table 4. Scenario 1: GAPSb/D X SA.

Distributions	Average Fitness			Standard deviation	
	GAPSb/D	SA	T-Test	GAPSb/D	SA
1	100.00	100.00	0.00	0.00	0.00
2	100.00	100.00	0.00	0.00	0.00
3	100.00	96.17	6.71	0.00	3.13
4	100.00	73.50	29.39	0.00	4.94
5	95.00	61.67	30.84	0.00	5.92
6	76.83	52.17	23.05	4.25	3.39
7	85.00	63.50	29.65	0.00	3.97
8	80.00	49.17	37.00	0.00	4.56
9	79.83	63.33	25.74	0.91	3.56
10	79.50	51.50	35.87	2.01	3.75

(Internal system-use, developed by the IT of Court of Justice). Hence, combining all possibilities of the problem size we obtain a search space of something around $\approx 10^{71}$.

Figure 3 shows the average fitness for 10 distributions, in which we can observe that GAPSb/D produces solutions with high quality if compared with SA. After the fourth distribution, the quality of solutions from SA decreases considerably, reaching an average fitness as small as 13.57.

Table 6 presents a comparison for the second scenario, in which we can see the differences start being meaningful from the fourth distribution on. An interesting fact is as the problem becomes harder to solve the GAPSb/S remains more stable presenting the most significant differences between the fifth and eighth distribution. The differences on the t-test show the instability of the SA algorithm to cover the search space.

Table 5. Scenario 2: districts of the central of warrants of São Luís.

Individual	Genes capacity	Combinations
Individual 1	3	95.284
Individual 2	5	30.872.016
Individual 3	5	30.872.016
Individual 4	7	4.529.365.776
Individual 5	7	4.529.365.776
Individual 6	5	30.872.016
Individual 7	5	30.872.016
Individual 8	6	406.481.544
Individual 9	3	95.284
Individual 10	10	2.761.025.887.620
Individual 11	8	30.872.016
Individual 12	4	43.595.145.594
Individual 13	3	1.929.501
Individual 14	6	406.481.544
Individual 15	4	1.929.501
Individual 16	3	84
Total:	84	$\approx 10^{71}$

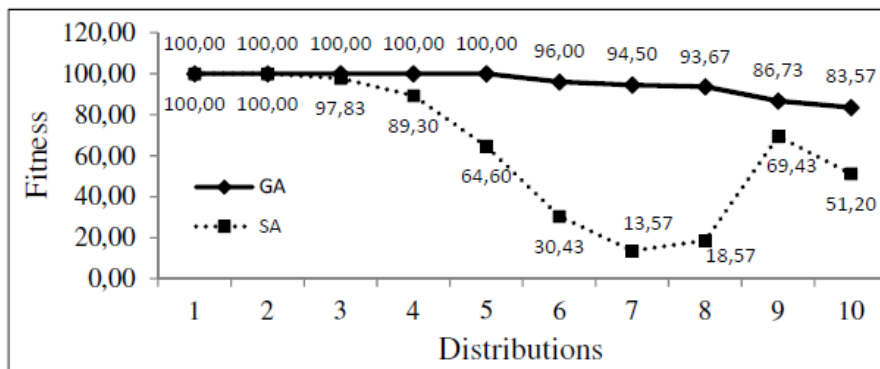


Fig. 3. Scenario 2: average fitness.

5 Conclusion

This work presented a selection-mutation GA for solving the problem of bailiffs distribution by districts. Results have proven that the implemented Genetic Algorithm is stable and reliable because solutions obey all constraint required by the Provision 18/2011. Furthermore, GAPS/D showed better results than Simulated Annealing and reduced considerably the time needed by doing the distribution manually. Moreover, the results indicate the possibility of using GA in bigger instances containing more districts and more bailiffs.

Future work includes testing integer representation providing more flexibility in selecting bailiffs; parallelizing bigger instance of scenarios using more districts

Table 6. Scenario 2: GAPSB/D X SA.

Distributions	Average Fitness			Standard deviation	
	GAPSB/D	SA	T-Test	GAPSB/D	SA
1	100.00	100.00	0.00	0.00	0.00
2	100.00	100.00	0.00	0.00	0.00
3	100.00	97.83	13.57	0.00	0.87
4	100.00	89.30	24.77	0.00	2.37
5	100.00	64.60	6.52	0.00	29.72
6	96.00	30.43	10.16	1.62	35.79
7	94.50	13.57	15.98	1.28	27.76
8	93.67	18.57	12.83	2.07	31.54
9	86.73	69.43	35.02	2.27	2.60
10	83.57	51.20	26.03	3.09	6.40

and bailiffs; test different meta-heuristics such as Differential Evolution and Particle Swam Optimization.

Acknowledgment. The authors would like to thank FAPEMA (Fundação de Amparo à Pesquisa e ao Desenvolvimento Científico e Tecnológico do Maranhão) for funding this research.

References

1. Berard, J.: Genetic algorithms in random environments: Two examples. *Probability Theory and Related Fields* 133, 123–140 (2005)
2. Bhawna, K., Kumar, G., Bhatia, P.K.: Software test case reduction using genetic algorithm: A modified approach. *international Journal of innovative Science, Engineering & Technology* 3(5), 6 (May 2016)
3. Bolton, C.C., Gatica, G., Barra, C.R., Parada, V.: A multi-operator genetic algorithm for the generalized minimum spanning tree problem. *Expert Systems With Applications* 50, 18 (2016)
4. Cortes, O.A.C., Barros, B.A.S., Lopes, R.F., Silva, J.C.D.: Um algoritmo híbrido paralelo cooperativo baseado em de, pso e ag: Uma avaliação em computadores multicore. *Congresso Brasileiro Em inteligência Computacional (CBIC)* (2013)
5. Cortes, O.A.C., Silva, J.C.: A local search algorithm based on clonal selection. In: *Eleventh Brazilian Symposium On Neural Networks*. p. 6 (2010)
6. Dombry, C.: A weighted random walk model, with application to a genetic algorithm p. 21 (2007)
7. General internal Affairs of Justice, SÃO LuÍS-Ma: Provision 18/2011 (Ago 2011)
8. Gomes, P.V., Saraiva, J.T.: Hybrid genetic algorithm for multi-objective transmission expansion planning p. 6 (2016)
9. Gomes, W.D.P., Gualda, N.D.F.: Modelagem integrada do problema de programação de tripulantes de aeronaves. *Transportes* 19(1), 2332 (Maio 2011)
10. Hassanat, A., Alkafaween, E., Al-Nawaiseh, N.A., Abbadi, M.A., Alkasassbeh, M., Alhasanat, M.B.: Enhancing genetic algorithms using multi-mutations p. 17 (2016)

11. Hu, L., Liu, J., Liang, C., Ni, F., Chen, H.: A phoenix++ based new genetic algorithm involving mechanism of simulated annealing. *international Journal of Distributed Sensor Networks* 2015, 8 (2015)
12. Krause, J., Parpinelli, R.S., Lopes, H.S.: Proposta de um algoritmo inspirado em evolução diferencial aplicado ao problema multidimensional da mochila p. 11 (2012)
13. Linden, R.: *Algoritmos Genéticos*. Brasport, Rio De Janeiro, 2a edn. (2008)
14. Linden, R.: *Algoritmos Genéticos*. Editora Ciência Moderna Ltda, Rio De Janeiro, 3a edn. (2012)
15. Montgomery, D.C., Runger, G.C.: *Applied statistics and probability for engineers* (2003)
16. Singh, V., Sharma, S.K., Vaibhav, S.: Transport aircraft conceptual design optimization using real coded genetic algorithm. *international Journal of Aerospace Engineering* 2016, 11 (2016)
17. Sousa, J., Cunha, M.D.C., Marques, A.S.: A simulated annealing algorithm for the optimal operation of water distribution networks. *Joint international Conference On Computing and Decision Making in Civil and Building Engineering* pp. 14–16 (June 2006)
18. Wang, J., Acharya, S., Kam, M.: Adaptive decision fusion using genetic algorithm p. 6 (2016)
19. Werner, J.C., Fogarty, T.C.: Genetic algorithm applied in clustering datasets. *Scism, South Bank University* p. 6 (2015)
20. Wijayaningrum, V.N., Mahmudy, W.F.: Optimization of ships route scheduling using genetic algorithm. *indonesian Journal of Electrical Engineering and Computer Science* 2(1), 180–186 (April 2016)

Artificial Vision System Using Mobile Devices for Detection of Fusarium Fungus in Corn

Pedro Salazar¹, Saul Ortiz¹, Talhia Hernández¹, Nestor Velasco²

¹ Instituto Tecnológico Superior del Occidente del Estado de Hidalgo,
Hidalgo, Mexico

² University of Central Florida,
USA

psalazar@itsoeh.edu.mx, ssoto@itsoeh.edu.mx, talhiah@hotmail.com,
nestorvb@gmail.com

Abstract. Artificial vision systems aims at mathematically modeling the visual perception systems of living beings and create programs that will allow the simulation of such capabilities by means of a computer system. The current frameworks that run on mobile devices allow both monochromatic and color image processing. The structure and properties of the 3D world that they try to describe aim at not just geometrical properties but also at properties such as material, light intensity/absorption on surfaces in an automated way. In Mexico, the implementation of such technologies in corn crops is almost nonexistent. However, by developing solutions the beneficial impact would boost the creation of technologies that may be able to detect plagues or diseases in crops. The following work proposes the use of an artificial vision system to identify the fusarium fungus on corn crops by integrating the technology in a smartphone and an implementation of javaCV to identify color patterns in the corn and be able to identify any anomaly.

Keywords: OpenCV, computer vision, fusarium, image processing, open source computer vision library.

1 Introduction

One of the most demanded agricultural product in Mexico is corn, as depicted in Figure 1. With the use of technology in agriculture, there has been significant beneficial changes, i.e., genetic manipulation of corn to provide the crop improved resistance to pests, worms or any additional threats.



Fig. 1. Corn crops in Mexico [1].

Agricultural technologies in Mexico are often not developed having small producers in mind, due to that, there aren't currently technology based tools that help with the plague detection process. Due to that situation, the proposed work aims at providing a solution based on an artificial vision system for mobile devices that will be able to detect the worst and most common corn fungus: "fusarium". With the use of a mobile device capable of detecting such fungus, common detection errors are avoided, noise factors such as light reflection and noise in color detection are not present.

2 State of the Art

There are currently various Computer Vision systems created entirely to agriculture, they are able to recognize not only size, shape, color and texture but assign a numeric value to objects or scenes that are being examined [2]. However, Computer Vision systems dedicated to pest detection are the less [3] but dedicate almost entirely to

providing advantages and suggestions on how to recollect information related to their current crops [4].

The two most important crops in Mexico are Beans and Corn, currently due to the high internal demand in the country there is a need to import corn and predictions state that given the high demographic growth there will be a need to double the production of such grain.

On the other hand, the irrigation of corn crops can increase substantially its production due to the high performance that can be achieved by duplicating technological tools focused on this grain.

Hidalgo in terms of agricultural land use possess a total of 153.938 hectares dedicated to irrigation; 56.926 of that land were dedicated to corn growth according to the 2007 P.V., 33.450 hectares belong to the Mixquiahuala DDR, where the Mezquital Valley is located.

Mezquital Valley covers 22 municipalities in which corn is produced but irrigated with wastewater, whilst the production potential can be up to 8.1 tons per hectare on average by introducing high yielding genotypes. However, some of them have some susceptibility to some diseases and pests that directly affects the production causing considerable economic losses to producers, the most significant and devastating ones are the smut, rot grain and army worm.

The smut (*Sporisorium reilianum*) is a fungal disease that affects corn production, destroying the male inflorescence (spike) and female (baby corn) replacing them with a powdery mass of spores [5]. Furthermore, the army worm is considered the most important pest of corn, in recent years it has become common to see it scuttling the stem of the plant to the neck of the root causing its wilting, it drills to the center of the stem and then continues feeding up, damaging the stigmata, the ears, and corn itself.

Due to the economic impact that these diseases and the direct negative effect in net income of producers, the aforementioned figures are an indicator of the risk posed by the smut and army worm and its possible spread throughout the state, and specifically in the Mezquital Valley, this coupled with the fact that this disease is endemic in some regions with geographical and climatic characteristics of the Valley imposes a big challenge.

3 Description of the problem

Due to the late detection along with the complications of properly detecting such corn diseases there is a low total production, Table 1 lists the main diseases that affect corn. It's worth mentioning how the fusarium fungus [6] not only attacks corn but also targets fruits such as melon, watermelon and pineapple. This disease causes a 40% drop of production due to decrease sick plants [7]. Identifying the fusarium fungus is not a simple task, often to make sure that the crop is sick it is necessary to send a sample to a lab to properly identify the type of disease infecting the crop, this traditional approach takes time and in most cases there is no solution to save the crop.

Table 1. Major corn diseases (pests) [8].

	ENFERMEDAD	MICROORGANISMO	GÉNERO O ESPECIE	
Plutición	Semilla	Hongo	<i>Fusarium</i>	
	Rizc	Hongos	<i>Fusarium</i> ; <i>Pythium</i>	
	Tallo	Bacterias	<i>Bacterial wilt</i> ; <i>Xanthomonas stewartii</i>	
	Tallo después de la floración	Hongos	<i>Pythium</i>	
	Mazorca y granos	Hongos	<i>Syntherisma</i> ; <i>Fusarium</i> ; <i>Ustilago</i> ; <i>Helminthosporium</i> ; <i>Marasmius</i> ; <i>Ustilago maydis</i> ; <i>Gibberella</i> ; <i>Zea</i>	
Foliar	Pudrición del cobro	Hongo	<i>Mycosphaerella</i>	
	Tizón de las hojas	Hongos	<i>Exserohilum</i> ; <i>Helminthosporium</i> ; <i>Ustilago</i>	
	Tizón del Sur	Hongos	<i>Bipolaris maydis</i> ; <i>Helminthosporium</i>	
	Hojas amarillentas	Hongo	<i>Pyricularia maydis</i>	
	Marchitamiento en bancas	Hongo	<i>Myrothecium</i>	
	Mancha de la hoja	Hongo	<i>Helminthosporium</i> ; <i>Marasmius</i> ; <i>Ustilago</i>	
	Mancha de la cara de la hoja	Hongos	<i>Ustilago</i> ; <i>Ustilago</i>	
	Arriacados	Hongo	<i>Ustilago</i> ; <i>Ustilago</i>	
	Mancha marón	Hongo	<i>Pyricularia maydis</i>	
	La mancha en ojo	Hongo	<i>Marasmius</i>	
	Mancha roja	Hongo	<i>Marasmius</i> ; <i>Ustilago</i>	
	La mancha en bander	Hongo	<i>Ustilago</i> ; <i>Ustilago</i>	
	Pictura de la hoja	Hongo	<i>Ustilago</i>	
	Raya común	Hongo	<i>Ustilago</i>	
	Raya del sur	Hongo	<i>Ustilago</i>	
	Raya tropical	Hongo	<i>Ustilago</i>	
	Infloración	Carabida del panizo	Hongo	<i>Ustilago</i>
		Falso carbón	Hongo	<i>Ustilago</i>
Carbón de la espiga		Hongo	<i>Ustilago</i>	
Carbón común		Hongo	<i>Ustilago</i>	
	Conocido	Hongo	<i>Ustilago</i>	

In order to identify the disease in the plant traditionally is done by image processing on a computer, image processing aims to improve the appearance of images and make clear some details that need to be evident, this process can be done by optical or digital methods. In order to perform image processing by means of an artificial vision system there is a need of coupling together digital methods implemented in a computer equipment following a series of steps to carry out the proper processing of in image.

In addition to the resources and methodology that requires image processing, another problem to address is how to train the end user because small farmers lack the knowledge and equipment on the methodology for image processing.

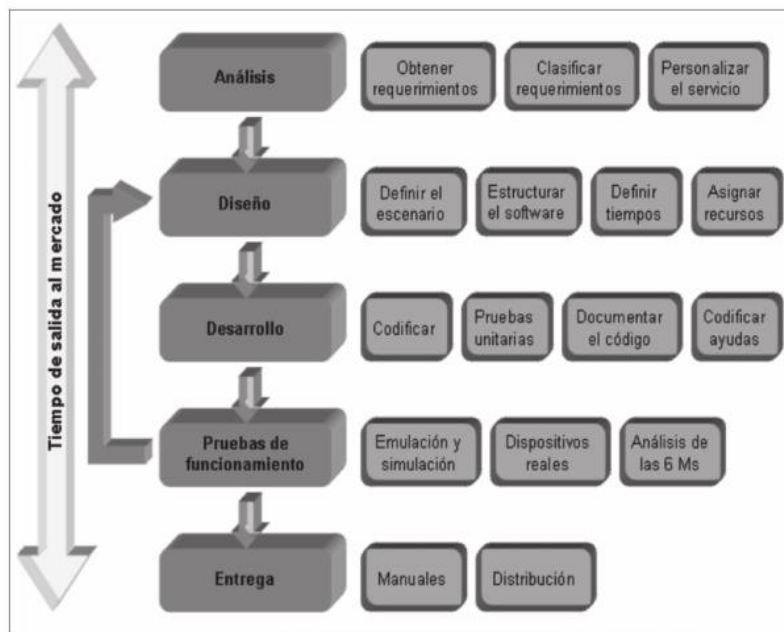


Fig. 2. Stages for mobile application development DrMovil.

4 A Mobile Application to Detect the Fungus Fusarium Corn Early

The methodology used to develop the mobile application is called DrMovil [9]. Figure 2 shows the stages.

4.1 Analysis

In this phase the requirements for the development of the mobile application were analyzed, as well as a field research to gather information.

For the field research in the experimental platform where samples of the fungus fusarium corn were obtained, as shown in Figure 3 and that helped define the mobile application should recognize a rectangle by same characteristics of corn stalk.



Fig. 3. Fusarium Fungus.

Coloring sick corn stalk is another be considered within the application development. The diseased stem has a particular coloration that by a PAM chemical analysis it's possible to identify the structure and chemical composition of some part of the plant, also when using the method of heat which consists of rising the temperature up to a steam saturation point at a given pressure It is obtained as a result the range of existing colors in the cornstalk, determining whether the fusarium fungus is present. With the support of the Autonomous University of Guadalajara, a study of colorimetry on the sample of the fungus and the results are shown in Figure 4.

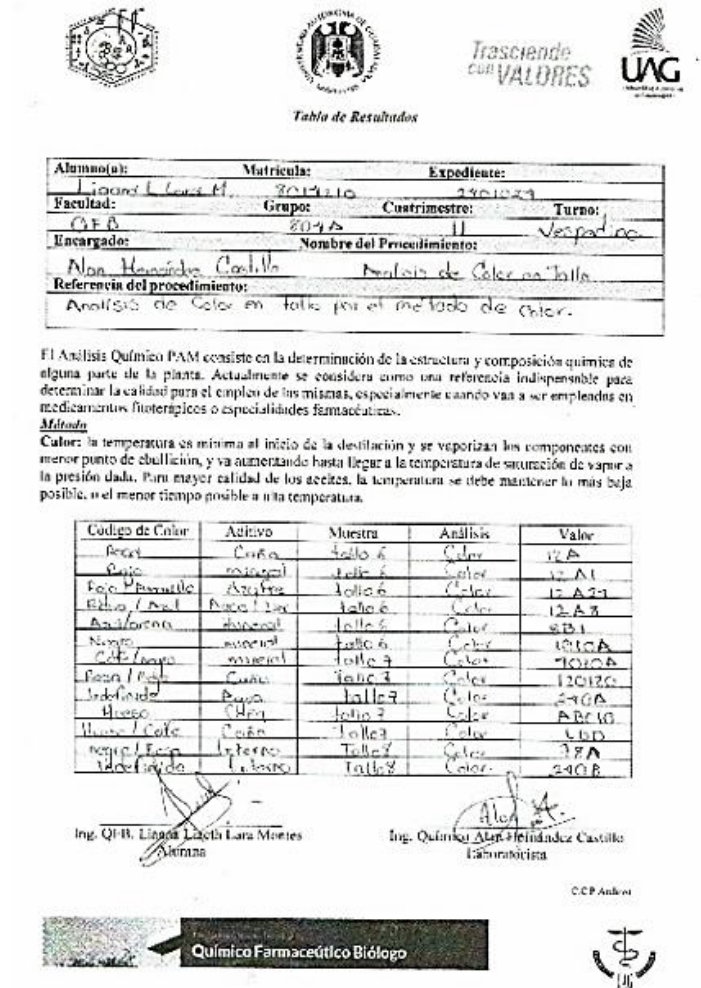


Fig. 4. Results of the color analysis by colorimetry.

To identify the fusarium pest, an OpenCV application was implemented as described by Paul Viola and Michael Jones [10], due to its multiple interoperable capabilities with languages such as C++, C, Python and Java along with the main operating Systems (Windows, Linux, Mac OS, iOS and Android) [11]. The technique used to detect the fungus is based on simple rectangles detection using a mathematical algorithm based on Haar Wavelets. The waves generated by this algorithm have a square shape per wavelength, to represent such wavelength a pair of adjacent rectangles are used. A light colored rectangle for negative intervals and a dark box for positive intervals (as shown in Figure 5) the formation of this squared wave allowed us to use Haar's features which basically detects the intensity of the pixels identifying the rectangles formed by the Wavelet algorithm of figure 5.

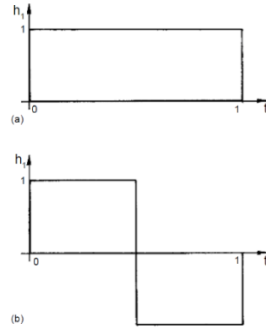


Fig. 5. Haar wavelet: (a) scaling function. (b) mother wavelet [12].

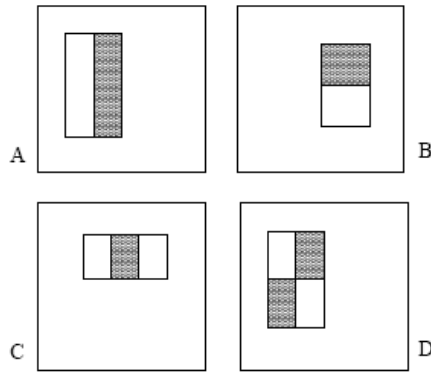


Fig. 6. Haar features [13].

The second feature that was used regarding the learning process is based on AdaBoost along with a combination of a staggered filters (Figure 6). The most intense colors were obtained from the colorimetry test and were used to train the filters that detect the fusarium fungus.

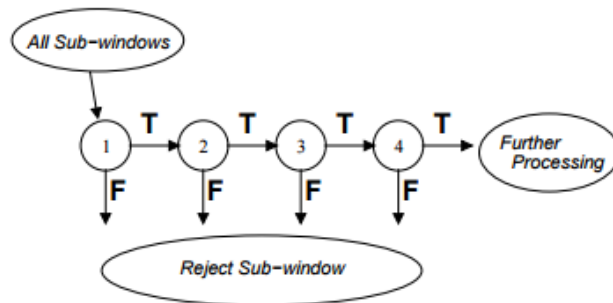


Fig. 7. Cascaded pattern detection.

The application was tested on a Smartphone with the following characteristics:

- Processor: Qualcomm Snapdragon™ 801 © Quad-Core CPUs 2.5GHz
- RAM: 3GB of RAM LP-DDR3
- Camera: 13 megapixels.

4.2 Design

The design of the application is intuitive and easy to use, the interface includes options to start the detection process and save the resulting data (Figure 8) (captured photos).

The “help” option contains a detailed description of each of the functions of the application.



Fig. 8. GUI Design.

4.3 Development

The application was created using API Android Studio 16, so it can be installed in any smartphone with Android 4.1 or higher which covers 60% of current devices on the market. Emulation and simulation tests were performed with the tools provided by Android Studio.

4.4 Performance Tests

Performance tests were performed to identify the fungus allocated at the corn stem. The a process is similar to the one implemented by Viola P. & Jones, M (2001) in which the shapes of the faces are detected, the application detects the shape of cornstalk in 100% of cases, additional tests were conducted with different plant images to make sure the effective recognition of the corn in a rectangular shape. Complimentary tests were performed using objects with similar shape of a cornstalk and although the shape of a stem was identified, the result was never a positive match for the fusarium fungus as shown in Figures 9 and 10.



Fig. 9. Application test with another plant.



Fig. 10. Recognition test of the fusarium fungus on cornstalk.

4.5 Current Findings and Future Work

In this paper the results of the implementation of artificial vision aims at solving an agriculture problem, the intended impact is to provide technological solutions for farmers who do not have the financial resources to cover the needed expenses for studies such as the colorimetry that is needed to determine whether corn is being affected by the fusarium fungus.

As Future work the goal of this work is the creation of a database of diseases like coal spike or army worm that also affects corn. With this catalog the application could not only identify the fusarium fungus but could provide the benefit the possibility of anticipating additional diseases that occur in important crops of agricultural products in the country.

References

1. SAGARPA, SIAP: Secretaría de Agricultura, Ganadería, Desarrollo Rural, Pesca y Alimentación, Servicio de Información Agroalimentaria y Pesquera (2011)
2. Yud-Ren, C., Kuanglin, C., Moon, S. K.: Machine vision technology for agricultural applications. *Computers and Electronics in Agriculture*, 36, pp. 173–191 (2002)
3. Camargo, A., Smith, J. S.: Image pattern classification for the identification of disease causing agents in plants. *Computers and Electronics in Agriculture*, 66, pp. 121–125 (2009)

4. Lili, N. A., Khalid, F. N., Borham, M.: Classification of herbs plant diseases via hierarchical dynamic artificial neural network after image removal (2011)
5. Bizzocchi, A.: Los Colores y su Significado. Ideas Marketing, Website: <http://www.ideas-chicago.com/los-colores-y-su-significado> (2013).
6. González, I., Arias, Y., Petei, B.: Aspectos Generales De La Interacción Fusarium oxysporum f. sp. lycopersici-tomate. *Revista de Protección Vegetal, La Habana*, 6 (2012)
7. Quintero, J. A., Apodaca, M. A.: Pudrición de la mazorca. *Manejo Sustentable del Maíz. Fundación produce Sinaloa, Sagarpa, Gobierno del estado de Sinaloa*, pp. 71–78 (2008)
8. El Maíz En Los Trópicos: Mejoramiento y producción. *Fao.org.*, Retrieved 23 September 2016, from <http://www.fao.org/docrep/003/x7650s/x7650s10.htm> (2016)
9. Gasca, M., Camargo, L., Medina, B.: Metodología para el desarrollo de aplicaciones móviles. *RT*, 18(40), pp. 20 (2014)
10. Viola, P. Jones, M.: Robust Real-time Object Detection. Cambridge, Massachusetts, Compaq Computer Corporation, Retrieved from: <http://www.hpl.hp.com/techreports/Compaq-DEC/CRL-2001-1.pdf> (2001)
11. OpenCV: OpenCV. *OpenCV.org*, retrieved from: <http://opencv.org/> (2016)
12. Stankovi ć, R.S., Falkowski, B.J.: The Haar wavelet transform: its status and achievements. *Comput Elec Eng.*, 29, pp. 24–44 (2003)
13. Características de Haar. Universidad Autónoma de Barcelona (2016)
14. Santacruz, V., Santacruz, C., Welti, J., Farrera, R. R., Alamilla, L., Chanona, J., Gutiérrez, G. F.: Effects of air-drying on the shrinkage, surface temperatures and structural features of apples slabs by means of fractal analysis. *Revista Mexicana de Ingeniería Química*, 7(1), pp. 55–63 (2008)
15. OpenCV: OpenCV, Open Source Computer Vision, Website: <http://opencv.org/> (2015)
16. Stack overflow. Learning JavaCV in pure Java, Stack overflow Website: <http://stackoverflow.com/questions/11494546/learning-javacv-in-pure-java> (2012)
17. Tlapale, A. D., Chanona, J. J., Mora, R., Farrera, R. R., Gutiérrez, G. F., Calderón, G.: Dough and crumb grain changes during mixing and fermentation and their relation with extension properties and bread quality of yeasted sweet dough. *International Journal of Food Science and Technology*, 45(3), pp. 530–539 (2010)
18. Lili, N. A., Khalid, F., Borhan, N. M.: Classification of herbs plant diseases via hierarchical dynamic artificial neural network after image removal using kernel regression framework. *International Journal on Computer Science and Engineering (IJCSE)*, 3(1), pp. 15–20 (2011)
19. Unisem: Carbón de la espiga en valle del mezquital: la solución es de todos. Retrieved from: <http://semillastodoterreno.com/2013/02/carbon-de-la-espiga-en-valle-del-mezquital-la-solucion-es-de-todos> (2013)
20. Fundación Hidalgo Produce: Carbón de la espiga del maíz. Retrieved from: <http://www.upfim.edu.mx/libro/libros/espigaMaiz.pdf> (2014)

Determination of the Ripeness State of Guavas Using an Artificial Neural Network

Edwin M. Lara-Espinoza¹, Monica Trejo-Duran¹, Rocio A. Lizarraga-Morales¹,
Eduardo Cabal-Yepez¹, Noe Saldana-Robles²

¹ Universidad de Guanajuato, Departamento de Estudios Multidisciplinarios,
Division de Ingenierias,
Guanajuato, Mexico

² Universidad de Guanajuato, Departamento de Ingenieria Agricola, Division de
Ciencias de la Vida,
Guanajuato, Mexico

{em.laraespinoza, mtrejo, ra.lizarragamorales, educabal, saldanar}@ugto.mx

Abstract. The determination of the ripeness state of fruits is an essential element in the agriculture research field. This is because the ripeness is related with quality and it can affect the commercialization of the product. In this paper, a classification system of the ripeness state of guavas is proposed. The guavas are classified into three states: green, ripe and overripe. The classification system is based on Artificial Neural Network (ANN) which uses color features as input. The characteristics used in our proposal are extracted from three different color spaces: RGB, CIELab and CIEluv. Specifically, we only use the components R, G, a and u, which gave us the best separability within classes. The system was tested using real images of guavas obtaining 97.44% of accuracy.

Keywords: Guavas, ripeness state, color, ANN.

1 Introduction

Nowadays, image analysis is of great interest for the development of applications in agriculture-oriented tasks. The determination of the ripeness state of fruits is an essential element in agriculture tasks because ripeness is highly related with quality and therefore, with their commercialization. The main issue is that only trained personnel can perform this task and a large amount of time is required to analyze each piece of fruit. The development of systems to determine fruits quality is very important. Specifically, guavas are of great interest in our society because, taking into account the benefit in the health, the guavas [5] have high content in quercetin, vitamin A and C which prevents the development of cataracts and the other diseases. Due to this, the global market of guavas [1] has achieved the exportation of 1.2 millions of tons per year.

Recently, a wide number of classification systems have been developed for the determination of the ripeness state of fruits. Such methods can be classified

into two groups: destructive and non-destructive. Destructive methods take a sample of the crop and it is chemically analyzed in order to determine its glucose composition. The main disadvantage of these methods is the destruction of the fruit. On the other hand, non-destructive methods analyze images of the fruit to determine the ripeness state. Among these approaches, different image features and classification methods have been proposed. In [8], color features are extracted from images of bananas with two different illuminations: natural and ultraviolet, and the corresponding images are submitted to a set of if-then rules for classification. On the same way, in [2] color features are extracted from bananas using two color spaces CIElab and HSV. Tomatoes images are analyzed in [15], where color features are extracted. In this case, the authors use two different cameras: conventional and near infrared. The classification is performed through an integration and analysis of the color variation in red-green. Using variation of color, in [14] an algorithm is developed to determine the ripeness state of watermelons. Another method used in classification tasks is the fuzzy logic, for example in [6] color features and texture features are extracted from images of tomatoes and they are submitted to an if-then rules system to get a classification. Different studies corresponding to the ripeness state of a fruit have been proposed using Artificial Neural Networks (ANN). For example, in [4] a system to determine the level of ripeness in palm oil using color features is proposed. The features are submitted as input to the ANN. Oranges are analyzed in [9], where color features and weight features are used for their classification.

In this paper, a classification system of guavas depending of their ripeness state is proposed. The guavas are classified into 3 states: green, ripe and overripe. The images were taken with a conventional camera and natural light. Color features are extracted from images using three color spaces RGB, CIElab and CIEluv. These features are used as input to the ANN where only the components R, G, a, u are used. Our system is tested with real images of guavas, attaining a high accuracy level. The rest of the paper is organized as follows: in the Section 2 the methodology is presented where it is described each state to details, Section 3 results and the accuracy percentage of the system is presented. Finally, in Section 4 conclusion is presented.

2 Methodology

The automatic determination of ripeness state of guavas is of a great interest. In this work, a system for the classification of guavas is proposed. In order to have a good set of guavas with exportation quality, a person has to classify each piece of fruit. For our application, image samples in three main states are studied: green, ripe and overripe. Samples of each state are shown in Figure 1. For this system, 72 images of guavas in different ripeness states were taken. All the images were taken in the same conditions and the guavas were pre-classified by an expert. The images are grouped in two sets training and testing, ensuring that these two sets are completely different.

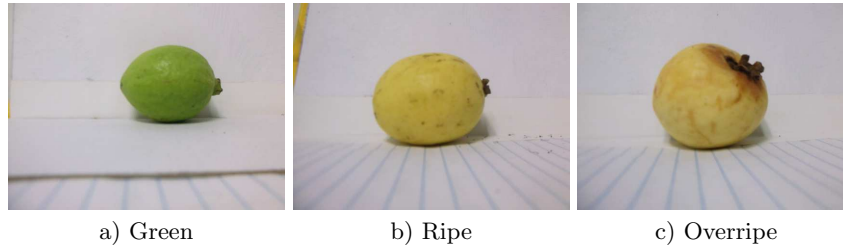


Fig. 1. Guavas in different ripeness states.

The proposed system is developed in two main stages: training and testing. The first stage is performed in three steps: image segmentation, features extraction, neural network training. The second step is achieved in four steps: image segmentation, features extraction, neural network testing and ripeness state classification. The process is shown in Figure 2. Each phase is described in detail in the next subsections.

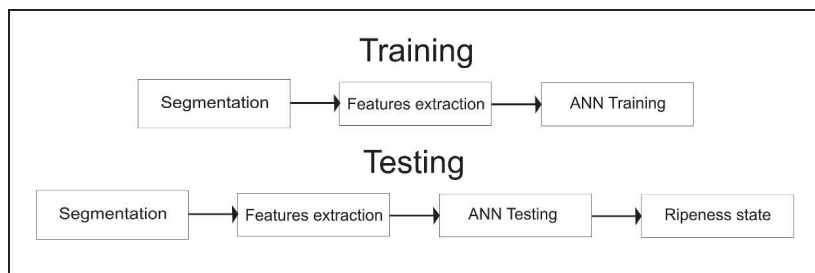


Fig. 2. Classification system.

2.1 Images Segmentation

In order to estimate which pixels correspond to the guava and which to the background, images were segmented. The image segmentation is performed through a sequence of two steps. The first step is to transform the image from RGB space to CIE Lab color space. After that, the image is submitted to the K-means algorithm [11] using the color components of a and b. In this step, the images are separated into two clusters: background and object. In order to select the cluster corresponding to the guava, we take the cluster with the smaller number of pixels. Since the resulting image is not perfectly segmented, it is necessary to apply an additional processing. In this case, we perform a closure operation of mathematical morphology, in order to remove not desire segments. In Figure 3 the complete image segmentation process is shown.

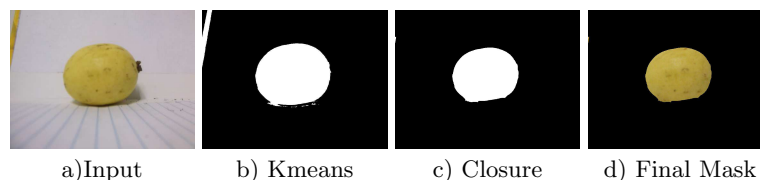


Fig. 3. Image segmentation process.

2.2 Feature Extraction

For the feature extraction, we only use the pixels that correspond to the guava. In this case, we transform the original images in RGB to its representations in CIELab and CIELuv color spaces. Such spaces are defined as follows:

- RGB Color Model: The RGB (Red, Green, Blue) color model is the most important one in digital image processing because it is used by all electronic devices, such as monitors, cameras, etc. In the RGB model, a color is expressed in terms of the amounts of Red, Green and Blue lights.
- CIELab color space: This color space is most commonly known because it is independent of the illumination [13]. L^* is the luminance or lightness component that goes from 0 (black) to 100 (white), the component a^* goes from green to red, and b^* from blue to yellow. The components a and b are the two chromatic components.
- CIELuv color space: This space is similar to CIELab and it is used in applications with low illumination[12]. L^* is the luminance component that goes from 0 (black) to 100 (white), u^* goes from green to red and v^* from blue to yellow, which are the two chromatic components.

The definition of $L^*a^*b^*$ and $L^*u^*v^*$ are based on the intermediate system CIEXYZ which emulates the human perception of color.

When the 3 corresponding images of each color space are obtained, only the pixels corresponding to the guava are used. In our application, we obtain the mean (see Eq.1) of each color component: R, G, a and u, which are the only features that we use for the ANN:

$$\bar{x} = \frac{1}{n} \sum_{i=1}^n x_i, \quad (1)$$

where x represent the value corresponding to the pixel intensity.

2.3 Artificial Neural Network for Guavas Classification

Artificial Neural Networks (ANNs) are a family of models inspired by biological neural networks which are used to estimate, or approximate functions that associate inputs and given outputs. The ANN can be designed using different

parameters [7], in this work, the following factors have been taken: number of layers, number of neurons per layer, activation function, and the learning rate. In our approach, each one of these factors are varied in a range in order to determinate the best parameters for our specific task. For the number of layers we explore in the range of [2, 3]. The number of neurons in the hidden layer were varied in [5,6,...,15]. The learning rate was explored in [0.2,0.5,0.8]. Finally, the activation function was explored using two of the most popular ones: tangent sigmoid (TS) and logarithmic sigmoid (LS). This is in order to get the best combination of parameters and build the optimal ANN for our task. The structure of ANN is shown in Figure 4, where $X = \{x_1, x_2, x_3, x_4\}$ is the input vector and $Y = y_1, y_2, y_3$ is the possible output with three options. In our system, $X = \{R, G, a, u\}$ and $Y = \{green, ripe, overripe\}$.

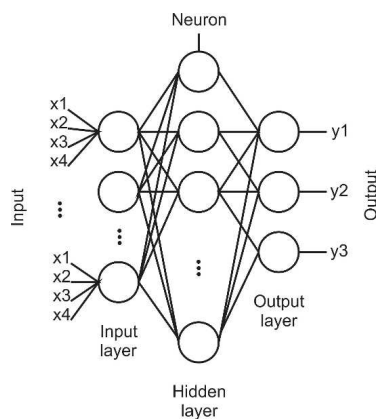


Fig. 4. Structure of Artificial Neural Network.

3 Results

At the end of our experiments, we have tested 786 different architectures with the different combinations of parameters. The performance of our system was evaluated using the number of images correctly classified. In our application, many architectures have achieved the same highest results of 97.44% of accuracy. However, the final results were obtained with the parameters: activation function = TS, learning rate = 0.2, two layers, input layer with 4 neurons and output layer with 3 neurons.

In Table 1 the confusion matrix for each class is shown. In this table we can see that the accuracy in each class is of 92.3%, 100%, and 100% for the green, ripe and overripe classes, respectively. As it was previously mentioned, 72 images were taken and they were grouped in two sets: training and testing, where 36 images were used to training and 36 for testing. As it can be seen in this table,

our method proposes a novel methodology, which is able to detect 3 different states of guavas with an accuracy of 97.44%.

Table 1. Confusion matrix of the ANN in our proposal.

	Green Ripe	Overripe	Average	
Green class	92.30	7.69	0	92.30
Ripe class	0	100	0	100
Overripe class	0	0	100	100
	Total average			97.44

In order to evaluate the performance of our method with other approaches we select some of the most common classifiers: Naive Bayes and Fuzzy Inference. Results of such classifiers using the basic parameters and the same set of images and features, are depicted in Table 2. As we can see, Naive bayes achieves an accuracy of 89.4737% and the fuzzy system achieve an accuracy of 84.2105%. Our method attains a performance higher than 97%.

Table 2. Table of accuracy of different methods.

Method	Accuracy
Neural network [7]	97.44%
Classifier of bayes [3]	89.47%
Fuzzy System [10]	84.21%

4 Conclusion

A ANN-based system for the classification of ripeness state of guavas has been discussed. Our method uses color features from 3 different color spaces, which allows us to properly discriminate between the three states. The proposed methodology explores different parameters of the ANN in order to achieve the best architecture for this specific task. In this sense, we can see that our system is an appropriate option for the agricultural industry for the automatic determination of the ripeness state of guavas.

Acknowledgements. This research was supported by the University of Guanajuato and the PRODEP through the NPTC project with number DSA/103.5/15/7007.

References

1. A. Yam Tzec, J., Villaseñor Perea, C. A. Romantchik Kriuchkova, M.S.E., Peralta, M.P.: Una revisión sobre la importancia del fruto de guayaba (*psidium guajava* l.) y sus principales características en la postcosecha. *Revista Ciencias Técnicas Agropecuarias* 19(4), 74–82 (2010)
2. Chaudhary, S., Prajapati, B.: Quality analysis and classification of bananas using digital image processing. *International Journal of Computer Science and Engineering (IJCSE)* 3, 29–36 (2014)
3. Ekdahl, M.: Approximations of bayes classifiers for statistical learning of clusters (2006), report code: LiU-TEK-LIC 2006:11.
4. Fadilah, N., Saleh, J.M., Ibrahim, H., Halim, Z.A.: Oil palm fresh fruit bunch ripeness classification using artificial neural network. In: *Intelligent and Advanced Systems (ICIAS), 2012 4th International Conference on*. vol. 1, pp. 18–21. IEEE (2012)
5. Filipovich, H., Ugarte, M.G., Cruz, D.E., Díaz, S.Q.: Beneficios de la guayaba para la salud. *Revista de Investigación e Información en Salud* p. 27
6. Goel, N., Sehgal, P.: Fuzzy classification of pre-harvest tomatoes for ripeness estimation—an approach based on automatic rule learning using decision tree. *Applied Soft Computing* 36, 45–56 (2015)
7. Hagan, M.T., Demuth, H., Beale, M., De Jesús, O.: *Neural network design*, vol. 20. PWS publishing company Boston (1996)
8. Intaravanne, Y., Sumriddetchkajorn, S., Nukeaw, J.: Ripeness level indication of bananas with visible and fluorescent spectral images. In: *Electrical Engineering/Electronics, Computer, Telecommunications and Information Technology (ECTI-CON), 2012 9th International Conference on*. pp. 1–4. IEEE (2012)
9. Kondo, N., Ahmad, U., Monta, M., Murase, H.: Machine vision based quality evaluation of iyokan orange fruit using neural networks. *Computers and Electronics in Agriculture* 29(1), 135–147 (2000)
10. Kuncheva, L.: *Fuzzy classifier design*, vol. 49. Springer Science & Business Media (2000)
11. Lloyd, S.: Least squares quantization in PCM. *IEEE Transactions on Information Theory* 28(2), 129–137 (1982)
12. Mahy, M., Eycken, L., Oosterlinck, A.: Evaluation of uniform color spaces developed after the adoption of cielab and cieluv. *Color Research & Application* 19(2), 105–121 (1994)
13. Mendoza, F., Dejmek, P., Aguilera, J.M.: Calibrated color measurements of agricultural foods using image analysis. *Postharvest Biology and Technology* 41(3), 285–295 (2006)
14. Nasaruddin, A.S., Baki, S.R.M.S., Tahir, N.: Watermelon maturity level based on rind colour as categorization features. In: *Humanities, Science and Engineering (CHUSER), 2011 IEEE Colloquium on*. pp. 545–550. IEEE (2011)
15. Wang, X., Mao, H., Han, X., Yin, J.: Vision-based judgment of tomato maturity under growth conditions. *African Journal of Biotechnology* 10(18), 3616–3623 (2011)

A BDI Agent System for the Collaboration of the Unmanned Aerial Vehicle

Mario Hernandez Dominguez, Jose-Isidro Hernández-Vega,
Dolores Gabriela Palomares Gorham, C. Hernández-Santos,
Jonam L. Sánchez Cuevas

Instituto Tecnológico de Nuevo León, División de Estudios de Posgrado e
Investigación, Nuevo León, Mexico

marioingmecatronica94@hotmail.com, jose.isidro.hernandez@itnl.edu.mx,
dolores.gabriela.palomares@itnl.edu.mx, carlos.hernandez@itnl.edu.mx,
jonam.leonel.sanchez@itnl.edu.mx
<http://posgrado2.itnl.edu.mx>

Abstract. This project describes the implementation of a BDI architecture for solving problems of collaboration and coordination among aerial mobile robots used through Unmanned Aerial Vehicle (UAV). A Multi-Agent System is implemented in people search and it is developed on Jason software. The benefits of developing this model is diverse such as optimizing the collaborative work among intelligent agents being able to use artificial intelligence in aerial mobile robots, improving the decision making process.

Keywords: Multi-agent system, distributed systems, collaborative agent.

1 Introduction

The purpose of this article is to present the simulation of a multi-agent model using the BDI architecture, where we can observe the way of communication to achieve a common goal of the agents. All this developed in a development environment in Jason 1.4.2.

This article contains an introduction, research related to multi-agent systems are exposed, then in the methodology we describe the theoretical resources that support the model of coordination and communication of multi-agent system, then we can locate the results, we expose images of the simulation model and we observe how agents are coordinated to achieve a common goal. And finally the conclusions of the authors of this investigation as well as discussions generated.

The contribution to the scientific community of this article is to disseminate the work being done on agents oriented programming with the help of Jason 1.4.2 software for the simulation and analysis of logic programming lines for multi-agent systems and to take this tool to improve the response of mobile robots.

Based on the “divide and conquer” principle, widely used in computer algorithms, it arises an existing problem in aerotronics area which consists in finding the way to work collaboratively between two unmanned aerial vehicles (UAV) in order to solve people searching jobs, using the Belief-Desire-Intention architecture coordination model (BDI).

Currently, UAVs are being implemented in various activities such as civilian areas (forest services, cartography, environment), agriculture, cinematography, military industry (security and border control), among others, and reviewing the history it shows that when the tasks are divided in an organized manner efficiency and breadth of the required objectives increases.

The collaboration and coordination among aerial mobile robot lies when an area is surrounded with more than one drone, there isn't collaboration between them to accomplish an assignment. On the other hand, the person to the assignment and the person controlling such equipment usually wastes time programming repeatedly the tasks to be performed, even when different drones do the same is the same work or part of the work, or while he is reviewing the information sent from both UAVs wasted in the searching that may be of vital importance to the victim or victims, an example would be in a mountain area where the forest guard service could have two drones that could generate the above described condition. As a result of the research, it is expected to build a communication bridge and coordination between drones, making it possible to collaborate between them. At the same time this will improve the autonomy of the unmanned vehicles insomuch as are based in BDI architecture.

After giving a short introduction to the investigation below is displayed in Figure 1 a very abstract model that may be taken to give a quick idea that we will see below in the simulation.

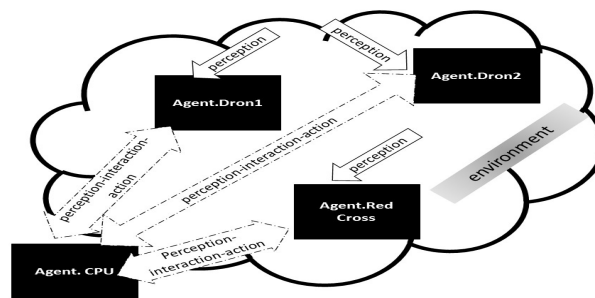


Fig. 1. An abstract model of the multi-agent system environment.

1.1 State of the Art

Agents using architecture BDI are characterized by having mental states (beliefs, desires, intentions) [13]. The great achievements of this architecture is due to

the component mixture as a philosophical model of simple human reasoning to understand, a large number of implementations [10] and an abstract logical syntax that has been accepted by the scientific community [9,17,19]. Reviewing the literature we have found various kinds of advances in the area of artificial intelligence and even more in the implementation of the theory of agents for improving processes, these developments are as follows:

The air traffic management system (OASIS) [8] are integrated mostly of agents, all these designed to following the structure of agents in any of their category. The odd in this system is the selection of a flight's trajectory. In this system the agents collaborate to choose the best path reduce the fuel consumption and rise the flight's productivity. This ensures the target in the estimated time of arrival. This system has been used in the Sidney airport. Tasks Control Air Traffic are divided into sub-blocks in architecture OASIS and an agent is selected to solve each one of those sub-blocks. Each agent solves its part independently and the social cooperation with the rest define the course of the Global System. An operation agent will then exist for each airplane other : In addition to agents acting as controllers path, sequencers, Wind Moderators, Coordinators [3]. A modeling system dogfight with the name SWARMM [16] which can encode the tactics adopted by pilots in combat areas and generate agents that real pilots can participate in simulation studies. The system models from the physical aspects of airplane like the tactical knowledge and way of thinking of the pilots.

In [5] a deliberative architecture the methodological framework in systems that provide case-based reasoning is observed. The system of reasoning leads building plans from the beliefs and intentions. Regarding the problem to be solved and methods used in each of the four stages defined by the system of reasoning, the agent can plan on the completion time using variational calculation [11]. This model has been handled in the development of industrial applications, the construction sector [4] and the promotion of mobile applications [5].

Agents comprising the AFRAS System(A Fuzzy Reputation Agent System) are dedicated to the buying and selling of services. The AFRASS system aims to simulate the operation of human society in the management and communication of this prestige generated by people when making a purchase, and the informal bargaining that takes place between individuals [2].

Agents were presented and formally defined a BDI architecture for high-level control of land mobile robots soccer . This architecture builds on top of a layer system . This system architecture provides the necessary level of abstraction that makes cognitive reasoning. This design allows abstraction and modulation of the different aspects of the complex domain represents the robotic football [12].

To the research area of UAVs, where the research results propose an integration between a UAV team and a camera for image processing automatically [20].

Das [7] proposes the implementation of an existing computer architecture to control the behavior of autonomous underwater vehicles (AUVs), reactive deliberative approach is the most effective and meaningful to control vehicle

behavior. However, little work has been done in the field of modeling the system to simulate and analyze the dynamic behavior run hybrid control architecture.

Christopher sets out the implementation of a distributed system client slave collaboration of three marine robots which maintains control of a formation preserving the distances between them and their positions [14].

The first steps for the integration of a system of distributed discrete event simulation within a framework of intelligent software agents are proposed. It begins with a single agent that implements the BDI approach which is applied to the monitoring for TBM excavation project [15].

The goal was to design and equalize a model based on a BDI architecture for collaborative search tasks between two drones. The innovation this model is the use of targeted agents under BDI architecture for collaborative work on unmanned aerial vehicles.

2 Methodology

According to [6] the organization in the multi-agent system (M.A.S.) depends on the kind of communication and the way agents cooperate between them, as well as the kind of agent the group comprises. Generally speaking there are three basic organizational configuration types:

1. Centralized Structure: In this type of configuration exist an agent that controls the interaction of the other agents of the system because it has the information or the functionality to do so.
2. Horizontal structure.
3. Hierarchical structure.
4. AD HOC structure.

The main goal that was accomplished with the model was to see how is the behavior of the entities based on the BDI architecture and how speaking actions will be executed to generate a collaboration and coordination environment between mobile flying robots. The table 1 describes PEAS (Performance, Environment, Actuators, Sensors) of the task environment that is used in this model and where some of the characteristics of the implemented agents are presented.

Table 1. PEAS description of the task environment for the multi-agent system.

Type Agent	Performance Measures	Environment – Forest	Actuators	Sensors
Agent – Controller – CPU-brain	Planning time	persons, agents	Sending messages	Message receiver
Agent – Receptor – DRON1,2	Minimize lost people searching time	Agents	Alarm	Camera, GPS
Agent – Receptor – Red-Cross	Number of rescued persons.	Persons, Agents	Motors figure	GPS

In the table 2 shown the task environment characteristics for this model are extended and described [18].

Table 2. Task environments and their characteristics.

task environment	Observable	Deterministic	Episodic	Static	Discreet	Agent
Searching environment	Totally	Stochastic	Sequential	Dynamic	Continue	Cooperative Multi-agent

- It is considered totally observable, due to the fact that sensors give the agent access to the complete state of environment in every moment of his route.
- It is considered the stochastic system, due to the fact that the next medium state isn't totally determined by the actual state and the executed action by the agent because it can't be possible to exactly predict neither human behavior nor the atmospheric or climatic conditions.
- It is considered sequential, due to the fact that decisions can affect future actions.
- It is considered dynamic, due to the fact that environment can change when the agent is delivering.
- It is considered Continuous, due to the fact that location of the drones goes through a range of continuous values in a soft way over time.
- It is considered Cooperative Multi-agent, due to the fact that finding missing people maximizes performance measure of the agents in a multi-agent environment that is partially cooperative.

2.1 Agents Characteristics and the Environment

Communication in multi-agent systems is usually based on the speaking actions paradigms and communication languages between agents KQML and FIPA [1]. The main speaking actions of the implemented agents in the model are represented in figure 2. These actions help us to generate a collaboration environment in order to reach the objective assigned to the agents.

States of Agents Tables 3, 4, 5 present how agent planning is defined and table 6 presents the environment methods.

Table 3. Agent CPU.

Plan	Description
+! Find (object)	This plan execute's the searching system starts working.
!+End (research1)	When this plan is executed, assumptions of a lost item are lowered.
! + Finish (base1):	When this plan is executed, assumption of returning to the base are lowered since it's already there.
+ Saving (person)	When this plan is executed, Red Cross is notified that has a person to rescue.
+! Protected (person)	When this plan is executed, Red Cross is notified that there isn't any person to be rescued.

Agents and Perceptions

- CPU Agent.
 - This agent is responsible for distributing and coordinating the main task.

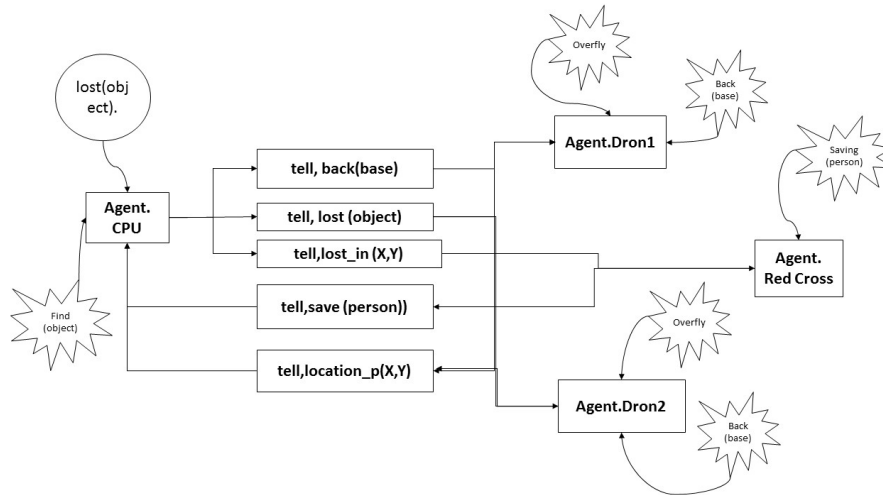


Fig. 2. System overview diagram.

Table 4. Agent Red Cross.

Plan	Description
+ Saving (person)	This plan is executed, a variety of rescuing plans are made.
+! Carry_to (R)	This plan is executed, victim is located in order to be rescued.
+ Attending (person)	This plan is executed, there is a transportation to the place where the person is.
+! At (L)	Corroboration about being in the same place as the victim is done.
+! Carry_to1 (R)	When this plan is executed, victim is returned to the right place.
! Take (S, L)	This plan is executed, a simulation of grabbing the victim is done.
+! Ensure_obj (S)	This plan is executed, a simulation of the victim being in the vehicle is done.
+! At1 (L)	This plan is executed, victim is returned to the starting spot.

- Perceptions of this type of agent are present in the speaking messages with the agent, mainly because perceptions depend on the other agents messages.
- UDOO1,2 Agent.
 - This agent is in charge of reviewing the assigned area by the CPU in the search for missing people.
 - Perceptions of this type of agent are generated by cameras and GPS.
- Red Cross Agent .
 - This agent is in charge of bringing help to people
 - Perceptions of this kind of agents are observed using a GPS.

Environment structure How environment in the JAVA programming language is structured, to go from the modeling state to the simulation part.

- Environment.
 - Libraries.- Java and Jason libraries were used in order to be able to use methods of both programming languages.

Table 5. Agent Dron1,2.

Plan	Description
+! Overfly (agent.CPU, object)	When this plan is executed, agents do the selected tour.
+ End.r (r2)	When this plan is executed, the CPU is notified that the tour is over.
+ Camera (r2)	When this plan is executed, a person is found on the map.
+! Back (base)	When this plan is executed, drones have to return from the selected point to the starting spot.

Table 6. Agent Environment.

Plan	Description
UpdatePercepts ()	This method includes the methods that are called by the agents.
NextSlot ()	Move one space to UDOO1 inside the grip.
NextSlot1 ()	Move one space to UDOO2 inside the grip.
MoveTowards (int x, int y)	Move the Red Cross to the victim spot.
To return()	Move one space from the grip to UDOO1 base.
To return1 ()	Move one space from the grip to UDOO2 base.
Pickobj ()	Grab the victim in the map.
Dropobj ()	Place the victim in the base.
Burnobj ()	Register the victim as sheltered.

- Environment extends Environment.- The model are declared as well as the starting locations that are sent to the agents "updatePercepts()".
- MarsModel extends GridWorldModel.- Locations are assigned to the graphic model and the methods to answer to a executeAction class calling.
- MarsView extends GridWorldView.- This class brings life to our simulation because color and labels to the model.
- ExecuteAction.-This type is where sent directions from the agents are classified. Directions have to be reflected on the environment.

In table 7 Speaking actions applied to the model are presented as well as one agents activities cycle, starting from CPU agent assuming the believing of having a missing person and going through the requirement to the drones of flying over certain area, the assistance of the Red Cross agent and concluding when drones return to the base.

3 Results

The results are presented as a simulation held in Jason software, hereafter it is presented a of images where the interaction among the agents and environment.The algorithm executed down filing a joint policy for multi-agent where making a comparison in the simulation between the algorithm with a single unmanned aerial vehicle in the environment and 2 UAV, which is presented below, we saw that the search time is reduced 50% on the search area.

Table 7. Speech acts within one simulation cycle.

Cycle	Agent	Actions	Belief	Goals	Plans
1	CPU		lost (object)		
2		.send ([agent_UDOO1, agent_UDOO2], tell, lost (object))			
3		.send ([agent_UDOO1, agent_UDOO2], achieve, overfly (agent_CPU, object))			
4	UDOO1,2		lost (object)		
5					! Overfly (agent_CPU, object)
6	Red Cross			saving (person)	
7	UDOO1,2				+ camera (r2)
8		.send (agent_CPU, tell, location_p (X, Y))			
9		.send (agent_CPU, achieve, save (person))			
10	CPU		location_p (X, Y)		
11					+ saving (person)
12		.send (agent_Red_Cross, tell, lost_en (X, Y))			
13		.send (agent_Red_Cross, achieve, save (person))			
14	Red Cross		lost_en (X, Y)		
15					save (person)
16		.send (agent_CPU, achieve, protected (person))			
17	CPU				protected (person)
18		.send (agent_Red_Cross, untell, lost_en (X, Y))			
19		.send (agent_Red_Cross, unachieve, save (person))			
20	Red Cross		-lost_en (X, Y)		
21					-save (person)
22	UDOO1,2				+ end_r (r2)
23		.send (agent_CPU, achieve, terminate (research1))			
24	CPU				end (research1)
25		.send ([agent_UDOO1, agent_UDOO2], untell, lost (object))			
26		.send ([agent_UDOO1, agent_UDOO2], tell, back (base))			
27		.send ([agent_UDOO1, agent_UDOO2], achieve, return (base))			
28	UDOO1,2		-lost (object)		
29			return (base)		
30					return (base)
31	UDOO1,2				+ end(r2)
32		.send (agent_CPU, achieve, terminate (base1))			
33	CPU				end (base1)
34		.send (agent_UDOO1, untell, back (base))			
35	UDOO1,2		-back (base)		

Time 1 Shows the beginning of the search within the organized environment by the CPU agent, thus, the collaboration between air agents UDOO1 and UDOO2, to make path in the area.

Time 2 Shows how the red cross land agent goes to the point located by air agents UDOO1, 2 where a person is.

Time 3 Shows how the red cross land agent returns with the victim to a safe area.

A BDI Agent System for the Collaboration of the Unmanned Aerial Vehicle

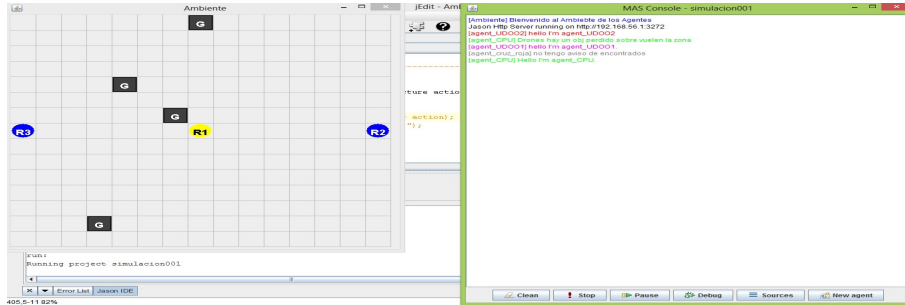


Fig. 3. Graphical interface of the multi-agent system environment.

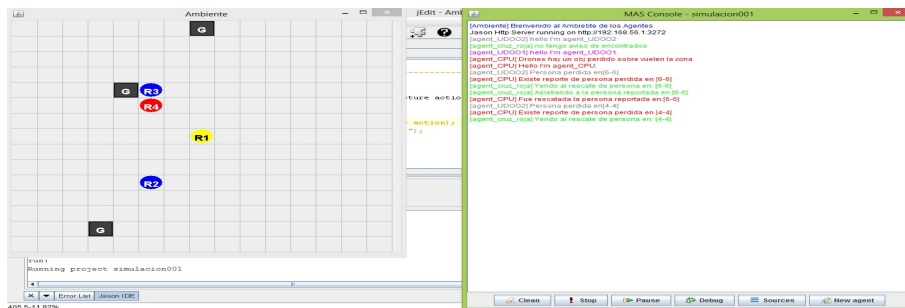


Fig. 4. Graphical interface of the multi-agent system environment.

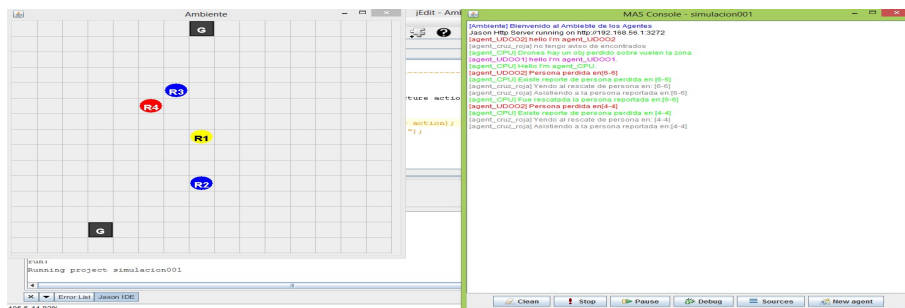


Fig. 5. Graphical interface of the multi-agent system environment.

Time 4 Shows how air agents UDOO1, 2 when arriving to the final point, they return to base.

Time 5 Shows all speech acts of agents in the environment as a result of the collaboration among them.

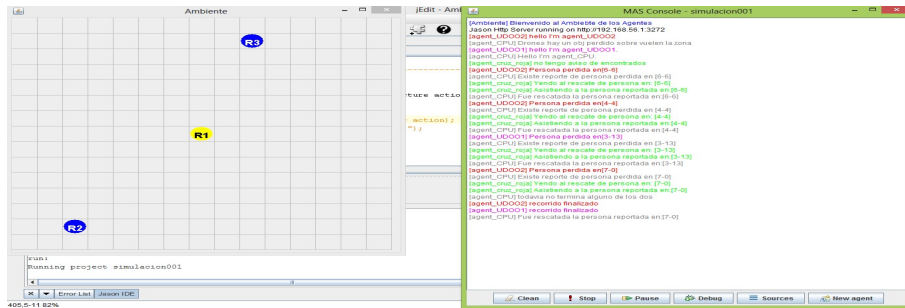


Fig. 6. Graphical interface of the multi-agent system environment.

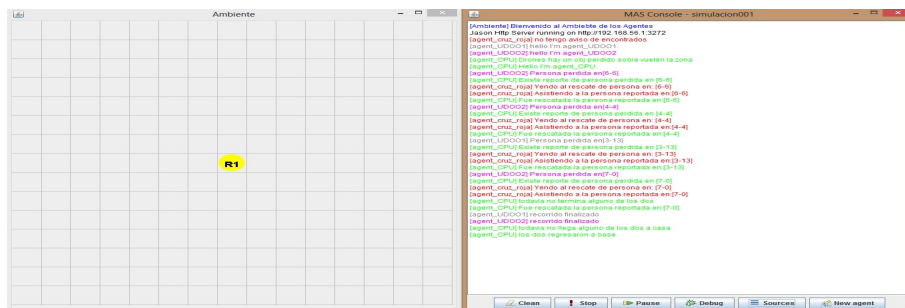


Fig. 7. Graphical interface of the multi-agent system environment.

4 Discussion

In the prior art can be seen that multi-agent developed in sequential programming models are more complex than those currently proposed to the programming paradigm agent oriented, where, as it is easier to the programmer to give the knowledge to the agent, since working with a high-level language, as for the agent that helps it having more autonomy to obtain information from the environment where it is and act accordingly. Having this kind of study done, it is expected it can channel new multi-agent models applicable to air mobile robots on this new type of programming paradigm.

5 Future Work

Future work will focus on bringing this simulation to practice and to be able to materialize using embedded cards as UDOO NEO as well as also to generate collaboration and coordination between UAVs as Parrot Bebop Drone and the laptop, which is shown in Figure 8.

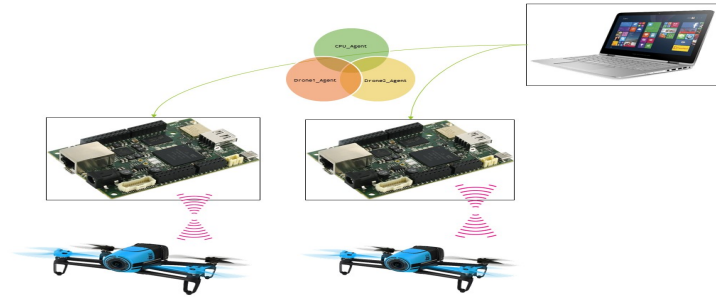


Fig. 8. Scheme of the multi-agent system.

6 Conclusion

It is concluded that collaborative communication environment may be generated among air mobile robots using intelligent agents so that we can get closer to human intelligence reproduction with the help of new programming paradigms as are, oriented agents and BDI architectures. It was, it was observed that the multi-agent systems facilitate solving tasks due to integration of diverse robotic entities within the same objective. In their daily basis because they can delegate to more complex robotic entities responsibilities. All the described above shows that these models are a new research tool with a very extensive application field in years to come. And we can conclude that the simulation based on the BDI architecture can generate a collaboration and coordination, including UAV's. because in the simulation UAVs share their tasks to achieve its objectives.

References

1. Bordini, R.H., Hübner, J.F., Wooldridge, M.: Programming multi-agent systems in AgentSpeak using Jason, vol. 8. John Wiley & Sons (2007)
2. Carbo, J., Molina, J.M., Davila, J.: Trust management through fuzzy reputation. *International Journal of Cooperative Information Systems* 12(01), 135–155 (2003)
3. Corchado, J.M.: *Agencia: Una puerta hacia la convergencia de la inteligencia artificial*. Universidad de Salamanca (1999)
4. Corchado, J.M., Laza, R.: Constructing deliberative agents with case-based reasoning technology. *International Journal of Intelligent Systems* 18(12), 1227–1241 (2003)
5. Corchado, J.M., Pavón, J., Corchado, E.S., Castillo, L.F.: Development of cbr-bdi agents: a tourist guide application. In: *European Conference on Case-based Reasoning*. pp. 547–559. Springer (2004)
6. Corchado, J.M.: 2 modelos y arquitecturas de agente
7. Das, S., Shome, S., Nandy, S., Pal, D.: Modeling a hybrid reactive-deliberative architecture towards realizing overall dynamic behavior of an auv. *Procedia Computer Science* 1(1), 259–268 (2010)
8. Georgeff, M., Rao, A.: Rational software agents: from theory to practice. In: *Agent technology*, pp. 139–160. Springer (1998)

9. Georgeff, M., Pell, B., Pollack, M., Tambe, M., Wooldridge, M.: The belief-desire-intention model of agency. In: International Workshop on Agent Theories, Architectures, and Languages. pp. 1–10. Springer (1998)
10. Georgeff, M.P., Lansky, A.L.: Reactive reasoning and planning. In: AAAI. vol. 87, pp. 677–682 (1987)
11. Glez-Bedia, M., Corchado, J., Corchado, E., Fyfe, C.: Analytical model for constructing deliberative agents. *Engineering Intelligent Systems for Electrical Engineering and Communications* 10(3), 173–185 (2002)
12. Gottifredi, S., Tucac, M., Corbatta, D., García, A.J., Simari, G.R.: A bdi architecture for high level robot deliberation. In: XIV Congreso Argentino de Ciencias de la Computación (2008)
13. Haddadi, A., Sundermeyer, K.: Belief-desire-intention agent architectures. *Foundations of distributed artificial intelligence* pp. 169–185 (1996)
14. Mas, I., Kitts, C.A.: Dynamic control of mobile multirobot systems: The cluster space formulation. *IEEE Access* 2, 558–570 (2014)
15. Ourdev, I., Xie, H., AbouRizk, S.: An intelligent agent approach to adaptive project management. *Tsinghua Science & Technology* 13, 121–125 (2008)
16. Rao, A.S., Georgeff, M.P.: An abstract architecture for rational agents. *KR* 92, 439–449 (1992)
17. Rao, A.S., Georgeff, M.P.: Decision procedures for bdi logics. *Journal of logic and computation* 8(3), 293–343 (1998)
18. Russell, S., Norvig, P.: *Inteligencia artificial: Un enfoque moderno* (2004)
19. Schild, K.: On the relation between standard bdi logics and standard logics of concurrence. In: *Proceedings of the Fifth International Workshop on Agent Theories, Architectures and Languages (ATAL-98)*, Lecture Notes in Artificial Intelligence. Springer-Verlag, Heidelberg (1999)
20. Srikanth, M., Bala, K., Durand, F.: Computational rim illumination of dynamic subjects using aerial robots. *Computers & Graphics* 52, 142–154 (2015)

CAD design and Identification of Hydrodynamic Parameters of an Underwater Glider Vehicle

Jorge Díaz Moreno¹, Reynaldo Ortíz Pérez¹, Eduardo Campos Mercado¹,
Luis Fidel Cerecero Natale^{1,2}

¹ Universidad Politécnica de Pachuca, Posgrado en Mecatrónica,
Zempoala, Hgo., Mexico

² Instituto Tecnológico de Cancún, Ingeniería en Mecatrónica,
Cancún, Quintana Roo, Mexico

jorge.diaz@micorreo.upp.edu.mx

Abstract. This article describes the design, modeling and identification of the main hydrodynamic parameters of an underwater glider vehicle is presented. The equations describing the dynamics of the vehicle is obtained from the Euler-Lagrange method. The main hydrodynamic parameters were obtained considering the geometry of the vehicle and its operating characteristics. Finally, simulation open loop system are presented.

Keywords: Hydrodynamic parameters, underwater glider vehicle.

1 Introduction

Unmanned underwater vehicles are classified in ROV's (Remotely Operated Vehicle) and AUV vehicles (Autonomous Underwater Vehicles) [8]. The Gliders are a type of AUV that control their own buoyancy and can spend long periods of time under water due to its autonomy low power consumption, because they usually do not use propellers or cables to the ship [4]. The diversity of underwater activities is wide and Gliders have efficient ways to perform tasks such as: to contribute to research, inspections and assessments, exploration of marine flora and fauna, deep-sea exploration for oil projects, search and rescue of objects in areas risk to humans [7].

The Gliders are underwater vehicles designed to carry out exploration, inspection, maintenance and surveillance, among others [8]. Most gliders have a cylindrical shape, this to minimize the effect of hydrodynamic damping and consequently the lower the energy required for vehicle propulsion [6].

The same laws of hydrodynamics governing the flow of the medium and the forces for air carriers can apply for underwater vehicles, but due to the high density of water (800 times greater than air) add effects buoyancy and masses added that they are significant in the dynamics of Glider [9]. The characteristic movement of a Glider describes a pattern in the form of sawtooth as shown in

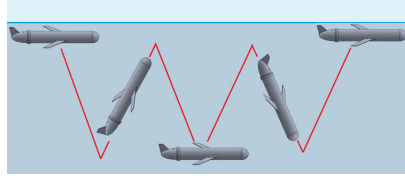


Fig. 1: Characteristic movement of a Glider.

Figure 1. They can carry sensors to measure physical environmental parameters, biogeochemical, acoustic and collect data on chlorophyll, I oxygen temperature, salinity [1] and if so, to estimate undercurrents or maritime density gradients, reproduction and primary study marine ecosystems, research on tracking whales and other marine mammals, among others [13].

Although usually these vehicles travel at low speed (average 0.4 m/s [9]), Glider design was adapted to improve performance in displacement and hydrodynamic forces, with the help of several sketches based on the mechanical design methodology Nigel Cross [10].

2 Description of a Glider

Gliders geometry is important for propulsion and maneuverability factor at different speeds. One of the most common ways in Gliders is torpedo-shaped consisting of a cylindrical body with its conical or spherical tips to simplify identification of the hydrodynamic parameters [11]. Accordingly, the geometry of the vehicle UPPGlider presented in this paper it is cylindrical, with a diameter of 15.4 cm and a length of 90 cm, see Figure 2. Based on the design of the vehicle and in order to simplify the mathematical model of UPPGlider, Assuming that the vehicle is moving at low speed, that is 0.25 m/s.

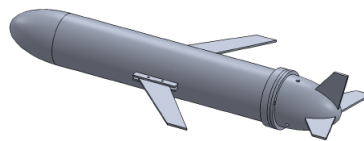


Fig. 2: UPPGlider: CAD design of the underwater vehicle.

Immersion and emersion (offset from the axis Z_I) vehicle is generated by changing its buoyancy ballast tank, while the displacement in the plane X_I, Y_I is produced by the wings, the orientation of the vehicle and changing buoyancy [3]. The angular position *roll* (ϕ) remains close to zero due to the location of the

center of buoyancy and the center of gravity of the vehicle, the side wings help the damping *roll*; while the rotational movement *pitch* (θ) It is produced by the effect of a moving mass and rotation *yaw* (ψ) It is governed by a rudder that is located in the tail of the vehicle [2].

The embedded system consists of a computer 2.9GHz Intel Core i7-3520M, 8GB of RAM, Windows 8.1 operating system and Visual Studio C++ 2010 to program the control strategy. Measurements of the inertial unit and the pressure sensor are performed with a USB-I2C interface connected directly to the PC. The main characteristics of the vehicle are described in Table 1.

Table 1: Main features of the UUP Glider.

Dough	15 kg
Buoyancy	9 N
Dimensions	90 cm (l) x 15.4 cm (w) x 15.4 cm (h)
Operating depth	100m
Operating Voltage	14V
Computer	NUC intel core i7 - 2.9GHz Windows 8.1 Professional 64 bits Microsoft Visual C++ 2010

3 Mathematical Model

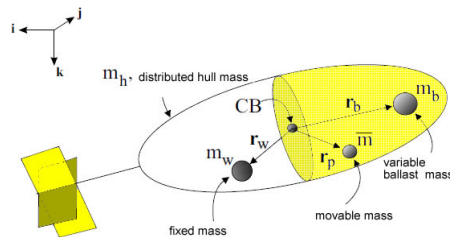


Fig. 3: Definition of mass of the Glider. [5]

The vehicle is modeled as a rigid body immersed in a fluid with fixed wings and tail, with the particularity that the total vehicle mass m_v , is the sum of the mass of the hull m_h , calibration mass m_w , the moving mass \bar{m} and mass ballast tank m_b ; whose location with respect to the coordinate system fixed to the vehicle body, is described by the vectors $r_h = 0$, r_w , r_p y r_b respectively, as shown in

Figure 3. It is noteworthy that the mass ballast tank is variable (m_b) but their position is constant, whereas the moving mass (\bar{m}) It is constant but is variable position.

To describe the force produced by the buoyancy has to the mass of the fluid displaced by the vehicle is denoted by m . Consequently, the net buoyancy is defined as: $m_0 = m_v - m$ so the vehicle has positive buoyancy if $m_0 > 0$.

The equations describing the dynamics of Glider are obtained starting in the momentum, which you have to p It represents the moment of translation of the vehicle and the fluid and π the angular momentum, momentum both expressed respect to the inertial coordinate system. In the case of translational momentum is must p_p It represents the total momentum of the moving mass \bar{m} , p_b they represent the momentum of the mass of ballast tank m_b and p_w describes the momentum of the mass m_w . Considering the above and Newton's laws we have:

$$\begin{aligned}
 \dot{p} &= \sum_{i=1}^I f_{ext_i}, \\
 \dot{\pi} &= \sum_{i=1}^I (x_i \times f_{ext_i}) + \sum_{j=1}^J \tau_{ext_j}, \\
 \dot{p}_p &= \bar{m}g\mathbf{k} + \sum_{k=1}^K f_{int_pointmass_k}, \\
 \dot{p}_b &= m_b g\mathbf{k} + \sum_{l=1}^L f_{int_ballast_l}, \\
 \dot{p}_w &= m_w g\mathbf{k} + \sum_{n=1}^N f_{int_w_n},
 \end{aligned} \tag{1}$$

where k is the unit vector in the direction of gravity, f_{ext_i} an external force is applied to the system and τ_{ext_j} It is an external torque. The vector x_i The vector is the location of the application point of force f_{ext_i} with respect to the inertial coordinate system. These external forces and torques include those due to gravity and buoyancy; however, gravity is explicitly included in the last three equations because it is the only force acting on the three masses. The force $f_{int_pointmass_k}$ is applied from the vehicle body to the mobile hub, it will be used as a control input. The forces $f_{int_ballast_l}$ y f_{w_n} are the forces applied from the vehicle body to the ballast system and mass calibration respectively.

In order to obtain the representation of the mathematical model with respect to the coordinate system fixed in the vehicle, it has to P It represents the momentum of the vehicle and Π the angular momentum, both expressed in the coordinate system of the vehicle. The momentum of the moving mass is represented by P_p , on the other hand; P_b y P_w They represent the momentum of the mass of the ballast tank and the mass calibration of the vehicle respectively. From the above it has the following expression:

$$\begin{aligned}
 p &= RP, \\
 \pi &= R\Pi + b \times p, \\
 p_p &= RP_p, \\
 p_b &= RP_b, \\
 p_w &= RP_w.
 \end{aligned} \tag{2}$$

Deriving the equations in (2) and using the expressions of kinematics and by substituting equation (1) it follows that:

$$\dot{P} = P \times \Omega + R^T \sum_{i=1}^I f_{ext_i}, \quad (3)$$

$$\dot{H} = H \times \Omega + P \times \nu + R^T \left(\sum_{i=1}^I (x_i - b) \times f_{ext_i} \right) + R^T \sum_{j=1}^J \tau_{ext_j}, \quad (4)$$

$$\dot{P}_p = P_p \times \Omega + \bar{m}g(R^T k) + R^T \sum_{k=1}^K f_{int_pointmass_k}, \quad (5)$$

$$\dot{P}_b = P_b \times \Omega + m_b g(R^T k) + R^T \sum_{l=1}^L f_{int_ballast_l}, \quad (6)$$

$$\dot{P}_w = P_w \times \Omega + m_w g(R^T k) + R^T \sum_{n=1}^N f_{int_w_n}, \quad (7)$$

where $R^T \sum_{k=1}^K f_{int_pointmass_k}$ is the internal force acting on the mass point \bar{m} in the coordinates of the vehicle body. Be:

$$\bar{u} = \begin{bmatrix} \bar{u}_1 \\ \bar{u}_2 \\ \bar{u}_3 \end{bmatrix} = P_p \times \Omega + \bar{m}g(R^T k) + R^T \sum_{k=1}^K f_{int_pointmass_k}. \quad (8)$$

such that

$$\dot{P}_p = \bar{u}.$$

\bar{u} internal strength is not the point mass in gravitational forces because centrifuged \bar{m} they have been included in the expression for \bar{u} , also is:

$$u_b = \begin{bmatrix} u_{b1} \\ u_{b2} \\ u_{b3} \end{bmatrix} = P_b \times \Omega + m_b g(R^T k) + R^T \sum_{l=1}^L f_{int_ballast_l}, \quad (9)$$

$$u_w = \begin{bmatrix} u_{w1} \\ u_{w2} \\ u_{w3} \end{bmatrix} = P_w \times \Omega + m_w g(R^T k) + R^T \sum_{n=1}^N f_{int_w_n}. \quad (10)$$

So:

$$\dot{P}_b = u_b,$$

$$\dot{P}_w = u_w.$$

The terms $\frac{d}{dt} I^{-1}(i, j)$ They are usually small in existing Glider. \dot{r}_w y \dot{r}_b they are zero. \dot{r}_p it is zero in balancing the gliders and is small during transitions

between equilibrium (due to the speed of actuators Glider). The magnitudes of the elements J generally they are large compared with the elements of r_p , r_b y r_w . The terms may be significant in designs Gliders very large or very small actuators or those with fast internal mass.

The full equations of motion for a submarine Glider in three dimensional space are:

$$\begin{bmatrix} \dot{R} \\ \dot{b} \\ \dot{\Omega} \\ \dot{v} \\ \dot{r}_p \\ \dot{r}_b \\ \dot{r}_w \\ \dot{P}_p \\ \dot{P}_b \\ \dot{P}_w \\ \dot{m}_b \end{bmatrix} = \begin{bmatrix} R\hat{\Omega} \\ Rv \\ J^{-1}\bar{T} \\ M^{-1}\bar{F} \\ \frac{1}{\bar{m}}P_p - v - \Omega \times r_p \\ \frac{1}{m_b}P_b - v - \Omega \times r_b \\ \frac{1}{m_w}P_w - v - \Omega \times r_w \\ \bar{u} \\ u_b \\ u_w \\ u_{ballast_rate} \end{bmatrix}, \quad (11)$$

where:

$$\begin{aligned} \bar{T} &= (J\Omega + \hat{r}_p P_p + \hat{r}_b P_b + \hat{r}_w P_w) \times \Omega + (Mv \times v) \\ &\quad + (\Omega \times r_p) \times P_p + (\Omega \times r_b) \times P_b + (\Omega \times r_w) \times P_w + (\bar{m}\hat{r}_p + m_b\hat{r}_b + m_w\hat{r}_w) gR^T k \\ &\quad + T_{ext} - \hat{r}_p \bar{u} - (\hat{r}_b u_b + \hat{r}_w u_w), \\ \bar{F} &= (Mv + P_p + P_b + P_w) \times \Omega + m_0 g R^T k + F_{ext} - \bar{u} - (u_b + u_w). \end{aligned}$$

Thus,

$$\begin{aligned} F_{ext} &= R^T \sum f_{ext_i}, \\ T_{ext} &= R^T \sum (x_i - b) \times f_{ext_i} + R^T \sum \tau_{ext_j}, \end{aligned}$$

where x_i is the point, where the inertial system f_{ext_i} acts represents external forces and moments including lift, drag and hydrodynamic moments associated with the system of the vehicle.

\bar{u} is a force control \bar{m} , and u_b and u_w are internal forces in the masses m_b and m_w . They will be restoring forces when the masses are fixed in one place.

4 Hydrodynamic Parameters Identification

When a body immersed in a fluid moves; a quantity of fluid is moved along with it (added mass), this amount of fluid will depend on the geometry of the vehicle [5], Likewise; There forces affecting movement direction in x,y,z (Hydrodynamic forces) and moments affecting the orientation roll (ϕ), pitch (θ), and yaw (ψ) (hydrodynamic moments) [4]. All measurements are made based on the center of buoyancy, because at this point systems coordinates fixed to the vehicle and the reference coordinate system are located fluid.

4.1 Aggregated mass

The added mass is a function of an increase in mass and thus increased acceleration inertia. Esas forms are represented by the added mass (M_f) added inertia (J_f) and cross terms (D_f):

$$M_A = \begin{bmatrix} M_f & D_f^T \\ D_f & J_f \end{bmatrix}.$$

Approximating the diagonal is considered acceptable, since the elements outside the diagonal are much smaller than diagonal elements itself, this is because the vehicle moves at low speed, so that the mass matrix added M_A is defined as:

$$M_A = - \begin{bmatrix} X_{\dot{u}} & 0 & 0 & 0 & 0 & 0 \\ 0 & Y_{\dot{v}} & 0 & 0 & 0 & 0 \\ 0 & 0 & Z_{\dot{w}} & 0 & 0 & 0 \\ 0 & 0 & 0 & K_{\dot{p}} & 0 & 0 \\ 0 & 0 & 0 & 0 & M_{\dot{q}} & 0 \\ 0 & 0 & 0 & 0 & 0 & N_{\dot{r}} \end{bmatrix}, \quad (12)$$

where $X_{\dot{u}}$, $Y_{\dot{v}}$ and $Z_{\dot{w}}$ is the added mass on the axle x , y and z respectively. $K_{\dot{p}}$, $M_{\dot{q}}$ and $N_{\dot{r}}$ are the moments of inertia about the axis added x , y and z respectively.

The equations describing each element of the diagonal matrix M_A based on the geometry proposed Glider, they are obtained from the vehicle profile Figure 4; the values are presented in table 2.

Table 2: Parameters of Figure 4.

Parameter	Value	Units	Description
D_{b_1}	168.28	mm	Diameter section b_1
D_{b_2}	190.5	mm	Diameter section b_2
a	84.14	mm	Length of the nose
b_1	750	mm	Section length b_1
b_2	43	mm	Section length b_2
b	793	mm	Total length of the cylindrical section
c	190	mm	Queue Length

In our case, we assume that the profile of the vehicle starts at the source positioning system coordinates in the nose of the vehicle, both the nose and tail are symmetrical, so they are governed by the equation of the ellipse on the horizontal axis outside the origin:

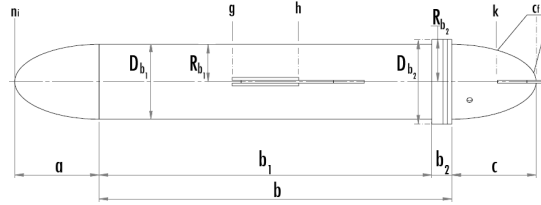


Fig. 4: Proposed Vehicle Profile.

$$\frac{(x - h_e)^2}{a_e^2} + \frac{(y - k_e)^2}{b_e^2} = 1. \quad (13)$$

Whereas the only center axis moves x so $k_e = 0$ and y , as function has:

$$y = \sqrt{\left(1 - \frac{(x - h_e)^2}{a_e^2}\right) b_e^2}. \quad (14)$$

The function y It is equal to the radius of the nose or tail of the hull so it can be considered for both cases $y = R(x)$ and Sections b_1 and b_2 Radio function $R(x)$ It can be considered constant.

These equations define the profile of the nose and tail of the vehicle without considering the fins, stabilizers, rudders or control surfaces.

Axial Added Mass ($X_{\dot{u}}$) To determine the axial added mass is considered the variation of vehicle shape in areas of the bow and stern:

$$X_{\dot{u}} = -m_{11} = -\frac{4\alpha_f \rho \pi}{3} \left(\frac{l}{2}\right) \left(\frac{D_{b1}}{2}\right)^2, \quad (15)$$

$$X_{\dot{u}} = -m_{11} = -\frac{4\beta_f \rho \pi}{3} \left(\frac{d_{b1}}{2}\right)^3, \quad (16)$$

where ρ To determine the axial added mass is considered the variation of vehicle shape in areas of the bow and stern. $\rho = 1030 \frac{kg}{m^3}$, α_f y β_f are parameters determined by the ratio of the length to the diameter of the vehicle according to Tables Blevins [14], such that on average; $\alpha_f = 0.047485$ y $\beta_f = 0.2733$ this because the value of $\frac{l}{D_{b1}}$ y $\frac{l}{D_{b2}}$ values are respectively 5 to 7.

Added Mass Crossflow ($Y_{\dot{v}}$, $Z_{\dot{w}}$, $M_{\dot{q}}$, $N_{\dot{r}}$) The added mass is calculated by the Strip Theory [12] It applied to the cross sections of the hull and consists in dividing the submerged part of the vehicle in a series of slices to determine the hydrodynamic coefficients of each section in two dimensions and be integrated

along the length of the body finally obtain the coefficients in three dimensions. Aggregate per unit length of a single cylindrical mass segment is given by:

$$m_a(x) = \pi\rho R(x)^2, \tag{17}$$

where ρ It is the density of the surrounding fluid and $R(x)$ is the radius of the hull as a function of axial position. The aggregate mass finned a circle is given by:

$$m_{af} = \pi\rho \left(a_{aleta}^2 - R(x)^2 + \frac{R(x)^4}{a_{aleta}^2} \right), \tag{18}$$

where a_{aleta} It is the maximum height of the fin measured from the axis of the ellipsoid. By integrating the equations 17 and 18 the length of the vehicle is reached:

$$\begin{aligned} Y_{\dot{v}} &= - \int_{n_i}^g m_a(x) dx - \int_g^h m_{af}(x) dx - \\ &- \int_h^k m_a(x) dx - \int_k^{c_f} m_{af}(x) dx, \\ Z_{\dot{w}} &= - \int_{n_i}^{c_f} m_a(x) dx, \\ M_{\dot{q}} &= - \int_{n_i}^g x^2 m_a(x) dx - \int_g^h x^2 m_{af}(x) dx - \\ &- \int_h^k x^2 m_a(x) dx - \int_k^{c_f} x^2 m_{af}(x) dx, \\ N_{\dot{r}} &= - \int_{n_i}^{c_f} x^2 m_a(x) dx. \end{aligned} \tag{19}$$

Due to Added Mass Balance ($K_{\dot{p}}$) To estimate the added mass due to rolling, only it considered the section of the hull containing the fins [12]:

$$K_{\dot{p}} = - \int_g^h \frac{2}{\pi} \rho a_{aleta}^4 dx. \tag{20}$$

Substituting measures and functions, parameters are obtained aggregate mass M_A .

Table 3: Results of the added mass.

Parameter	Value	Units
$X_{\dot{u}}$	-0.7738890384	kg
$Y_{\dot{v}}$	-60.49746284	kg
$Z_{\dot{w}}$	-22.49920646	kg
$K_{\dot{p}}$	-0.8306898369	$\frac{kg \cdot m^2}{rad}$
$M_{\dot{q}}$	-15.85575167	$\frac{kg \cdot m^2}{rad}$
$N_{\dot{r}}$	-7.843744090	$\frac{kg \cdot m^2}{rad}$

4.2 Aerodynamic Forces and Moments

The forces F_{hydro} and aerodynamic moments M_{hydro} viscous effects appear water during movement of the glider and are usually expressed under the fluid as [14]:

$$F_{hydro} = \begin{bmatrix} -D \\ SF \\ -L \end{bmatrix} = \begin{bmatrix} (K_{D0} + K_D \alpha^2) V^2 \\ K_\beta \beta V^2 \\ (K_{L0} + K_\alpha \alpha) V^2 \end{bmatrix}, \quad (21)$$

$$M_{hydro} = \begin{bmatrix} T_{DL1} \\ T_{DL2} \\ T_{DL3} \end{bmatrix} = \begin{bmatrix} (K_{MR} \beta + K_p p) V^2 \\ (K_{M0} + K_M \alpha + K_q q) V^2 \\ (K_{MY} \beta + K_r r) V^2 \end{bmatrix}, \quad (22)$$

where: K_{D0} , K_D are coefficients of the drag force (x) in D with respect to V^2 , $\alpha^2 V^2$.

K_β It is the coefficient of force (y) side L with respect to βV^2 .

K_{L0} , K_α are coefficients of force (z) supporting L with respect to V^2 , αV^2 .

K_{MR} , K_p are coefficients roll moment T_{DL1} with respect to βV^2 , $p V^2$.

K_{M0} , K_M , K_q are coefficients pitch moment T_{DL2} with respect to V^2 , αV^2 , $q V^2$.

K_{MY} , K_r coefficients are time yaw T_{DL3} with respect to βV^2 , $r V^2$.

Analysis of the Data To determine the values of the coefficients of the hydrodynamic forces and moments has been used data collection through various fluid simulations with CFD module called SolidWorks Flow Simulation. The simulations are to be changing angles of attack α and sideslip β , where:

$$\alpha = \tan^{-1} \left(\frac{V_3}{V_1} \right),$$

$$\beta = \tan^{-1} \left(\frac{V_2}{\sqrt{V_1^2 + V_2^2 + V_3^2}} \right).$$

The coordinate system flow shown in Figure 5 together with the angles of attack α and sideslip β plus speeds on each axis.

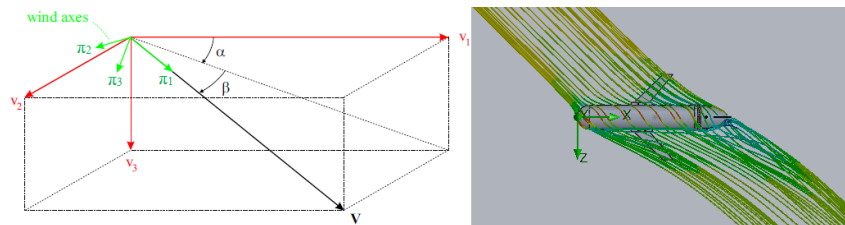


Fig. 5: Vehicle reference systems and fluid and Fluid direction in Flow Simulation respectively.

Glider speed is represented transforming the speed displayed in the fluid system attached to the body system as:

$$\begin{bmatrix} V_1 \\ V_2 \\ V_3 \end{bmatrix} = R_{WB} \times \begin{bmatrix} V \\ 0 \\ 0 \end{bmatrix} = \begin{bmatrix} V \cos \alpha \cos \beta \\ V \sin \beta \\ V \cos \beta \sin \alpha \end{bmatrix}.$$

To determine the values of the coefficients of the hydrodynamic forces in these simulations is configured that the total speed that will move the glider is $V = \sqrt{V_1^2 + V_2^2 + V_3^2} = 0.5m/s$, varying angles α and β It is to vary the velocity components of the fluid and then let the software determine the hydrodynamic forces.

The table 4 shows the values of the obtained coefficients.

Table 4: Values of the constants of aerodynamic forces and moments.

Parameter	Value	Units
K_{D0}	5.04	kg/m
K_D	-4.2863	kg/m/rad ²
K_β	-42.3403	kg/m/rad
K_{L0}	0.7	kg/m
K_α	95.3556	kg/m/rad
K_{MR}	-16.7381	kg/rad
K_p	-174.3244	kg s/rad
K_{M0}	0.392	kg
K_M	-40.2293	kg/rad
K_q	-117.804	kg s/rad
K_{MY}	20.794	kg/rad
K_r	-41.2834	kg s/rad

5 Simulation and Results

In Figure 6 the mathematical model in MatLab Simulink shown. Table data used 3 column of the results according to the equations describing the actual profile and the values of constants Table 4.

The conditions for the simulation were that the vehicle has a rudder that between 50 and 210 seconds is kept rotated 20 degrees and 210 to 410 seconds is maintained at -20 degrees while the rest of the time is kept 0. moving mass changes $r_p = [0.3, 0, 0]$ to $r_p = [-0.3, 0, 0]$ and the value of m_b changes from 0.5 to -0.5 every 30 seconds initial conditions are: $x = 0, y = 0, z = 0, \phi = 0, \theta = 0, \psi = 0$ and $\nu = 0$. The result can be seen in the graphs of Figures 6, 7 and 8.

You can see that the roll angle (ϕ), practically remains unchanged due to the fixed side wings in the vehicle, the yaw angle (ψ) obeys the programmed rotation of the wheel, while the angle pitch (θ) semiperidico shows the constant pitch all the way due to the change of the moving mass r_p and m_b every 30 seconds.

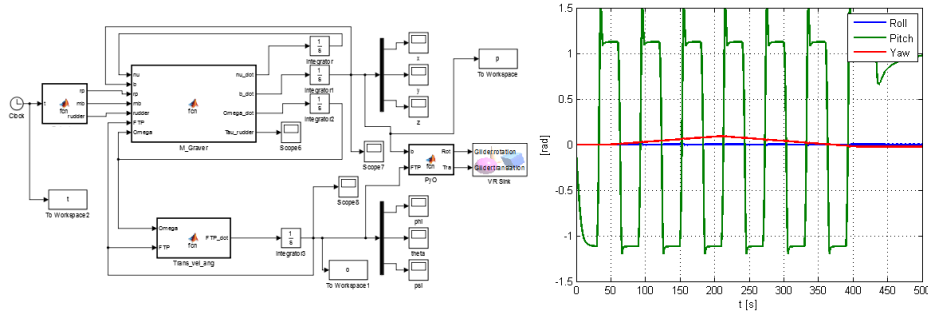


Fig. 6: Graver model in Simulink and Orientation respectively.

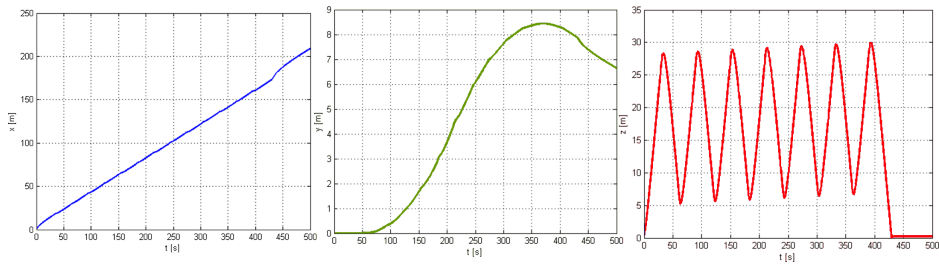


Fig. 7: Displacement in X, Y, and Z respectively.

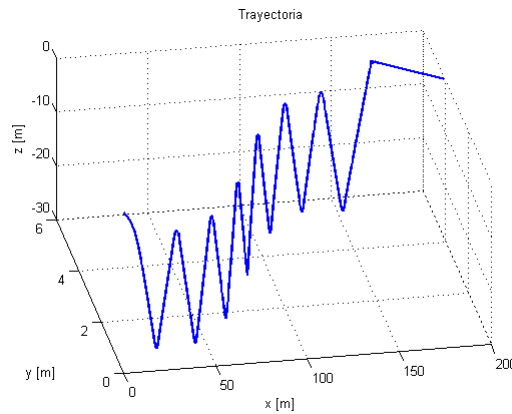


Fig. 8: Position.

Also, in the printing position, it can be seen that the vehicle travels a slightly longer distance on the shaft 250m X during the duration of the test 500s travel, while displacement in Y the way evidence produced due to scheduling helm of the vehicle and finally the characteristic zig-zagueo the Glider due to the angle in pitch (θ) and the wings of the vehicle.

Acknowledgments. This work was partially supported by a CONACyT CVU: 637204.

References

1. Akyildiz, I.F., Pompili, D., Melodia, R.: Underwater acoustic sensor networks: research challenges. *Science Direct* (2005)
2. Bender, A., Matthew, D., Lee, A., Williams, S.B.: Analysis of an autonomous underwater glider. *Australian Centre for Field Robotics* (2006)
3. Campos, E., J.Torres, S.Mondi, Lozano, R.: Deep control using artificial vision with time-delay of an auv. 9th International Conference on Electrical Engineering, Computing Science and Automatic Control (2012)
4. Fossen, T.I.: *Marine control systems guidance, navigation, and control of ships, rigs and underwater vehicles* (2002)
5. Graver, J.G.: *Underwater gliders: Dynamics, control and design* (2005)
6. Jun, B.H., Park, J.Y., Lee, F.Y., Lee, P.M., Lee, C.M., Kin, K., Lim, Y.K., Oh, J.H.: Development of the auv 'isimi' and a free running test in an ocean engineering basin. *Ocean Engineering* (2009)
7. Liang, X., Zhang, J., Qin, Y., Yang, H.: Dynamic modeling and onputer simulation for autonomous underwater vehicles with fins. *Ocean Engineering* (2012)
8. Mercado, E.C.: Design, modelling and control of auv's using artificial vision (2014)
9. Naomi Ehrlich Leonard, J.G.G.: Model-based feedback control of autonomous underwater giders. *IEE Journal of Oceanic Engineering*, Vol. 26, No 4 (2001)
10. NigelCross: *GEngineering Design Methods Strategies for Product Design* (2000)
11. Pellicer, A.G.: Estimacin de los coeficientes hidrodinmicos de vehculos autonomos submarionos mediante CFD
12. Presterio, T.: Verification of a six-degree of freedom simulation model for the remus autonomus underwater vehicle
13. Smith, S.N., Smith, S.L., Rus, D., ad Burton H. Jones, M.S., Sukhatme, G.S.: Persistent ocean monitoring with underwater gliders. *Open Access Articles* (2011)
14. Zhang, S., Yu, J., Zhang, A., Zhang, F.: Spilaring motion of underwater gliders: Modeling, analysis, and experimental results. *Ocean Engineering* (2012)

Oncological Analysis Using Data Mining

Doricela Gutiérrez Cruz¹, Ricardo Rico Molina¹, Liliana Rodríguez Páez¹, Karla Vilchis Hernández¹, Bernardo Soto Rivera², Yaroslaf Albarrán Fernández¹, Alma Gutierrez Cruz², Mónica Ortega¹

¹ Unidad Académica Profesional Nezahualcóyolt UAEM,
Mexico

² Hospital Regional 1º de octubre,
Mexico

gutierrezcruzdo@yahoo.com.mx, rico_molina@hotmail.com

Abstract. Data mining is a technique that involves the application of specific algorithms, which generate a list of patterns based on large volumes of information that is useful for decision making in wide fields of application, as detection of patterns in diseases. This paper proposes to carry out a cancer analysis by means of data mining techniques, applied on a sample of 3365 cases, using association algorithms as Apriori and J48 classification algorithm. The data were obtained from clinical reports of patients from the Palliative Care Unit of the Hospital Regional 1o de Octubre. Once the data mining process was completed, it was possible to identify some of the most relevant types of cancer, age as characteristic factor in the emergence of diseases, as well as the sex affected.

Keyword: Data mining, cancer, apriori, J48 classification algorithms.

1. Introduction

The increasing volume and variety of information computerized in digital databases has grown in the last decade [3], a considerable part of this information is historical, it represents transactions or situations that have occurred and it may be useful for understanding future information [14, 15,16].

Technological development both in the computer and data transmission fields, promotes a better handling and storage of information; as is the case of Data Mining (DM), which can be defined as the consistent use of specific algorithms that generate a list of patterns based on preprocessed data that is useful for decision-making. [17, 10, 13]. That list of patterns is closely related to statistics, using sampling techniques and data visualization. Research and development to analyze large volumes of data became increasingly necessary, and they can be done based on files. Even if the advantages increase when there are large volumes of data [4], to discover knowledge from this huge volume of data is a challenge in itself. DM is an attempt to make sense of the explosion of information that currently can be stored [5]. The phase of data mining is the representation of the type of model obtained. It focuses on searching, which will have

one or more forms of representation, depending on the type of model obtained [6]. The data analysis can provide real knowledge to help in decision making [7].

Cancer is one of the main causes of death in the world. In 2012 about 14 million new cases and 8.2 millions of chronic and degenerative deaths related to this condition were reported; 30% of those deaths were due to dietary and behavioral risk factors. On the other hand, over 60% of total annual new cases in the world occur in Africa, Asia, and Central and South America, these regions represent 70% of cancer deaths in the world [1].

The historical behavior of cancer mortality has been on an upward trend, and international registers allow the problem that cancer represents to be visualized, however existing information in Mexico is limited, therefore it is difficult to have access to it to determine the real impact of cancer on health more accurately [2].

It should be noted that the methodology DM is part of a process called "Knowledge Discovery in Databases" (KDD), which indicates the necessary steps to reduce risks in the search of knowledge models when applying DM techniques. For example, in the KDD process the data require a substantial preprocessing to be modeled (cleaning and preparation) [9, 10, 11].

In the clinical setting the DM is helpful for the identification and diagnosis of diseases. Likewise, it has significance for the discovery of possible interrelationships between diverse diseases [8]. In medical applications, where it is not possible to ignore the importance of the temporal component, data mining techniques have acquired major significance [11]. In this context, the aim of this paper is to characterize and classify the types of cancer and their impact on the population using data mining techniques, in the expectation of finding underlying relationships that cannot be identified by a classic statistical treatment.

2. Case Study

The Hospital Regional 1o de Octubre (HR1O) was inaugurated on December 5th, 1974 and the population attended is diverse: urban, suburban, rural and marginalized.

In accordance with the above, regarding our area of influence, the population figures are as follows: covered population 2172,49, registered population 1086,124, user population 651,674. Approximately 50% of the beneficiaries are workers and pensioners, and nearly a quarter are children under the age of 18.

Since each year 10 million people suffer from pain caused by a disease, and cancer represents 5.5 million of them, palliative care practices were implemented in the Hospital eight years ago; they are focused on controlling pain and attending the psychosocial aspects of the patient and the family members who support him during the process.

3. Experimental Development

To carry out this study, the general process KDD was applied in order to discover patterns and relationships in data that can be used to make valid predictions [9, 17], the universe of the study were 3365 cases of cancer; while the WEKA software was

used for the analysis and construction of the data mining model (<http://www.cs.waikato.ac.nz/ml/weka/>).

3.1 Data Selection

To conduct this study, the representative variables to address the problem: *sex*, *year*, *age*, *diagnosis* and *type of beneficiary*, were taken from the clinical reports provided by the palliative care unit of the hospital.

3.2 Pre-Processing Data

This step consisted of a data cleansing, in order to get quality patterns; that is: without outliers or null values. The data obtained from clinical reports were analyzed to identify inconsistencies using the WEKA system. This process was only performed in the data related to diagnosis, as these were either oncological or not oncological.

The description of the five most important attributes for conducting this research is shown in Table 1, while Table 2 shows the attributes of the different types of cancer addressed in this research.

Table 1. Description of the most important attributes.

Attribute	Definition	Description
S	Sex	Gender of patients
Y	Year	Year when the diagnostic is reported to the unit
Dx	Cancer	Type of cancer suffered by the patient

Table 2. Description of the attributes associated with different types of cancer.

Attribute	Definition
ca co	heart cancer
ca ce	brain cancer
ca ab	abdominal cancer
ca ceu	cervical cancer
ca a	appendix cancer
ca c v	spinal cancer
ca cvcr	spinal and rectal cancer
ca es	esophagus cancer
ca e	stomach cancer
ca h	liver cancer
ca av	cancer of ampulla of Vater
ca meo	bone marrow cancer
ca ov	ovarian cancer
ca pi	skin cancer
ca p	prostate cancer
ca pu	lung cancer
ca r	rectal cancer
ca ri	kidney cancer
ca te	testicular cancer

Attribute	Definition
ca v	bladder cancer
ca sl	cancer of lymphatic system
ca m	breast cancer
ca o	oral cancer
ca os	bone cancer
ca pa	pancreatic cancer
le	leukemia
ca mm	multiple myeloma
sa te b	soft tissue sarcoma

3.3 Analysis of Data

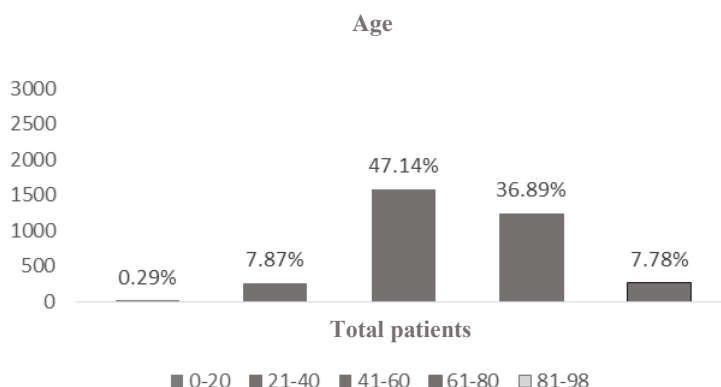
The search and finding of unsuspected patterns is carried out during the data mining stage where discovery tasks, such as classification [22, 23], clustering [18, 19], sequential patterns [20], associations [21], among others, are applied.

One of the differences in gender condition was observed in a study on disease burden with higher rates of morbi-mortality in men [33]. Higher mortality rates for men or women, depending on the location of the tumor, were identified in other studies carried out in work places, whereas women were the most affected in other studies [33, 34].

Age is a characteristic factor in the onset of chronic diseases [32], since at the time of the diagnosis it was evaluated as a prognostic element, and it was reported that elderly patients have lower life expectancy, even in early stages, when compared with younger patients.

The effect of age represents a change in rates associated with age, which is important given that the onset of chronic diseases is usually greater with increasing age [31, 35].

Figure 1 shows the frequency analysis of some of the variables studied. As it can be denoted, during 2009-2015, 61% of the patients reported by the palliative care unit of HR10 were women, and the remaining 33% men. Concerning the types of cancer and their incidence reported during the same period, breast cancer had an incidence of case of 19%, followed by of spinal and rectal cancer with 9%, lung and prostate cancer with 8%, and cervical and bone marrow cancer with 7%.



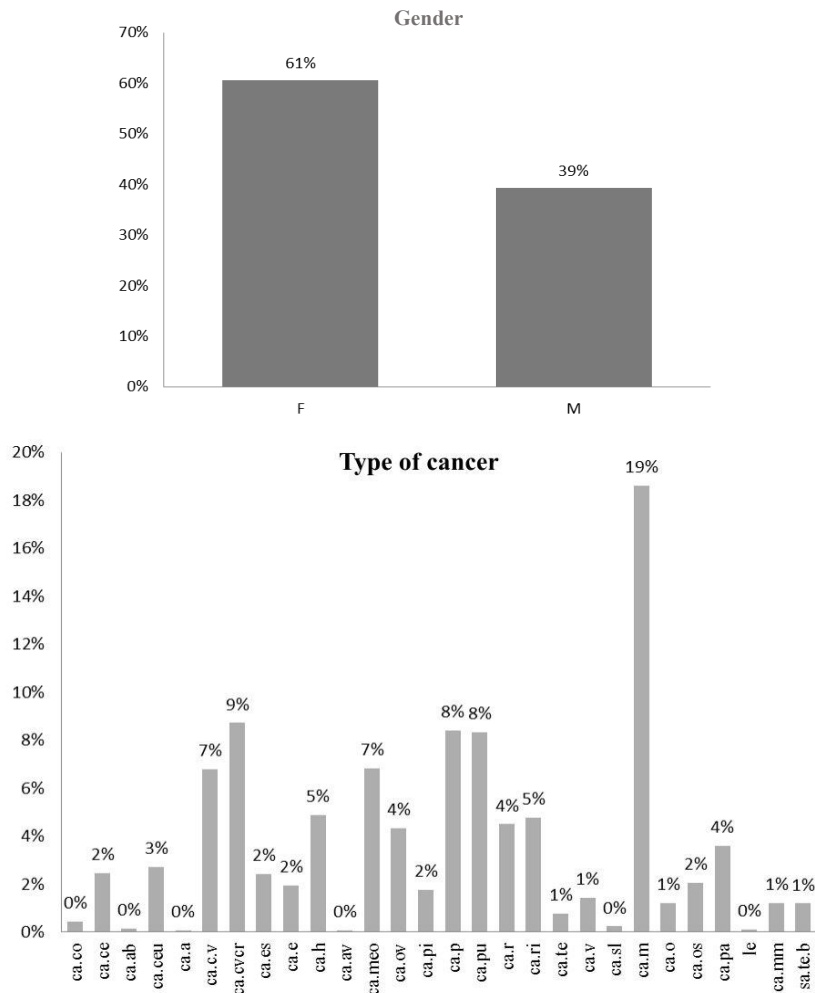


Fig. 1. Frequency analysis of the gender, age and types of cancer with highest incidence during 2009-2015 (Own elaboration, 2016).

3.4 Classification

For this activity, as mentioned, WEKA software was used. It was selected owing to the data included in the data set are mostly categorical, and because it uses decision trees. From the available algorithms, the algorithm J48 corresponding to the C4.5 algorithm was used [30]. Default specifications of WEKA and the stratified cross-validation method were used for its execution, as well.

To generate the tree an attribute as root must be selected, and a branch with each of the possible values of that attribute must be created; this process is carried out with each resulting branch. An attribute to continue dividing must be selected on each node, to do this the attribute that best separate the examples according to the class is selected.

Figure 2 shows that, by gender, most of the patients treated for some type of cancer during the reported period were women (91.8%).

```

Number of Leaves :    138

Size of the tree :    235

Time taken to build model: 0.03 seconds

=== Stratified cross-validation ===
=== Summary ===

Correctly Classified Instances      2932           87.1322 %
Incorrectly Classified Instances    433           12.8678 %
Kappa statistic                    0.7269
Mean absolute error                 0.118
Root mean squared error             0.269
Relative absolute error             37.0597 %
Root relative squared error         67.4235 %
Total Number of Instances          3365

=== Detailed Accuracy By Class ===

                TP Rate  FP Rate  Precision  Recall  F-Measure  ROC Area  Class
                0.802   0.084   0.86       0.802   0.83       0.896    m
                0.918   0.198   0.878     0.918   0.897     0.899    f
                0       0       0         0       0         0.723    m
Weighted Avg.   0.871   0.153   0.87       0.871   0.87       0.898
    
```

Fig. 2. Classification of patients by sex suffering from cancer during 2009-2015 (Own elaboration, 2016).

Figure 3 shows that the types of cancer with highest incidence during the reported period were: prostate cancer with 71.4%, breast cancer 68.7%, pancreatic cancer 68.6%, esophageal cancer 65.7%, whereas the type with the lowest incidence was eye cancer with 9.1%.

Subsequently, the Apriori algorithm was applied to mine data, which were used to obtain association rules between sets of a data repository [36]. It shows the results of 3365 cases of cancer:

Apriori algorithm association rules

1. Dx=cacvcr 172 ==> Ano=2009 172 conf:(1)
2. Sexo=f Dx=cacvcr 118 ==> Ano=2009 118 conf:(1)
3. Edad=41_60 Dx=cameo 109 ==> Ano=2009 107 conf:(0.98)
4. Sexo=f Dx=cameo 116 ==> Ano=2009 113 conf:(0.97)
5. Dx=cameo 169 ==> Ano=2009 164 conf:(0.97)
6. Edad=41_60 Dh=2 221 ==> Sexo=f 213 conf:(0.96)
7. Edad=41_60 Dh=2 Ano=2009 186 ==> Sexo=f 179 conf:(0.96)
8. Dh=2 327 ==> Sexo=f 310 conf:(0.95)
9. Dh=2 Ano=2009 278 ==> Sexo=f 263 conf:(0.95)
10. Dx=cam 130 ==> Sexo=f 119 conf:(0.92)

```

=== Stratified cross-validation ===
=== Summary ===

Correctly Classified Instances      1623          48.2318 %
Incorrectly Classified Instances    1742          51.7682 %
Kappa statistic                    0.4331
Mean absolute error                 0.0292
Root mean squared error             0.1326
Relative absolute error             66.5038 %
Root relative squared error         89.5113 %
Total Number of Instances          3365

=== Detailed Accuracy By Class ===

```

TP Rate	FP Rate	Precision	Recall	F-Measure	ROC Area	Class
0.224	0.078	0.215	0.224	0.22	0.652	cacvcr
0.267	0.001	0.5	0.267	0.348	0.893	caco
0.145	0.014	0.207	0.145	0.17	0.725	cace
0.198	0.014	0.281	0.198	0.232	0.798	caceu
0.487	0.038	0.485	0.487	0.486	0.802	cacv
0.467	0.065	0.342	0.467	0.395	0.799	cameo
0.473	0.052	0.449	0.473	0.46	0.811	capu
0.05	0.004	0.125	0.05	0.071	0.772	sateb
0.714	0.059	0.527	0.714	0.607	0.877	cap
0.687	0.114	0.579	0.687	0.628	0.847	cam
0.658	0.005	0.735	0.658	0.694	0.895	caes
0.541	0.02	0.549	0.541	0.545	0.857	caov
0.458	0.007	0.529	0.458	0.491	0.843	capi
0.375	0.011	0.407	0.375	0.39	0.843	cae
0	0	0	0	0	0.871	le
0	0	0	0	0	0.483	cameo
0	0	0	0	0	0.482	capu
0.522	0.016	0.619	0.522	0.567	0.846	cari
0.344	0.016	0.5	0.344	0.408	0.798	car
0	0	0	0	0	0.673	casl
0.167	0.002	0.417	0.167	0.238	0.764	cao
0	0	0	0	0	0.497	caab
0.488	0.006	0.513	0.488	0.5	0.792	camm
0	0	0	0	0	0.497	caa
0	0	0	0	0	0.496	caav
0.417	0.002	0.741	0.417	0.533	0.828	cav
0	0	0	0	0	0.497	cam
0.569	0.005	0.685	0.569	0.622	0.811	caos
0	0	0	0	0	0.499	caos
0.323	0.017	0.438	0.323	0.372	0.769	cah
0	0	0	0	0	0.499	caes
0	0	0	0	0	0.497	caceu
0	0.001	0	0	0	0.493	caes
0	0	0	0	0	0.497	cam
0.569	0.005	0.685	0.569	0.622	0.811	caos
0	0	0	0	0	0.499	caos
0.323	0.017	0.438	0.323	0.372	0.769	cah
0	0	0	0	0	0.499	caes
0	0	0	0	0	0.497	caceu
0	0.001	0	0	0	0.493	caes
0	0	0	0	0	0.986	cam
0.686	0.01	0.722	0.686	0.703	0.916	capa
0	0	0	0	0	0.5	cari
0.241	0.003	0.389	0.241	0.298	0.827	cah
0	0	0	0	0	0.497	caos
0	0	0	0	0	0.494	cae
0.091	0.001	0.2	0.091	0.125	0.809	cao
0.423	0.005	0.407	0.423	0.415	0.915	cate

Fig. 3. Classification of types of cancer reported during 2009-2015 (Own elaboration, 2016).

The results obtained through algorithms of apriori classification include 10 association rules, each and every one of them with a certainty that goes from 0.92 to 1. It can be stressed that Rule 3 shows that, in 2009, there were 2 related attributes: age "41-60" years, and "cameo" diagnosis; whereas Rule 4 registers that female gender and "cameo" diagnosis were more significant during the same period; Rule 6 shows that beneficiary patients type 2 between 41 and 60 years were women; Rule 10 exposes that the type of cancer "Cam", is associated with the attribute "woman". Finally, there is an association between Rules 4 and 10, related to diagnosis and sex attributes, the latter being women.

4. Conclusions

Based on the analysis, it can be said:

1. The latest report from the World Health Organization shows that the burden of cancer is increasing at an alarming rate and underlines the need for effective prevention strategies to curb the disease. Also, that the most frequent types of cancer are different in men and women [33, 37, 38, 39]. This research confirms the latter, since from the 3365 reported patients, 91.8% of the women were the most affected by some type of cancer, compared to 80.2 % of men.
2. Currently, the emergence of new chronic diseases has impacted many people around the world, the predominant types of cancer worldwide with the highest annual number of deaths include: lung, liver, stomach, colon and breast [37]. The predominant types of cancer in the palliative care unit of HR10 were: prostate cancer 71.4%, breast cancer 68.7%, pancreatic cancer 68.6%, and esophageal cancer 65.7%.
3. Age is a factor in the onset of chronic diseases, the older the patient, the greater the incidence of diseases [32, 40], as it was shown, the most incidences of cancer are reported in patients between 40 and 60 years.

Among the existing chronic diseases, the study of cancer has become very important; since it has been a worldwide public health problem for several decades. The costs of cancer burden are even hurting economies, besides exerting pressure on health care systems.

Cancer is one of the chronic degenerative disease with highest incidence among adults [1, 2], and currently one of the leading causes of morbid-mortality among the population younger than 20 [3]. The most representative factors are the male gender and the group of 70 years or older. The most common locations of cancer in both genders were trachea, bronchus and lung, followed by prostate in man cancer and breast cancer and uterus (body and neck) in women [4].

In general, the lifestyle habits that most influence on the risk of suffering from cancer are smoking and obesity, in both genders; whereas, hormonal aspects in women exclusively [5]

Acknowledgements. The authors thank the information, monitoring and facilities granted to this research by Hospital Regional 1° de Octubre to the "Universidad

Autónoma del Estado de México” “Unidad Académica Profesional Nezahualcóyotl”, and appreciate the support given by Eng. Luis Antonio Gutierrez Perez.

References

1. Organización Mundial de la Salud (OMS): Mortalidad a nivel mundial: Las 10 causas principales de defunción en el mundo. <http://www.who.int/mediacentre/factsheets/fs310/es/index2.html> (2015)
2. Rizo, P., González, A., Sánchez, F., Murguía, P.: Tendencia de la mortalidad por cáncer en México: 1990-2012. *Evidencia Médica e Investigación en salud*, 8(1), pp. 5–15 (2015)
3. Hernández, J., Ramírez, J., Ferri, C.: Introducción a la Minería de Datos. Departamento de Sistemas Informáticos y Computación, Universidad Politécnica de Valencia, Madrid (2004)
4. Chiotti, S. M., Cidisi, O.: Minería de Datos en Base de Datos de Servicios de Salud – UTN – FRSF. Ingar UTN- CONICET (2013)
5. Riquelme, J., Ruiz, R., Gilbert, K.: Minería de Datos: Conceptos y Tendencias. Departamento de Lenguajes y Sistemas Informáticos, Universidad de Sevilla (2006)
6. Quesada, Y., Wong, D., Rosete, A.: Minería de Datos aplicada a la Gestión Hospitalaria. En: 14 Convención Científica de Ingeniería y Arquitectura, CUJAE (2008)
7. Marcano, Y. J., Talavera, R.: Minería de Datos como soporte a la toma de decisiones empresariales. *Opción*, Año 23, No. 52, pp. 104–118 (2007)
8. Zamarrón, C., García, V., Calvo, U., Pichel, F., Rodríguez, J. R.: Aplicación de la Minería de Datos al estudio de las alteraciones respiratorias durante el sueño. Hospital Clínico Universitario de Santiago de Compostela, Servicio de Neumología (2006)
9. Han, J., Kamber, M.: *Data Mining: Concepts and Techniques*. Morgan Kaufmann Publishers, USA (2006)
10. Hand, D., Mannila, H., Smyth, P.: *Principles of Data Mining*. Cambridge, MA: The MIT Press (2001)
11. Hernández, J., Ramírez, M. J., Ferri, C.: Introducción a la Minería de Datos. Madrid, Pearson Educación, S A (2004)
12. Fayyad, U. M., Grinstein, G., Wierse, A.: *Information Visualization in data Mining and Knowledge discovery*. Morgan Kaufmann, Harcourt Intl. (2001)
13. Frawley, W., Piatetsky-Shapiro, G., Matheus, C.: Knowledge discovery in databases: An Overview. *AI magazine*, Vol. 13, No. 3, pp. 57 (1992)
14. Simon, A.: *Data Warehouse, data Mining and OLAP*. John Wiley & Sons, USA (1997)
15. Berson, A., Smith, S. J.: *Data Warehouse, Data Mining & OLAP*. McGraw Hill, USA (1997)
16. White, C. J.: *IBM Enterprise Analytics for the Intelligent e-business*. IBM Press, USA (2001)
17. Fayyad, U., Piatetsky-Shapiro, G., Smyth, P.: The KDD process for extracting useful knowledge from volumes of data. *Communications of the ACM*, Vol. 39, No. 11, New York, USA, pp. 27–34 (1996)
18. Zhang, T., Ramakrishnan, R., Linny, M.: An efficient data clustering method for very large databases. In: *ACM SIGMOD International Conference on Management of Data* Montreal, Canada (1996)
19. Agrawal, R., Srikant, R.: Mining sequential patterns. In: *The 11th International Conference on Data Engineering, ICDE, Taipei, Taiwan* (1995)
20. Agrawal, R., Ghosh, S., Imielinski, T., Iyer, B., Swami, A.: An interval classifier for database mining applications. In: *Proceedings VLDB Conference, Vancouver, Canada* (1992)

21. Agrawal, R., Srikant, R.: Fast algorithms for mining association rules. In: VLDB Conference, Santiago de Chile, Chile (1994)
22. Witten, I., Frank, E.: Data mining: Practical machine learning tools and techniques with Java Implementations. Morgan Kaufman Publishers, San Francisco, CA, USA (2000)
23. Ng, R., Han, J.: Efficient and effective clustering method for spatial data mining. In: The 20th International Conference on Very Large Data Bases (VLDB 94), Santiago de Chile, Chile (1994)
24. Hernández, E., Lorente, R.: Minería de datos aplicada a la detección de Cáncer de Mama. Universidad Carlos III, Madrid, España, <http://www.it.uc3m.es/jvillena/irc/practicass/08-9/14.pdf> (2009)
25. Yépez, M. C.: Supervivencia de mujeres con cáncer de cuello uterino. Municipio de Pasto Revista Universidad y Salud, Vol.2, No.14, pp 7–18 (2011)
26. Mora, R.: El papel de la minería de datos en la detección y diagnóstico de cáncer. Universidad de Salamanca, Salamanca, España, <http://sistemaminergescon.blogspot.com> (2011)
27. Febles, J. P., González, A.: Aplicación de la minería de datos en la bioinformática. ACIMED, Vol. 10, No. 2, pp. 69–76, http://scielo.sld.cu/scielo.php?script=sci_arttext&pid=S1024-94352002000200003&lng=es&nrm=iso (2002)
28. Dávila, F., Sánchez, Y.: Técnicas de minería de datos aplicadas al diagnóstico de entidades clínicas. RCIM, Vol. 4, No. 2, pp. 174–183, http://scielo.sld.cu/scielo.php?script=sci_arttext&pid=S1684-18592012000200007&lng=es&nrm=iso (2012)
29. Camacho, S. S.: Método Heurístico para el Diagnóstico de Cáncer de Mama basado en Minería de Datos. Revista PGI, No. 1, pp. 97–101, http://www.revistasbolivianas.org.bo/scielo.php?script=sci_arttext&pid=S3333-7772014000100020&lng=es&nrm=iso (2014)
30. Basilio, A.: Aprendizaje Automático: conceptos básicos y avanzados, Aspectos prácticos utilizando el software Weka. Vol. 10, pp. 84–832 (2006)
31. Mery, C.M., Pappas, A.N., Bueno, R., Colson, Y.L., Linden, P., Sugarbaker, D.J.: Similar long-term survival of elderly patients with non-small cell lung cancer treated with lobectomy or wedge resection within the surveillance. Epidemiology and end results database, 128, pp. 237–245 (2005)
32. González, J.R., Llorca, F.J., Moreno, V.: Algunos aspectos metodológicos sobre los modelos edad-período-cohorte. Aplicación a las tendencias de mortalidad por cáncer, Nota Metodológica (2002)
33. Rodríguez, P., Fernández, J., Delgado, L., Garrote, I., Morales, J.M., Achiong, F.J.: Mortalidad por cáncer y condición de género. Rev méd electrón (2009)
34. Borràs, J.: La perspectiva del género en el cáncer: Una vision relevante necesaria. Universidad de Barcelona (2015)
35. Organización Mundial de la Salud (OMS): Salud Mundial: Retos actuales
36. La salud de los adultos en peligro: El ritmo de las mejoras disminuyen y las diferencias se acentúan. <http://www.who.int/whr/2003/chapter1/es/index3.html> (2003)
37. Paresh, T., Yogesh, G.: Using Apriori with WEKA for Frequent Pattern Mining. International Journal of Engineering Trends and Technology (IJETT), 12(3), pp. 121–131 (2014)
38. Stewart, B.W., Wild, C.P.: World Cancer Report 2014. International Agency for Research on Cancer (2014)
39. Menvielle, G., Luce, D., Goldberg, P., Leclerc, A.: Smoking, alcohol drinking, occupational exposures and social inequalities in hypopharyngeal and laryngeal cancer. Int J Epidemiol, 33(4), pp. 799–806 (2004)
40. Hansen, R.P., Olesen, F., Sorensen, H.T., Sokolowski, I., Sondergaard, J.: Socioeconomic patient characteristics predict delay in cancer diagnosis: a Danish cohort study. BMC Health Serv. Res., 8(49) (2008)

41. Serrano-Olvera, A., Gerson, R.: Supervivencia en relación con la edad en cáncer pulmonar de células no pequeñas. *Gac. Méd. Méx.*, Vol.145, No.1 (2009)

Feature Subset Selection and Typical Testors Applied to Breast Cancer Cells

Alexis Gallegos, Dolores Torres, Francisco Álvarez, Aurora Torres

Universidad Autónoma de Aguascalientes, Aguascalientes,
Mexico

alexisEdm@gmail.com, mdtorres@correo.uaa.mx,
fjalvar@correo.uaa.mx, atorres@correo.uaa.mx

Abstract. One of the most significant concerns around the world has been human health. So far, there have been little discussion about how the Computer Science can help to improve diagnostics of many diseases. In this paper, the aim is to prove that the Computer Science can offer techniques to help the improvement of the diagnosis of medical pathologies. For that, Feature Subset Selection and Typical Testors will be applied to a breast cancer database. Nowadays, cancer is a medical condition difficult to ignore, which has special interest by the specialists for finding effective methods to prevent and cure it. The database contains a feature set of breast cancer cells, which were subjected to an analysis of testors in order to find the minimum feature set that best describes benign and malignant cells. As a result, each typical testor found contains risk factors recognized by medical experts.

Keywords. Typical testor, feature subset selection, breast cancer, cancer cells, combinational logic.

1 Introduction

Breast Cancer is the most common female neoplasia¹ and the first death cause from tumor disease among women worldwide [2], accounting for 16% of all female cancers [3]. Nowadays, cancer has been become increasingly difficult to ignore. Every day, new studies on the causes and treatments are published; however, everyone agrees that the critical point of this studies is the timely diagnosis or cancer screening [4]. According to the National Cancer Institute, cancer screening means checking for cancer in people who have no symptoms that help doctors find and treat several types of cancer.

¹ Neoplasia is an abnormal mass of tissue whose growth exceeds the normal tissues, and it persists after cease the stimulus that triggered the change [1] D. Zicre, "Cátedra de Anatomía y Fisiología Patológicas," in *Neoplasia*, ed: Facultad de Ciencias Médicas. UNR, 2012.

Early detection is important because when abnormal tissue or cancer is found timely, it may be easier to treat. By the time symptoms appear, cancer has begun to spread and is harder to treat [5]. However, there are effective methods for screening only for some cancers.

Despite the usefulness of early detection, it can have some risks, as well as the methods used. For example, screening test can present a false-positive results; it means that the test indicates that the cancer is present when this is not true. Also, the test can have false-negative results, this indicates that cancer is not present even though it is.

Furthermore, over diagnosis is possible, this happens when screening test correctly shows that a person has cancer, but the cancer is slow growing and would not have harmed that person in his or her lifetime [5]. This justifies the need to improve the diagnosis of cancer.

The clinical diagnosis is a cognitive process that starts from the sensitive concrete thinking. It is linked to objective reality; it develops in abstract thinking and has the criterion of truth in practice [6]. It involves training, experience, pattern recognition and calculation of conditional probability, among other components, that human treatment has and therefore, is not free of errors that can cause sickness, damages, expenses and even death, especially in sensitive diseases such as cancer [7].

The errors represent an estimated 150 out of 1000 patients with misdiagnosis [8]. As such, the medical field is one of the areas that could be most benefit from close interaction with Computing Science and Mathematics to improve processes such as medical diagnosis [7]. Reason why it is decided to apply comprehensive mathematical methods to support diagnosis and prognosis of diseases such as cancer, in this case breast cancer.

This paper has been divided into three parts and organized the following way. The first part deals with important concepts in Typical Testors, Featured Subset Selection in computer science, Breast Cancer and its impact around the world. Next, the second section will examine the framework of this analysis, such as the previous research related to Testors Theory and the review of the methodology applied to breast cancer cells. Finally, the third section describes the results of the methodology and its review.

2 Important Concepts

2.1 Typical Testors

Testors Theory was formulated as an independent scientific direction of Mathematical Cybernetics in the 60's in the former Union of Soviet Socialist Republics (USSR), whose origin is linked to the use of mathematical logic methods for locating faults in electrical circuits that perform Boolean functions [9].

Later, testors were used to perform supervised classification and selection of variables in problems of geology [9, 10]. The use given in this article to the testors and typical testors is related to feature subset selection, whose precursor is Dmitriev, Zhuravlev and colleagues [10].

In this way, a testor is a subset of features that distinguishes objects from different classes [10]. According to Santiesteban and Pons [11], Shulcloper [9], and Torres [10], a typical testor is a testor that it is no longer possible to remove any feature without losing its status of testor. Otherwise, a typical testor is already formed by the minimum set of features needed to ensure the identification of the class to which a specific object belongs.

Typical testors determine issues such as evaluation of informational weight of traits and selection of variables. They can reduce the dimension of the space of representation of objects [11] and they can be used as a set of support for classification algorithms [12]. So, consequently, the aim of this study is to prove that testor analysis can help to classify cells based on a real dataset; this will be explained in chapter 3.

2.2 Featured Subset Selection

Regularly, Featured Subset Selection (FSS) [13] is used to reduce dimensionality [14], which is used to efficiently reduce the number of variables, attributes or characteristics with which should describe the objects and to find their influence in a problem. This is an alternative method that starts by using the set of typical testors, taking out irrelevant or redundant features [11, 14].

FSS really has importance because reducing the number of features may help to decrease the cost of acquiring data and also make the classification models easier to understand [14, 15]. Also, the number of features could affect the accuracy of classification. Some authors have also studied the bias feature subset selection for classification learning [14].

The FSS problem has been studied by the statistics and machine learning communities for many years with high attention because of the enthusiastic research in data mining [16]. There are many potential benefits of variable and feature selection [17]:

- Facilitating data visualization and data understanding,
- Reducing the measurement and storage requirements,
- Reducing training and utilization times,
- Defying the curse of dimensionality to improve prediction performance.

Selecting the most relevant variables is usually suboptimal for building a predictor, particularly if the variables are redundant [17]. For example, the brute-force selection method evaluates exhaustively all possible combinations of the input features, and then finds the best subset [16]. Later, chapters 3 and 4 will describe a brute-force method applied to the already mentioned dataset related to breast cancer cell with the aim of evaluating if a cell is malign or benign and calculate the informational weight of every feature.

2.3 Informational Weight

The use of the informational weight for feature subset selection is an excellent tool that shows tangible results [14]. Informational weight of a feature is a score, in other words, is the measure of significance to predict whether an object belongs to a group or to another (Classification) [10, 18].

2.4 Breast Cancer

Firstly, cancer is a collection of related diseases. In all types of cancer, some body's cells begin to divide without stopping and spread into surrounding tissues. Cancer can start almost anywhere in the human body, which is made up of trillion of cells [19]. It is the result of mutations, or abnormal changes in the genes that regulate cell growth. Normally, human cells grow and divide to form new cells as the body needs them. When cells grow old or become damaged, they die, and new cells take their place [19, 20].

When cancer develops, this orderly process breaks down. Mutations can „turn on“ certain genes and „turn off“ others in a cell. The modified cell acquires the ability to divide without any control or order, which produces more identical cells and generates a tumor [19, 20].

Consequently, breast cancer is a malignant tumor that has been developed from the breast cells [21]. The breast is made up of glands called lobules that can make milk and thin tubes called ducts that carry milk from the lobules to the nipple, generally breast cancer originates in cells of those lobules [20, 21].

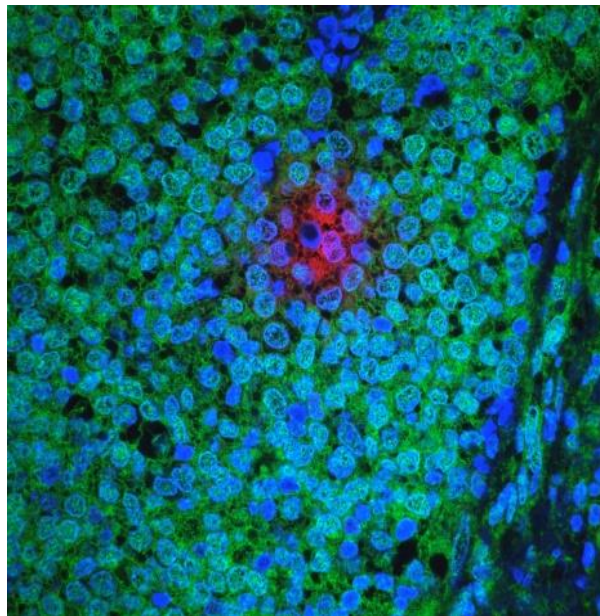


Fig. 1. Invasive breast cancer tumor [19].

Breast cancer has had a great impact worldwide, according to the Pan American Health Organization (PAHO) in the American continent breast cancer is the most common between the women with 29% of the cancer cases. PAHO estimates more than 596,000 new cases and more than 142,100 deaths in the region by 2030, mainly in the area of Latin America and the Caribbean [22]. Next figure shows the incidence of breast malignant tumors in women over age 20 years divided by age group, year 2014:

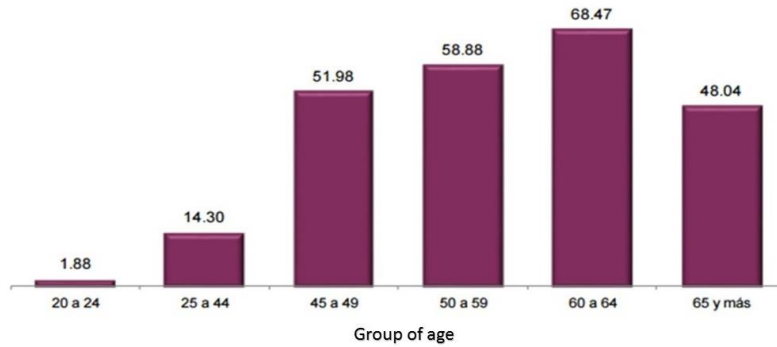


Fig. 2 Incidence of breast malignant tumors in women over age 20 years divided by age group. For 100 thousand women for each age group, INEGI [22].

In general, any type of cancer represents an important impact to the physical state of the person, his or her emotional sphere, a high cost of treatment and can even undermine the economy of the countries; so the prevention and a timely diagnosis are critical to address this problem [23]. Hence, this paper is focused in the application of Feature Subset Selection and Typical Testors to improve the diagnosis of cancer in body's cells. Next chapters will explain the study done.

3 Framework

The general methodology used for this paper is shown in figure 3 below:

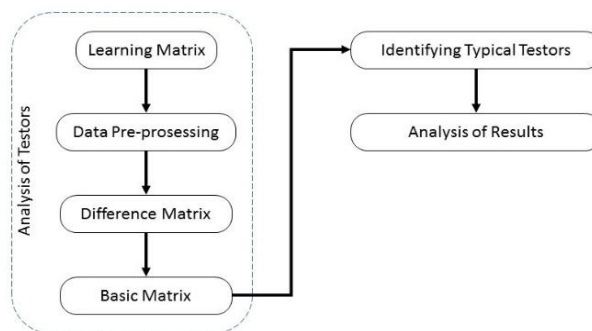


Fig. 3. General Methodology.

As seen if Figure 3 the methodology used needs a Learning Matrix (LM), which is the source of the information that contains descriptions of objects [9, 11]. For this paper, the LM comes from the University of California and their Machine Learning Repository. The repository is Wisconsin Diagnostic Breast Cancer [24].

The database contains the diagnosis and 10 features computed from a digitized image of a fine needle aspirate of a breast mass and describes characteristics of a cell nucleus present in the image [24]. The image below shows an example of this images.

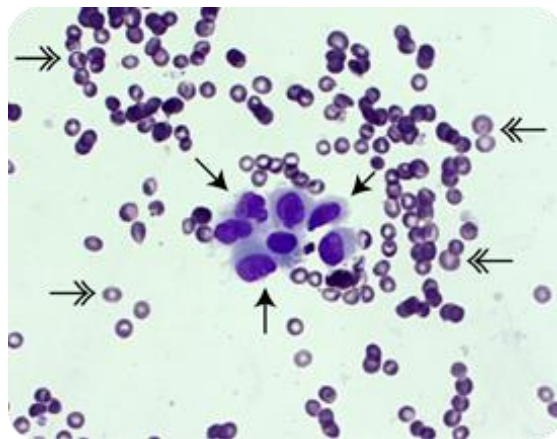


Fig. 4. Fine needle aspirate of a breast mass [25].

The real-valued features for each cell nucleus are [24, 26]:

1. Diagnosis (M=malignant, B=benign)
2. Radius,
3. Texture,
4. Perimeter,
5. Area,
6. Smoothness,
7. Compactness,
8. Concavity,
9. Concave points,
10. Symetry,
11. Fractal dimension

Diagnosis is the final result of evaluating the characteristics of the cell with a computer vision diagnostic system [26-28]. Each cell in the database has one of two possible diagnoses, it can be a malignant cell registered with an uppercase letter M or a benign cell registered with an uppercase letter B.

The radius of a cell was measured by averaging the length of radial lines segments defined by the centroid of the cell and the individual points in the boundary of the cell. The radial lines were defined by Street, Wolberg and Mangasarin in [26, 27] as can be seen in figure 5.

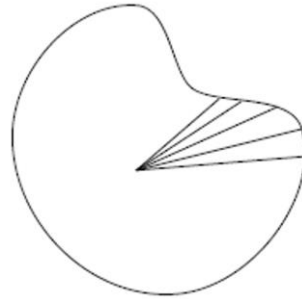


Fig. 5. Radial lines measured in a cell [26].

As mentioned earlier, each cell feature was extracted by a computer vision system, so, the texture was measured by finding variance of gray scale intensities in computer pixels [26, 27]. See Figure 6.

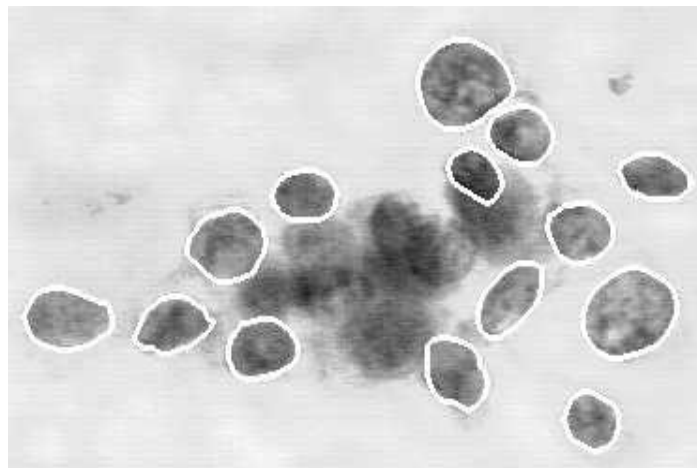


Fig. 6. Example of image taken by a computer vision system and boundary cell [26].

The perimeter is defined as the total distance between individual points named snake points in [26]. Those individual points comprise the white lines in the boundary of the cells (see Figure 6).

The area is measured by counting the number of pixels on the interior of the white line adding one-half of the pixels in the perimeter [26].

Meanwhile, the smoothness of a nuclear contour is quantified by measuring the difference between the length of a radial line and the mean length of the lines surrounding it [26], see Figure 5. Basically, the smoothness is a local variation in radius lengths [24].

Perimeter and area are combined to calculate a measure of compactness, which is a measure of shape [26, 27]. The compactness is given by the formula:

$$\text{Compactness} = \text{perimeter}^2 / \text{area}.$$

This number is minimized by a circular disk and increases with the irregularity of the boundary and also increases for elongated cell nuclei, which can indicate an increased probability of malignancy [26].

Concavity analyzes the shape irregularities in a cell nucleus. Street, Wolberg and Mangasarian [26] measure the number and severity of concavities or indentations in a cell nucleus. They draw chords between non-adjacent white points and measure the extent to which the actual boundary of the nucleus lies on the inside of each chord. See Figure 7.



Fig. 7. Chords used to compute Concavity [26].

Concave points uses similar measure than Concavity but this feature only measures the number, rather than the magnitude, of contour concavities [26].

Symmetry is found the longest chord through the center. Then, according to [26], the length difference between lines perpendicular to the longest chord to the cell boundary in both directions was measured. This is illustrated in Figure 8.

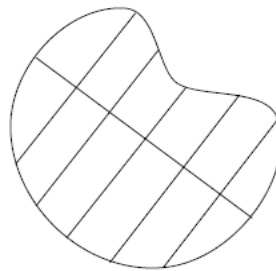


Fig. 8. Segments used in Symetry computation [26].

Finally, the Fractal Dimension is a shape feature [27], so, a higher value corresponds to a less contour and thus to a higher probability of malignancy [26]. The fractal dimension is aproximated using the coastline approximation by Madelbrot [26, 29]. The perimeter of the nucleus is measured using increasingly larger ,rulers'. This is, as the ruler size increases, decreasing the precision of the measurement, the observed

perimeter decreases. Now, Plotting these to values on a log scale and measuring the downward slope gives the negative of an approximation of the fractal dimension [26]. This measurement is illustrated in Figure 9.



Fig. 9. Sequence of measurements for computing Fractal Dimension [26].

The database contains a total of 569 instances with 357 benign instances and 212 malignant instances. This dataset was preprocessed (Data Preprocessing, see Fig. 3), it means that is necessary a depth analysis of the database looking for duplicate instances in each class and contradictions (delete equal records but different diagnosis). Consequently, the database most contain unique instances.

At the end of Data Preprocessing, the dataset contains 130 benign instances and 146 malignant instances. Those 276 instances were analysed with the next steps of the methodology.

With the LM and C_1, \dots, C_n comparison criteria specified [11] by a pathologist of each feature described earlier, a Difference Matrix (DM) is computed by comparing each instance from a class with each instance in the other classes following the comparison criteria of the corresponding feature. When a couple of feature are equal the matrix receives a 0, and 1 when the features are different [11]. A DM contains information that distinguishes objects from differents classes, which contains descriptions of objects [11, 30, 31].

Following this, the Basic Matrix (BM) is determined. The BM contains the basic differences from the DM without duplicates [11, 30]. According to Pons and Shulcloper [9, 32]: be i_q a row of the Difference Matrix, the row i_q is essential if there is not a row i_p that is subline of i_q , then the Basic Matrix contains the essential rows of the DM.

Next step is identifying typical testors. As mentioned earlier, typical testors are formed by the minimum set of features needed to ensure the identification of the class to which a specific object belongs.

The subset $\tau = \{X_{i_1}, \dots, X_{i_s}\}$ of features from a LM is a Testor if each column from its BM is deleted, except those corresponding elements of τ , there is not a row composed by full of zeros. The subset τ is a Typical Testor whether any feature is deleted, the subset is no longer a testor [9, 11, 32].

Finally, the informational weight is calculated and it is possible begin an analysis of results. This information is explained below.

4 Results and Conclusions

At the end of the process, a validation is required which is done by a specialist in the area. For breast cancer and its cells, the specialists are the Oncologist and Pathologist. The final information must be attached to reality, for this reason a Computer Science specialist can not validate this information.

Finally, the typical testors and their informational weight is shown below:

Table 1. Typical Testors.

Feature	Typical Testors (In column)	
	1	2
Radius	0	1
Texture	1	1
Perimeter	1	1
Area	1	0
Smoothness	1	1
Compactness	1	1
Concave points	1	1
Symetry	1	1
Fractal dimension	1	1

As can be seen, Table 1 shows the typical testors. The process found two typical testors and their resulting information that states that most of the features are critical to determine if a instance of the cell is malignant or benignant.

The Typical Testor 1 states a 0 in the radius feature and 1 in the other features. On the other hand, the Typical Testor 2 sets a 0 in the area and 1 in the other features. This means that the radius and the area ar interchangeable.

Table 2. Informational weight according to the typical testors.

Feature	Informational weight
Radius	50%
Texture	100%
Perimeter	100%
Area	50%
Smoothness	100%
Compactness	100%
Concave points	100%
Symetry	100%
Fractal dimension	100%

In other words, it is possible to classify a cell instance knowing at least one of the two features, the radius or the area. For example, an instance can be classified knowing its texture, perimeter, smoothness, compactness, concave points, symmetry and fractal points but if radius is unknown, the area must be known. However, if the area is unknown, the radius must be known. Finally, in the best case, both values are known but it is not possible to classify a cell if both features are unknown.

The informational weight is obtained by calculating a percentage factor that indicates the frequency of each variable in the set of typical testors [33]. Table 2 shows the informational weight of each feature.

The value of the informational weight represents the degree of importance of each feature analyzed in a classification process. A value of 100% indicates that the feature is critical and it can not be ignored in any case.

Also, it can be possible that one or more features have 0% of informational weight meaning that is not necessary, therefore the number of features is reduced and make the problem easier. Remember, this is one of the objective of the analysis.

5 Future Work

The analysis described in this paper is an exhaustive method to find the typical testors. Next step, is to apply a Metaheuristic as an alternative.

The main goal is to find typical testors through metaheuristic algorithms taking advantage of the already identified basic matrix. In this way, the alternative process will be a hybrid method.

Moreover, it is intended to apply both processes (hybrid and exhaustive) in more cases they represent the behavior of different pathologies.

Acknowledgements. We thank Dr. Luis Muñoz Fernandez for all his assistance and advices and Angela Paulina Pérez Díaz for her advices. We really appreciate your help.

References

1. Zicre, D.: Cátedra de Anatomía y Fisiología Patológicas. In: Neoplasia, ed: Facultad de Ciencias Médicas, UNR (2012)
2. Guerra Merino, I.: Factores pronóstico del cáncer de mama en 108 mujeres menores de 36 años. Universidad Complutense de Madrid (2000)
3. CEAMEG: Cancer de Mama. Cancer de Mama, Vol. 1, pp. 1 (2014)
4. Canceronline. Detección Precoz de Cáncer. Available: http://www.canceronline.cl/index.php?option=com_content&view=article&id=48&Itemid=57
5. NIH.: Cancer Screening. Available: <http://www.cancer.gov/about-cancer/screening> (2015)
6. Pérez, N. M.: El diagnóstico médico: algunas consideraciones filosóficas. (2009)

7. Lugo-Reyes, S. O., Maldonado-Colín, G., Murata, C.: Inteligencia artificial para asistir el diagnóstico clínico en medicina. *Artificial Intelligence to Assist Clinical Diagnosis in Medicine*, Vol. 61, No. 2, pp. 110–120 (2014)
8. Reed, K.: HealthGrades Patient Safety in American Hospitals Study. Available: <https://www.hospitals.healthgrades.com/>
9. Ruíz, J., Alba, E., Lazo, M. : Introducción a la Teoría de Testores. Departamento de Ingeniería Eléctrica, CINVESTAV-IPN, pp. 197 (1995)
10. Torres, M. D., Torres, A., Torres, M. L., Bermudez, L., Ponce, E. E.: Factores Predisponentes en Relajación Residual Neuromuscular. *Research in Computing Science*, Vol. 93, pp. 163–174 (2015)
11. Santiesteban, Y., Pons, A.: LEX: A New Algorithm for the Calculus of all Typical Testors. Vol. 1, pp. 85–95
12. Lias-Rodríguez, A., Pons-Porrata, A.: Un nuevo Algoritmo de Escala Exterior para el Cálculo de los Testores Típicos. pp. 10, http://www.rcs.cic.ipn.mx/2015_93/Factores%20predisponentes%20en%20relajacion%20residual%20neuro muscular.pdf (2015)
13. Wang, G., Song, Q., Sun, H., Zhang, X.: A Feature Subset Selection Algorithm Automatic Recommendation Method. China: Cornell University Library, pp. 1–34 (2013)
14. Torres, D., Ponce de León, E., Torres, A., Ochoa, A., Díaz, E.: Hybridization of Evolutionary Mechanisms for Featured Subset Selection in Unsupervised Learning. *MICAI 2009, Advances in Artificial Intelligence*, pp. 610–621 (2009)
15. Pelikan, M., Sastry, K., Cantú-Paz, E.: *Scalable Optimization vía Probabilistic Modeling: From Algorithms to Applications*. Springer (2006)
16. Deng, K.: OMEGA: On-line Memory-Based General Purpose System Classifier. Doctor, School of Computer Science, Carnegie Mellon University, Pittsburgh, PA (1998)
17. Guyon, I., Elisseeff, A.: An Introduction to Variable and Feature Selection. *Journal of Machine Learning Research*, Vol. 3 (2003)
18. Cotilla, M. O.: *Un Recorrido por la Sismología de Cuba*. Cuba: Editorial Complutense, S. A. (2006)
19. N. C. Institute: What is Cancer? <http://www.cancer.gov/about-cancer/understanding/what-is-cancer> (2015)
20. Breastcancer.org.: ¿Qué es el Cáncer de mama? <http://www.cancer.gov/about-cancer/understanding/what-is-cancer>(2014).
21. NIH: Breast Cancer - Patient Version. National Cancer Institute.
22. INEGI: Estadísticas a Propósito del Día Mundial de la Lucha contra el Cáncer de Mama. In: *Estadísticas Nacionales*, ed. México, Instituto Nacional de Estadística y Geografía (2015)
23. INEGI: Estadísticas a Propósito del Día Mundial Contra el Cáncer. México, Instituto Nacional de Estadística y Geografía (2016)
24. Wolberg, W. H., Street, N., Mangasarian, O. L.: *Wisconsin Diagnostic Breast Cancer (WDBC)*. California, Ed., USA (1995)
25. V. B. Imaging: Fine Needle Aspiration. <http://www.breastimaging.vcu.edu/services/guided/fineneedle.html> (2016)

26. Street, W. N., Wolberg, W. H., Mangasarian, O. L.: Nuclear Feature Extraction for Breast Tumor Diagnosis. In: International Symposium on Electronic Imaging: Science and Technology, Vol. 1905, pp. 861–870
27. Wolberg, W. H., Street, W. N., Heisey, D. M., Mangasarian, O. L.: Computerized breast cancer diagnosis and prognosis from fine- needle aspirates. Archives of surgery (Chicago, Ill.: 1960), Vol. 130, No. 5, pp. 511 (1995)
28. Wolberg, W. H., Street, W. N., Heisey, D. M., Mangasarian, O. L.: Computer-derived nuclear features distinguish malignant from benign breast cytology. Human Pathology, Vol. 26, No. 7, pp. 792–796 (1995)
29. Mandelbrot, B. B.: The fractal geometry of nature. New York, W.H. Freeman (1982)
30. Ochoa-Somuano, J.: Técnicas de Selección de Atributos para la Categorización Automática de Escenas Visuales. Maestría, Centro Nacional de Investigación y Desarrollo Tecnológico, Cuernavaca, Morelos (2005)
31. Martínez-Sánchez, N., García-Lorenzo, M. M., García-Valdivia, Z. Z.: Modelo para Diseñar Sistemas de Enseñanza-Aprendizaje Inteligentes Utilizando el Razonamiento Basado en Casos. Revista Avances en Sistemas e Informática, Colombia, Vol. 6 (2009)
32. Pons-Porrata, A.: Desarrollo de Algoritmos para la Estructuración Dinámica de Información y su Aplicación a la Detección de Sucesos. Doctorado, Departamento de Lenguajes y Sistemas Informáticos, Universidad Jaume I, Castellón (2004)
33. Rodríguez de León, P.: Heurística lógico combinatoria para la selección de subconjuntos de características en diabetes mellitus. Tesis (maestría en informática y tecnologías computacionales), Universidad Autónoma de Aguascalientes, Centro de Ciencias Básicas, Aguascalientes, Ags., Méx. (2016)

Fuzzy Logic Controller for Speed and Torque in AC Servo System

L. Rodrigo Silva Sánchez, Antonio Hernández Zavala,
Jorge A. Huerta Ruelas

Centro de Investigación en Ciencia Aplicada y Tecnología Avanzada del
Instituto Politécnico Nacional (CICATA-IPN-QRO), Querétaro,
Mexico

lrodrigo.silva.s@gmail.com, anhernandez@ipn.mx, jhuertar@ipn.mx

Abstract. This paper presents the application of a fuzzy-logic controller for an AC servomotor. The fuzzy-logic controller is coupled to conventional methods for AC Servo commutation, such as a field-oriented flux control and voltage amplifiers. A test bench platform was designed specifically to test the controller at different load values. The behaviour of the speed and torque variables got stable while maintaining the error deviation lower than 5%, being a competitive option compared to the current literature.

Keywords: AC servomotor, fuzzy logic controller, speed control, torque control.

1 Introduction

Industrial automation is based in motion control of different mechanisms, for which induction motors and servomotors are used given its robustness and reliability. The controllers for motors and servomotors have become a key requirement for precise automation. The use of artificial intelligence in the fields of power electronics and speed control has increased significantly. These methods use fuzzy logic and artificial neural networks, which require little mathematical knowledge to describe the operation of the system, along with a logical instead of a mathematical analysis to control the system to facilitate decision-making.

This trend is accompanied of the electrical machine optimization for maximum performance, which involves the use of electronics that are more sensitive to disturbances, making necessary to implement compensation equipment taking into account factors that were previously not relevant. Fuzzy systems allow modelling a plant out of the knowledge of its functioning, and the controller realization is straightforward. Artificial neural networks need to have a learning stage, in which the user provides the input data and it shows which is the output or the expected response.

In many papers there is coupling between fuzzy and PID control techniques [1, 2, 3]. For servomotor systems, it obtains better results than separately. The importance of

this work is the implementation of fuzzy control to measure performance with the lowest number of membership functions in the three-phase inverter developed. Several papers have described how to couple the Fuzzy control to AC servo systems [1-15]. The controller responds according to the application of rules or algorithms that are related to the mechanism dynamics. Inferences are made according to the in line behaviour of the motor and its dynamic response [4, 5, 6, 7].

The application of artificial neural networks and fuzzy logic is based on the application of rules or algorithms that are not related to the mechanism, but to its behaviour. The advantages found were self-tuning, fast torque and flux response, without problems during low-speed operation [8, 9, 10].

The work presented by Bor-Ren Lin [11], proposes a neural network for states interruptions voltage inverter using current control of hysteresis. In the case of L. Cabrera and Zinger [12], they present four training algorithms to emulate the sector stator in a DTC (Direct Torque Control).

The paper is organized as follows: Section 2 presents the electrical, mechanical and mathematical models of the servomotor in order to understand how it is controlled. Section 3 presents the design of the fuzzy logic controller for speed and torque. Section 4 shows the experiments realized along with the testing platform. The results are analysed and discussed in section 5, to finally present the conclusion.

2 Model of the AC Servomotor

Vectorial control began in the decade of the 70s in West Germany, with the principles stated in the work of Hass and Blaschke. The method focuses on the coupling and uncoupling of the magnetic flux of the motor, resulting in a dynamic behaviour similar to direct current motor. The simplified equations to obtain are convenient for the control system and for implementation. They can be written in the form of Ec. 1:

$$\begin{pmatrix} V_{qs} \\ V_{ds} \\ 0 \\ 0 \end{pmatrix} = \begin{pmatrix} R_s + d(L_{ls} + M) & W_e(L_{ls} + M) & dM & W_e M \\ -W_e(L_{ls} + M) & R_s + d(L_{ls} + M) & -W_e M & dM \\ dM & -(W_e - W_r)M & R_r + d(L_{lr} + M) & -(W_e - W_r)(L_{lr} + M) \\ -(W_e - W_r)M & dM & -(W_e - W_r)(L_{lr} + M) & R_r + d(L_{lr} + M) \end{pmatrix} \begin{pmatrix} i_{qs} \\ i_{ds} \\ i_{qr} \\ i_{dr} \end{pmatrix}, \quad (1)$$

where

d : differential operator,

V_{qs}, V_{ds} : stator voltage of synchronously rotating $d^e - q^e$ reference frame,

i_{qs}, i_{ds} : stator current of synchronously rotating $d^e - q^e$ reference frame,

R_r, R_s : stator and rotor resistances, respectively,

W_e, W_r : synchronous and rotor angular velocities, respectively,

$$M = \frac{3}{2} L_{ms}, \quad (2)$$

where

L_{ms} : the stator magnetizing inductance.

The rotor speed and torque are related by the equation

$$\frac{2}{p} J d(W_r) = T_e - T_l, \quad (3)$$

where

p : Number of poles,

J : the inertia of the rotor,

T_e : electromagnetic torque,

T_l : load torque.

The three-phase inverter topology was used. The circuit consists of three half-bridges, their respective phase input is formed by a DC power supply and an inductive-capacitive LC filter, as shown in Fig. 1.

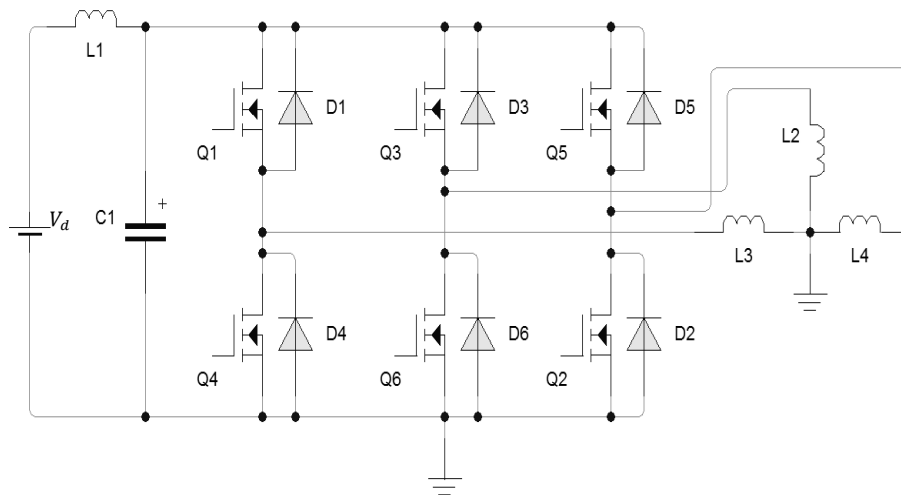


Fig. 1. Three-phase inverter (Half Bridge).

3 Fuzzy Logic Controller

The principal blocks that compose a fuzzy system are shown in Fig. 2. its operation requires first to convert one or more input data from a continuous universe (crisp) into fuzzy values in the fuzzification stage. Then, at the inference stage, it uses those fuzzy values to obtain a response out of the rule base which was previously filled with an expert knowledge to handle the system. Once a set of results is inferred, it is necessary to realize the inverse transformation, to convert the fuzzy value into a crisp value for modifying the system, the defuzzification stage.

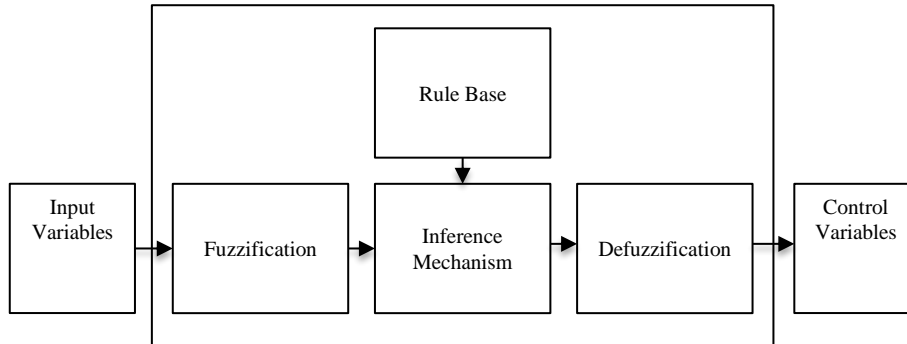


Fig. 2. General Block Diagram of Fuzzy System.

3.1 Membership Function Definition

The membership functions (MF) are proposed by the user. In this case, the definition of the membership functions was performed using three triangular membership functions for the input and output variables. Each MF is defined by the triangular MF general equation (4):

$$\mu(x) = \begin{cases} 0, & a < b \\ mx + b, & b \leq c \\ -mx + b, & c \leq d \\ 0, & d \leq e \end{cases} \quad (4)$$

For the case of the input variable error, the linguistic terms used to identify each MF are: Negative Small (NS), Zero (ZE), and Positive Small (PS), they are distributed graphically as shown in Fig. 3. The corresponding equations are (5)-(7). The same configuration was used for the output variable as in Fig. 4.

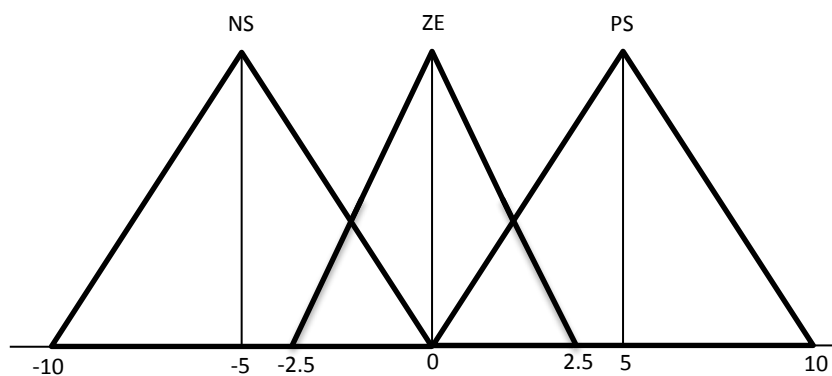


Fig. 3. The membership functions for error input.

$$\mu_{NS}(x) = \begin{cases} 0, & -\infty < -10 \\ 0.2x + 2, & -10 \leq -5 \\ -0.2x + 0, & -5 \leq 0 \\ 0, & 0 \leq \infty \end{cases} \quad (5)$$

$$\mu_{ZE}(x) = \begin{cases} 0, & -\infty < -2.5 \\ 0.4x + 1, & -2.5 \leq 0 \\ -0.4x + 1, & 0 \leq 2.5 \\ 0, & 2.5 \leq \infty \end{cases} \quad (6)$$

$$\mu_{PS}(x) = \begin{cases} 0, & -\infty < 0 \\ 0.2x + 0, & 0 \leq 5 \\ -0.2x + 2, & 5 \leq 10 \\ 0, & 10 \leq \infty \end{cases} \quad (7)$$

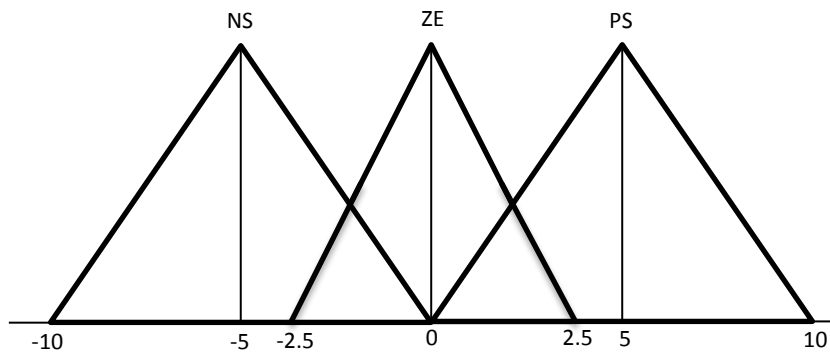


Fig. 4. Membership function for output.

3.2 Inference Mechanism and Rule Base

The inference mechanism is responsible for evaluating the fuzzy data membership values, obtained by the fuzzifier into the fired rules from the rule base. In this sense, the inference mechanism delivers the membership values, corresponding to the output membership functions. To generate the rule base, It is required a prior knowledge of an expert because without this it is very difficult generating a rule base applicable to process control.

Our controller uses the Mamdani model, which establishes rules defined by the following equation:

$$R_i: IF x = A_i \text{ and } y = B_i \text{ THEN } z = C_i. \quad (8)$$

For example:

$$Rule_1: IF In \text{ is } NP \text{ and } Out \text{ is } NP \text{ THEN } z \text{ is } PP. \quad (9)$$

The number of rules used in this controller is seven. Table 1 shows the rule base distribution used to describe the input and output variables relation.

Table 1. Rule-Base.

IN/OUT	NP	ZE	PP
NP	PP	NP	X
ZE	NP	ZE	PP
PP	X	PP	NP

3.3 Defuzzification

Defuzzification stage is responsible for converting the fuzzy values obtained after the evaluation, into crisp values.

For this controller, the Mean of Maxima MOM defuzzifier is used. This defuzzifier, analyses the fuzzy values and determines the values in which $\mu_B(y)$ is a maximum. Subsequently, it calculates the average of these values as output if the maximum value of $\mu_B(y)$ occurs only once:

$$y = MOM \sum_{j=1}^l \frac{\mu(x_j)}{l}. \quad (10)$$

4 Fuzzy Logic Controller

The suggested speed control system was implemented for the AC servomotor coupled to a test bench. To implement the fuzzy controller we used an 8-bit microcontroller coupled to a synchronizer phase and a three-phase inverter, which were developed as in Fig. 5. Table 2 shows the characteristics of the servomotor that was used for testing.

Fig. 7 shows: a) the controller response for a 100-rpm set point, b) torque and c) Magnetic flux with a fixed preload of 1,156 N.m. All variables were taken simultaneously to verify control responses. The overshoot is too large at the beginning, and then it slowly declines until it stabilizes.

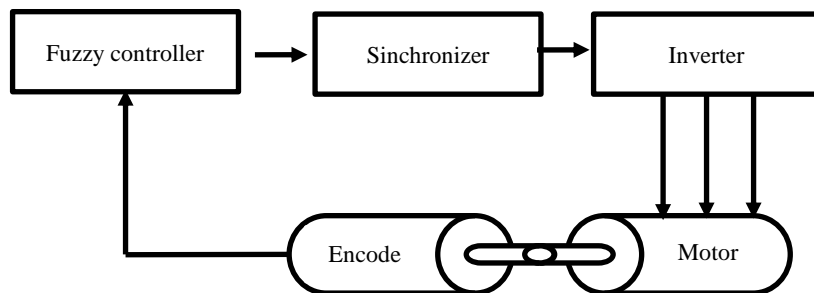


Fig. 5. Diagram of the implementation of fuzzy control.

Fig. 6 shows the developed test bench and driver in which the torque and speed experiments were performed.

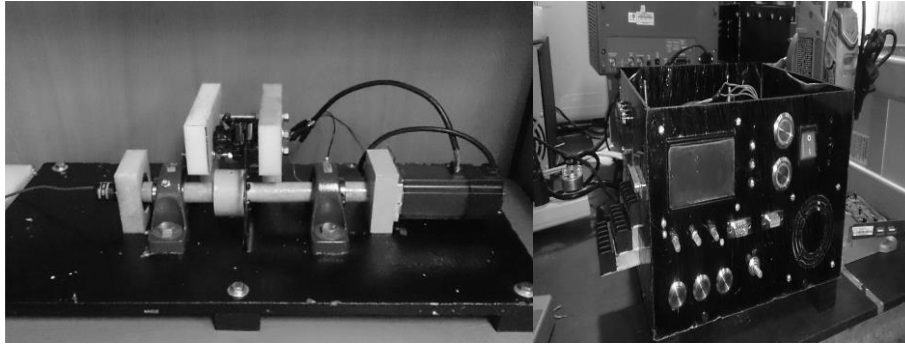


Fig. 6. Photograph of the AC Servomotor Test Bench and driver developed.

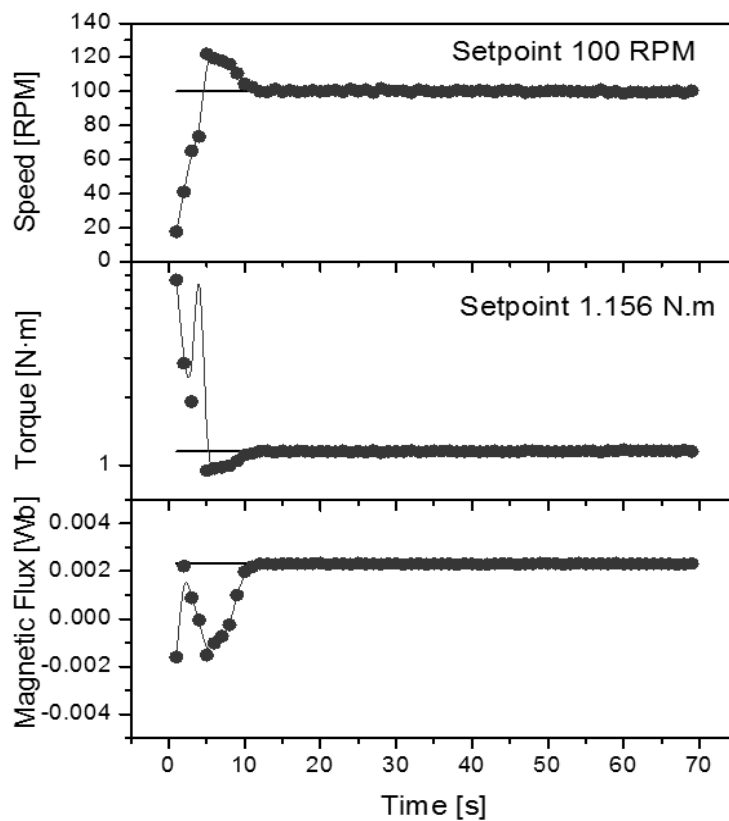


Fig. 7. Motor response tuned to a set point of 100 RPM's and a fixed preload of 1.156 Nm. a) the controller response b) torque and c) Magnetic flux.

Table 2. Main data for AC servomotor used to test Fuzzy controller.

Description	Symbol	Quantity	Unit
Stator voltage	V_d	220	V
Rotor resistance	R_r	0.816	Ω
Stator resistance	R_s	0.918	Ω
Slip index	S	0.16	
The stator magnetizing inductance	L_{ms}	1.311	H
The inertia of the rotor	j	0.0143	$\text{Kg}\cdot\text{m}^2$

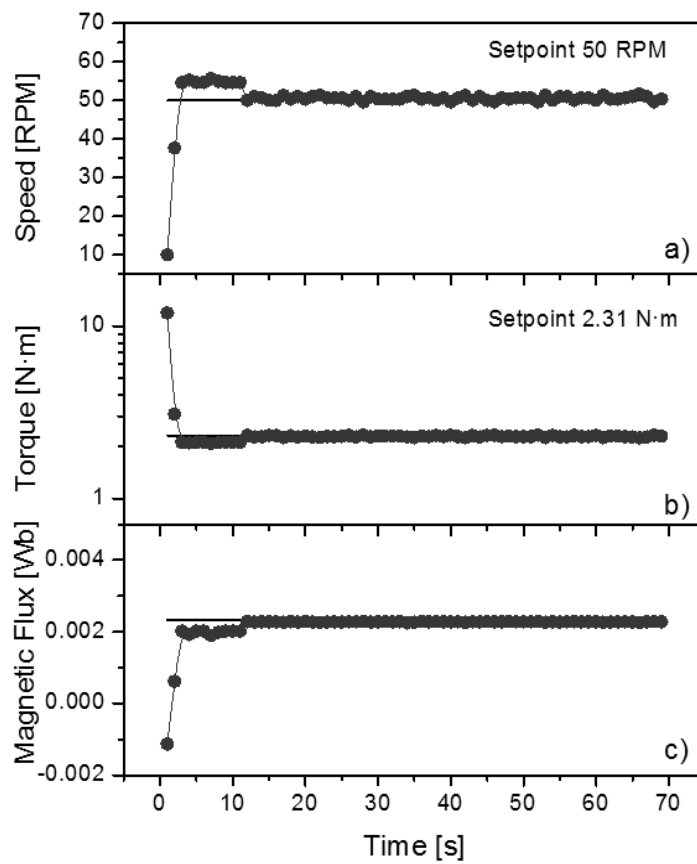


Fig. 8. Motor response tuned to a set point of 50 RPM's and a fixed preload of 2.31 Nm. a) the controller response b) torque and c) Magnetic flux.

Fig. 8 shows: a) the controller response for a 50-rpm set point, b) torque and c) Magnetic flux with a fixed preload of 2.31 N.m. All variables were taken simultaneously to verify control responses. The overshoot is too large at the beginning, and then it slowly declines until it stabilizes.

The nominal AC servomotor torque is 1.3 N.m. therefore is difficult for the controller to stabilize in the 5% error range. It is seen that the magnetic flux is below that the set point, since the preload is greater than the nominal for this AC servomotor.

5 Discussion

From the results, it can be deduced that it is possible to couple the fuzzy control technique with vector control techniques.

It is seen that different tests have a similar behaviour, notorious from the responses of control graphs at different reference values (50, 100) rpm. The controller stabilizes effectively in the 5% range despite of the few membership functions used for the controller.

Table 3. Error comparison in FLC with vector techniques in AC Servomotor.

Authors	Control technique in the inverter	Control	Variable to Control	Test	Error (e)
Silva et al.	FOC	Fuzzy	Torque Speed	Real	e< 5%
Feng-Fu Chen [13]	FOC	Fuzzy	Torque Speed Position	Simulation / Real	e< 6%
Gilberto C. D. [14]	FOC	Fuzzy	Torque Speed	Real	e< 6%
Pawel Grabowski [9]	DTC	Neuro Fuzzy	Torque	Real	e< 7%
Faa-Jeng Lin [10]	FOC	Neuro Fuzzy	Torque speed Position	Simulation	e< 7%
Giuseppe Buja [15]	DTC	Fuzzy	Torque	Real	e< 2%

It is important to notice that an increase in the number of membership functions used for input and output, will lead us to better results. Nevertheless, if we consider that we require an 8-bit microcontroller implementation, we cannot use many membership functions to define the fuzzy system, since it will consume much more memory and processing time. In this sense, we chose a basic implementation

for our speed controller in order to maintain a reasonable response time and resource consumption.

It can be concluded that the steady state error remains between 3% and 5%, which, if compared to commercial drivers is still high, since most of them handle 1% standard error. However, when compared with other paper works, they present a similar error as seen in Table 3. Another aspect observed in control graphs is that you can see a bigger overshoot, causing the generation of harmonics in the stator phases resulting in overheating.

6 Conclusions

The proposed controller was successfully implemented in the AC servomotor, by coupling techniques for vector control of induction motors and fuzzy logic. It was also achieved that the steady state error remains lower than 5% in tests at different speeds and preloads.

Compared to other drivers developed by researchers, the proposed controller is competitive, since it was implemented in an 8-bit microcontroller using the simplest structure in order to efficiently use the computational resources. Implementing neural networks coupled with fuzzy logic and vector control error would increase the response time due to large information processing.

Acknowledgments. Authors would like to thank CONACYT and the Instituto Politécnico Nacional (IPN), for their financial support.

References

1. Manikandan, R.: Design of Equivalent Fuzzy PID Controller From The Conventional PID Controller. *Int Conf Control Commun Comput Technol*, India, pp. 356–362 (2015)
2. Zhao, Z.Y., Tomizuka, M., Isaka, S.: Fuzzy gain scheduling of PID controllers. In: *Proceedings First IEEE Conf Control Appl*, pp. 698–703 (1992)
3. Choi, H.H., Yun, H.M., Kim, Y.: Implementation of Evolutionary Fuzzy PID Speed Controller for PM Synchronous Motor. *IEEE Trans Ind Informatics*, Vol. 11, pp. 540–547 (2015)
4. Kung, Y., Wang, M., Huang, C.: Digital Hardware Implementation of Adaptive Fuzzy Controller for AC Motor Drive. In: *Ind Electron Soc 2007 IECON 2007 33rd Annu Conf IEEE*, Taiwan, pp. 1208–1213 (2007)
5. Lubin, T., Mendes, E., Marchand, C.: Fuzzy Controller in A.C. Servo Motor Drive. In: *Electrical Machine Drives, Seventh Int Conf (Conf Publ No 412)*, pp. 11–13 (1995)
6. Uddin, M.N., Rebeiro, R.S.: Fuzzy Logic Based Speed Controller and Adaptive Hysteresis Current Controller Based IPMSM Drive for Improved Dynamic Performance. pp. 1–6 (2011)
7. Suyitno, A., Strefezza, M., Dote, Y.: Variable - Structured Robust Control by Fuzzy Logic and Stability Analysis for AC Drive System. Singapore, pp. 51–56 (1993)
8. Dazhi, W., Guoqing, J., Jun, L.: A Novel Hysteresis Current Control Strategy Based on Neural Network. Vol. 2, pp. 369–372 (2010)

9. Grabowski, P.Z., Member, A., Kazmierkowski, M.P.: A Simple Direct-Torque Neuro-Fuzzy Control of PWM-Inverter-Fed Induction Motor Drive. Vol. 47, pp.863–870 (2000)
10. Lin, F.J., Chiu, S.L.: Adaptive Fuzzy Sliding-Mode Control for PM Synchronous Servo Motor Drives. IEEE Proc Control Theory Appl., Vol. 145, pp. 63–72 (1998)
11. Lin, B.R., Hoft, R.G.: Power Electronics Inverter Control With Neural Networks. Appl Power Electron Conf Expo Eighth Ann, pp. 128–134 (1993)
12. Cabrera, L.A., Elbuluk, M.E., Zinger, D.S.: Learning Techniques to Train Neural Networks as a State Selector. In: Power Electron Spec Conf PESC'94 Rec 25th Annu IEEE, Vol. 12, pp. 233–242 (1994)
13. Cheng, F.F.: Application of Fuzzy Logic in the Speed Control of AC Servo System And an Intelligent Inverter. IEEE Trans Energy Convers, Vol. 8, pp. 312–318 (1993)
14. Sousa, G., Bose, B.K., Cleland, J.G.: Fuzzy logic based on-line efficiency optimization control of an indirect vector-controlled induction motor drive. IEEE Trans Ind Electron, Vol. 42, pp. 192–198 (1995)
15. Buja, G.S., Kazmierkowski, M.P.: Direct Torque Control of PWM Inverter-Fed AC Motors—A Survey. IEEE Trans Ind Electron, Vol. 51, pp. 744–757 (2004)

Impreso en los Talleres Gráficos
de la Dirección de Publicaciones
del Instituto Politécnico Nacional
Tresguerras 27, Centro Histórico, México, D.F.
noviembre de 2016
Printing 500 / Edición 500 ejemplares

